UNIVERSITÄT BERN

Graduate School for Health Sciences

University of Bern

FROM REST TO TASK:
Functional Brain Networks in Schizophrenia

PhD Thesis submitted by

Anja Katharina Bänninger

from **Embrach ZH**

for the degree of

PhD in Health Sciences (Neurosciences)

Thesis advisor
Prof. Dr. Thomas Koenig
University Hospital of Psychiatry and Psychotherapy
Faculty of Medicine of the University of Bern

Thesis co-advisor
Prof. Dr. med. Roland Wiest
Institute for Diagnostic and Interventional Neuroradiology
University Hospital of Bern
Faculty of Medicine of the University of Bern

Accepted by the Faculty of Medicine and the Faculty of Human Sciences of the University of Bern

Bern, Dean of the Faculty of Medicine

Bern, Dean of the Faculty of Human Sciences

TABLE OF CONTENTS

"*A science of the mind must reduce … complexities (of behavior) to their elements. A science of the brain must point out the functions of its elements. A science of the relations of mind and brain must show how the elementary ingredients of the former correspond to the elementary functions of the latter.*"

William James (1890)

LIST OF ABBREVIATIONS

ACC	Anterior cingulate cortex
BOLD	Blood oxygen level-dependent
dAN	Dorsal attention network
DMN	Default mode network
DTI	Diffusion tensor imaging
EEG	Electroencephalography
EC	Eyes closed
EO	Eyes open
ERP	Event-related potential
FM	Frontal-midline
fMRI	Functional magnetic resonance imaging
GFS	Global field synchronization
Hz	Hertz
ICA	Independent component analysis
IPL	Inferior parietal lobule
LFP	Local field potential
lWMN	Left working memory network
MEG	Magnetoencephalography
mPFC	Medial prefrontal cortex
MRI	Magnetic resonance imaging
PCC	Posterior cingulate cortex
PET	Positron emission tomography
PrC	Precuneus
rWMN	Right working memory network
ROI	Region of interest
RSN	Resting state network
tDCS	Transcranial direct current stimulation
TCN	Temporally coherent network
TMS	Transcranial magnetic stimulation
WM	Working memory

SUMMARY

A primary goal of neuroscience research on psychiatric disorders such as schizophrenia is to enhance the current understanding of underlying biological mechanisms in order to develop novel interventions.

Human brain functions are maintained through activity of large-scale brain networks. Accordingly, deficient perceptual and cognitive processing can be caused by failures of functional integration within networks, as reflected by the *disconnection hypothesis* of schizophrenia. Various neuroimaging techniques can be applied to study functional brain networks, each having different strengths. Frequently used complementary methods are the electroencephalography (EEG) and functional magnetic resonance imaging (fMRI), which were shown to have a common basis. Given the feasibility of combined EEG and fMRI measurement, EEG signatures of functional networks have been described, providing complimentary information about the functional state of networks. Both at rest and during task completion, many independent EEG and fMRI studies confirmed deficient network connectivity in schizophrenia. However, a rather diffuse picture with hyper- and hypo- activations within and between specific networks was reported. Furthermore, the theory of state dependent information processing argues that spontaneous and prestimulus brain activity interacts with upcoming task-related processes. Consequently, observed network deficits that vary according to task conditions could be caused by differences in resting or prestimulus state in schizophrenia.

Based on that background, the present thesis aimed to increase the understanding of aberrant functional networks in schizophrenia by using simultaneous EEG-fMRI under different conditions. One study investigated integrative mechanisms of networks during eyes-open (EO) resting state using a common-phase synchronization measure in an EEG-informed fMRI analysis (study 3). The other two studies (studies 1&2) used an fMRI-informed EEG analysis: The second study was an extension of the first, which was performed in healthy subjects only. Hence, the same methodologies and analyses were applied in both studies, but in the second study schizophrenia patients were compared to healthy controls. The associations between four temporally coherent networks (TCNs) – the default mode network (DMN), the dorsal attention network (dAN), left and right working memory networks (WMNs) – and power of three EEG frequency bands (theta, alpha, and beta band) during a verbal working memory (WM) task were investigated.

Both resting state and task-related studies performed in schizophrenia patients (studies 2&3) revealed altered activation strength, functional states and interaction of TCNs, especially of the DMN. During rest (study 3), the DMN was differently integrated through common-phase synchronization in the delta (0.5 – 3.5Hz) and beta (13 – 30Hz) band. At prestimulus states of a verbal WM task, however, study 2 did not reveal differences in the activation level of the DMN between groups. Furthermore, from pre-to-post stimulus, the association of the DMN with frontal-midline (FM) theta (3 – 7Hz) band was altered, and a reduced suppression of the DMN during WM retention was detected. Schizophrenia patients also demonstrated abnormal interactions between networks: the DMN and dAN showed a reduced anti-correlation and the WMNs demonstrated an absent lateralization effect (study 2).

The view that schizophrenia patients display TCN deficiencies is supported by the results of the present thesis. Especially the DMN and its interaction to the task-positive dAN showed specific alterations at different mental states and their interaction (during rest and from pre-to-post stimulus). Those alterations might at least partly explain observed symptomatology as attentional orientation deficits in patients. To conclude, functional networks as the DMN might represent promising targets for novel treatment options such as neurofeedback or transcranial direct current stimulation (tDCS).

1. INTRODUCTION

Human brain functions and cognition rely on activity within large-scale and distributed brain networks (McIntosh 1999, McIntosh 2000). A network consists of integrated distributed regions that facilitate specific perceptual or cognitive operations. Hence, the resulting mental operation underlying a network reflects an integration of all those single operations from included regions. Aberrant perceptual and cognitive states can thus be attributed to functional integration failures within brain networks. This idea was translated to psychiatry with the description of schizophrenia as a *disconnection syndrome* (Friston and Frith 1995). When complementary neuroimaging techniques such as functional magnetic resonance imaging (fMRI) and electroencephalography (EEG) are independently used, different network properties are revealed without knowing whether they both originate from the same network: Using fMRI, functionally co-activated regions can be identified with high spatial resolution, whereas the high temporal resolution of the EEG can provide information regarding frequency, amplitude and phase synchronization of oscillating neuronal populations measured on the scalp. Examining the brain's intrinsic functional activity provides additional information to the study of task-related activity to characterize human brain functions and to detect biological markers of neurological and psychiatric diseases (Fox and Raichle 2007). Additionally, according to the framework of state dependent information processing, the brains intrinsic state interacts with the typical response patterns elicited by internal (e.g. memories, thoughts, and emotions) or external (e.g. sensory information, task performance) stimuli. Consequently, inter-trial variability in healthy subjects, as well as altered activation patterns found in patients, is potentially explainable by differences in the brain's prestimulus or resting state.

The present thesis aimed to elucidate functional large-scale networks in schizophrenia patients from different angles: during rest and within task-related states from pre-to-post stimulus, as well using the combined measurement of EEG and fMRI. The thesis is structured into four chapters. The first chapter covers the theoretical background including schizophrenia, cerebral networks, the disconnection hypothesis of schizophrenia, as well as the hallmark theory of state dependent information processing. The second chapter, *Empirical contribution,* contains the results of the three studies conducted within this project: The first study "*Pre-stimulus BOLD-network activation modulates EEG spectral activity during working memory retention*", the second study "*Inefficient Preparatory fMRI-BOLD Network Activations Predict*

Working Memory Dysfunctions in Patients with Schizophrenia", and the third entitled "*Delta EEG synchronization linked to DMN activity in schizophrenia*". The third chapter concludes with a discussion of the overall findings within the context of the current status. And finally, some future directions for research are presented in the chapter *Perspectives*.

1.1 Schizophrenia

1.1.1 Epidemiology and phenomenology

Every year, it is estimated that roughly 1% of the worldwide population is diagnosed with schizophrenia and that two third of those people developing schizophrenia require professional assistance within a few years after illness onset (Andreasen 2000). The heterogeneity of this severe mental illness is illustrated by the variety of characteristic symptoms covering a broad range of human functions including: Reality distortions as seen in delusions and hallucinations, disorganized communication and behavior, reduced volition and motivation, abnormal motor behavior and affective experience, cognitive impairments, as well as social withdrawal. Psychotic episodes are usually preceded by a prodromal phase or so-called at-risk mental state and typically occur for the first time in late adolescence or early adulthood with men tending to experience earlier onsets (around 21 years of age) and more severe illness courses than women (around 27 years of age; Lieberman, Perkins et al. 2001, Saha, Chant et al. 2005, McGrath, Saha et al. 2008, Addington and Heinssen 2012). The mortality risk for schizophrenia patients is two to three times higher than that of the general population: Suicide is one cause, but multiple medical comorbidities (partly representing side effects from medication) including cardiovascular disease, obesity, diabetes, and substance abuse also contribute (Auquier, Lancon et al. 2006). This indicates that, in general, mental health care systems need to be optimized in terms of rehabilitation of affected individuals (Saha, Chant et al. 2005). Despite lower prevalence compared to other mental illnesses (e.g. depression with worldwide yearly prevalence of 3%; Moussavi, Chatterji et al. 2007), schizophrenia bears enormous health, social, and economic burden for patients, their families, as well as caregivers and the wider society (Global Burden of Disease Study 2015, Chong, Teoh et al. 2016).

To date, current diagnostic systems have not improved the understanding of the etiology and pathophysiologic mechanisms of schizophrenia. Typically, diagnosis is based either on the Diagnostic and Statistical Manual of Mental Disorders (DSM;

American Psychiatric Association) or the International Classification of Diseases (ICD; World Health Organization, WHO). These systems date back to early classification attempts by Emil Kraeplin (1887), Eugen Bleuler (1911) and Kurt Schneider (1939). The division into first and second rank symptoms as defined by Kurt Schneider particularly influenced these diagnostic systems. First rank symptoms, considered as especially representative for the disease, mainly included auditory hallucinations, passivity experiences, thought withdrawal, thought insertion, thought broadcasting, or diffusion and delusional perception. In contrast to Kraeplin and Bleuler, Schneider did not attempt to link symptoms with neurophysiological correlates.

However, there is strong evidence that biological causes underlie schizophrenia. First, besides small but important environmental effects (around 11%), there is a high heritability of the disease, estimated around 81% (Sullivan, Kendler et al. 2003). Second, evidence comes from the fact that patients respond to pharmacological treatment, and that it is possible to induce psychotic-like symptoms in healthy subjects by ketamine intake (Kleinloog, Uit den Boogaard et al. 2015).

1.1.2 From the perspective of biological psychiatry

As other fields of medicine demonstrated improved diagnosis, treatment prediction and prognosis of certain diseases by means of precise biological tests, similar attempts were undertaken in psychiatry (Kapur 2011). Over a century of biological research has been conducted in the field of schizophrenia, yet the knowledge about its underlying neuropathology has remained diffuse. Despite the early conviction of Kraeplin and Bleuler that schizophrenia could be linked to an organic brain disorder, the interest of biological research diminished due to conflicting results, as reflected for example by the statement of Plum in 1972 that "schizophrenia is the graveyard of neuropathologists" (Plum 1972). Thanks to advances in neuroimaging techniques such as computer tomography (CT) and magnetic resonance imaging (MRI) in the 1970's, some encouraging reports initiated a new interest in the biology of schizophrenia. Shenton et al (2001) reviewed fMRI studies from the years 1988 until 2000 and summarized more definite brain abnormalities reported across studies. These abnormalities included mainly ventricular enlargement, reduced grey matter volume of medial temporal lobe structures (including the amygdala, hippocampus, parahippocampal gyrus and neocortical temporal lobe regions), and grey and white matter reductions of superior temporal gyrus. Less consistent were findings of frontal

and parietal lobe abnormalities, and mixed evidence of subcortical regions (e.g. basal ganglia and the thalamus) was reported (Shenton, Dickey et al. 2001). An even though a tremendous number of studies applying varied neuroimaging techniques found biological abnormalities in all major mental disorders, it has not yet lead to useful clinical tests for their diagnosis and treatment (Kapur, Phillips et al. 2012). According to Linden (2013), this lack of viable biomarkers despite the availability of sophisticated methods can be ascribed, among others, to the following two essential problems: First, the diagnosis and classification of diseases (DSM or ICD; Chapter 1.1.1) is still based on the collection of reported symptoms and observed behaviors, not biomarkers and etiology. Second, our understanding of mechanisms underlying effective biological treatments such as psychotropic drugs or brain stimulation is still scarce (Linden 2013).

Nevertheless, candidate endophenotypes for schizophrenia have been extracted from structural brain imaging, EEG, sensorimotor integration, eye movements and cognitive performance (Allen, Griss et al. 2009). A promising approach to gain further insights into potential biomarkers and possible treatment targets is through the study of large-scale neuronal networks: First, observed deficits as described earlier are diffuse, affecting different brain circuitries involving executive function, language, emotion, and motor domains. Second, attempts to use specific individual brain regions to explain the disorder failed. Third, the investigation of cerebral networks is enabled due to major advances in neuroimaging techniques since the last 25 years.

1.2 Cerebral networks

In this chapter, essential terms and concepts regarding brain networks will be specified, followed by short descriptions of two widely applied methodologies used to characterize brain networks.

The structural and dynamic properties of complex networks have received increased attention in various disciplines, ranging from systems neuroscience, physics, economics, to informatics and social sciences in recent years (e.g. Strogatz 2001, Sporns, Chialvo et al. 2004, Newman 2006). In systems neuroscience, the study of brain networks is conceptually divided into three main categories: Structural, functional, and effective connectivity. *Structural connectivity* refers to the anatomical skeleton of networks, the actual physical connections between neurons or population or neurons. It thus includes local circuits up to large-scale networks. *Functional connectivity* is

defined as brain regions being simultaneously activated and therefore forming a functional entity. The last category, *effective connectivity*, investigates temporally delayed activation between regions and thus reveals directional information of functional causality between regions. These categories are not independent of each other, as patterns of functional or effective connectivity are circumscribed by structural connectivity, whereas anatomical substrates undergo plastic changes depending on functional interactions (Sporns, Chialvo et al. 2004).

This thesis focused on functionally connected large-scale networks. In this regard, the differentiation into functional segregation and integration needs to be clarified. In the 19th century, there were the two dominating perspectives of localizationism (functional segregation) versus connectionism (functional integration) of brain functioning (Friston 2011). *Functional segregation* reflects the idea of mapping certain mental functions onto circumscribed brain areas. But as Logothetis (2008) nicely pointed out, despite the modular architecture of the brain, we will never be able to link modules of the mind to brain structures due to the fact that a "*unified mind has no such separable elements*" (Logothetis 2008). *Functional integration*, on the other hand, represents the interaction of those functionally specialized systems (i.e., populations of neurons, cortical areas and sub-areas) needed for the integration of sensorimotor information, and cognition (representing large-scale networks; Friston 2002). Thus, both functional segregation and integration are mutually dependent.

In the following, broadly applied methods in cognitive neuroscience, EEG and fMRI, and the features of brain networks they describe are presented.

1.2.1 Electroencephalography (EEG)

Since the German psychiatrist Hans Berger invented the EEG and reported the first study in 1929, it has found broad scientific applications both in basic and also clinical research. The EEG is a direct measure of synchronous, cortical neuronal activity. The firing of neurons is based on postsynaptic potentials, leading to electric bipolar fields surrounding the cell membranes. Local field potentials (LFPs) are bioelectric potentials measured from the extracellular neuronal space generated by synchronous excitation of several hundreds of neurons (Nicholson 1973) that reflect integrative dendritic events and neuronal input rather than output signals. The EEG measures the electric bipolar field resulting mainly from instantaneous LFPs produced by synchronously active, parallel oriented pyramidal cells (perpendicular to the pial surface) on the

human scalp. The EEG is well suited to study human information processing due to its high temporal resolution (the minimal duration of a stimulus for visual perception is around 80-120msec; Efron 1970). However, its ability to spatially localize the active neuronal populations (i.e., *generators*) accounting for the measured signal is restricted due to a combination of *volume conduction* and *additivity* of sources, which lead to the so-called *inverse problem* of the EEG. *Volume conduction* represents the tissue properties that allow a flow of electric currents. In the case of EEG, these currents are elicited by LFPs in the brain, and flow through the brain volume to the sensors on the scalp. *Volume conduction* depends on physiological factors such as human skin, skull, and cerebral spinal fluid that all differently modulate the current flow that is measured on the scalp. Furthermore, there is the problem of *additivity* of sources, which means that any measured electric field on the scalp reflects the sum of all electric fields produced by instantaneously active sources. As there are uncountable possibilities in source constellations producing the same electric field on the scalp, it becomes impossible to uniquely identify the different generators involved in the finally measured signal without additional a priori assumptions (Pascual-Marqui, Sekihara et al. 2009).

The recorded EEG signal is characterized by voltage differences between each electrode and the measuring reference. Resulting oscillations can be divided into different frequency bands (delta ≅ 0.5 – 4Hz, theta ≅ 4 – 8Hz, alpha ≅ 8 – 13Hz, beta ≅ 13 – 30Hz, and gamma ≅ 30 – 70Hz), which have been linked to relevant functions such as vigilance, arousal, and specific mental operations. Currently, many different approaches and analysis techniques are available and may be combined to interpret the EEG signal. These approaches can be categorized into the temporal and the spatial domain. The temporal domain involves the investigation of the waveforms of oscillations with amplitude or power of frequencies or event-related potentials (ERPs), as well as phase-synchronization. The spatial domain involves the analysis of scalp topographies such as the so-called *microstate* analysis (Koenig and Wakermann 2009).

EEG is the method of choice for the study of sleep stages and epilepsy, but typical markers have also been found in other neurologic and psychiatric diseases. In schizophrenia, EEG indices both during resting-state as well as during a broad range of perceptual and higher cognitive tasks were found: During rest, there is solid evidence for increased power in slower frequencies such as delta and theta bands and to some degree decreased power in alpha band (Sponheim, Clementz et al. 2000, Boutros,

Arfken et al. 2008, Galderisi, Mucci et al. 2009, Siekmeier and Stufflebeam 2010). Furthermore, reductions in ERPs such as the N100 (Rosburg, Boutros et al. 2008), and the highly replicable P300 component (Ford 1999) have been reported. Regarding spatial analysis, differences in *microstates,* a concept introduced by Lehmann et al (Lehmann 1971, Lehmann, Ozaki et al. 1987) between patients and controls were found. Microstates represent quasi-stable topographies lasting about 80 – 120msec and were consistently clustered into four typical scalp distributions of the electric fields labeled A, B, C, and D (Koenig, Prichep et al. 2002). It was found that certain mental operations were related to specific microstates (Lehmann, Strik et al. 1998, Milz, Faber et al. 2016) and that there was a lawful evolution of microstates across developmental stages supporting the view that they represent "*building blocks of human information processing*" (Koenig, Prichep et al. 2002). In schizophrenia, a recent meta-analysis proved evidence of a shortened duration of microstates D, while C occurred more frequently (Rieger, Diaz Hernandez et al. 2016).

To measure large-scale networks, there are theoretically two methods using EEG: First, the microstate analysis from the spatial domain and second, phase-synchronization measures from the time domain. Given that the excellent temporal resolution of the EEG allows for analyses of the timing of interactions, we approached the study of networks by phase-synchronization outlined in the following chapter.

1.2.1.1 Synchronization as binding mechanism

In neuroscience, synchronization measures how the phases of different oscillations are systematically related or not, and informs about the temporal relation of ongoing brain signal. This relation is thought to imply the presence of functional interactions. It should be noted that several synchronization measures exist within the field, which originate from different conceptual backgrounds and thus inform about other aspects of network activities. Table 1 provides an overview of these categories pointing out several important differences.

USAGE OF THE TERM SYNCHRONIZATION					
	Stability of phase relationship	**Lag sensitive**	**Amplitude matters**	**Basis of calculation**	**Conceptual background**
ERD / ERS	no	no	yes	single electrode	activation / deactivaton of "networks"
PLI / ITPC / Coherence	yes	only variance of lag	no	pair of electrodes / processes (problematic to separate)	timely ordered interaction of regions, potentially sequential, causal
GFS	yes	yes (zero-lag)	no	global (across electrodes)	simultaneity of activation / non causal integration / "binding" / common excitability

Table 1: Overview of different synchronization measures. ERD = Event related desynchronization, ERS = Event related synchronization; PLI = Phase locking index; ITPC = Inter-trial phase coherence; GFS = Global field synchronization

The historically oldest concepts are the event related synchronization (ERS) and event related desynchronization (ERD), which reflect an increase or decrease, respectively, of signal amplitude in a given frequency. Examples for this type of synchronization are the well-known alpha ERD in occipital areas in response to visual stimulation or the mu rhythm suppression contralateral to somatomotor stimulation (Pfurtscheller and Lopes da Silva 1999). Typically, the phase locking index (PLI), inter-trial phase coherence (ITPC) and other coherence measures investigate whether the phase difference between two signals *x* and *y* of a dominant oscillatory or frequency signal, independent of signal amplitude, is constant over a limited time (usually around hundreds of milliseconds; Varela, Lachaux et al. 2001). On the one hand, those indices do not consider the magnitude of the phase angle difference, and consider only if it is stable across electrodes (PLI) or trials (ITPC). On the other hand, they may inform about causality if it is possible to argue which part of a signal pair leads (cause) and which part follows (effect). The last category, GFS, is non-causal, but indicates simultaneity of activation as it considers no lag between phases, and is also called common-phase synchronization.

Common-phase synchronization was proposed as a main candidate mechanism to integrate spatially distributed brain areas into transiently stable networks (Singer 1999, Singer 2001, Varela, Lachaux et al. 2001). The so-called *binding problem* – how single features of an object are bound together into a unitary percept – was first addressed in studies of visual perception. Most investigations in visual binding confirmed the relevance of gamma band synchronization both in animal (e.g. Gray, Konig et al. 1989, Gray and Singer 1989) and human studies (e.g. Tallon-Baudry, Bertrand et al. 1997, Rodriguez, George et al. 1999, Lachaux, George et al. 2005, Uhlhaas, Roux et al. 2009, Kottlow, Jann et al. 2012), albeit applying different synchronization measures. According to the review of Uhlhaas and Singer (2006), beta and gamma band synchronization of neuronal oscillations facilitate many different cognitive functions such as perceptual awareness and grouping, attention-dependent stimulus selection, routing of signals across distributed cortical networks, sensory-motor integration and working memory (Uhlhaas and Singer 2006). The relevance of binding processes for efficient cognitive processes is demonstrated by psychiatric and neurological disorders exhibiting binding deficits, such as the Balint's syndrome,

Parkinson's disease, schizophrenia, autism, epilepsy, or Alzheimer's disease (Uhlhaas and Singer 2006, Burwick 2014).

For the purposes of this thesis, we were interested in instantaneous synchronization to measure functional connectivity, and therefore used the GFS measure, introduced by Koenig et al, indicating the degree of zero-lag synchronization across all electrodes with a single value ranging from 0 (no synchronization) to 1 (total synchronization; Koenig, Lehmann et al. 2001). Given that by definition functional networks inherently consist of several distributed active sources, EEG cannot describe their anatomical substrates unambiguously due to the *additivity* of active sources (Chapter 1.2.1). However, fMRI, as presented in the following chapter, provides detailed spatial information (in the range of a few millimeters) of functional networks.

1.2.2 Functional Magnetic Resonance Imaging (fMRI)

Regional brain activation changes are measured in fMRI by means of the blood oxygenation level-dependent (BOLD) signal (Ogawa, Lee et al. 1990). The underlying principle is that neural activation leads to increased energy consumption and therefore more arterial blood flows into the specific area. As deoxygenated blood has a different magnetic moment as oxygenated (paramagnetic versus magnetic), the relative preponderance of one over the other leads to different signal properties measured using MRI. Consequently, the BOLD signal reflects a mixture of the cerebral blood flow (CBF), cerebral blood volume (CBV) and the oxygen consumption rate (CMRO2), which are all mutually dependent (Obata, Liu et al. 2004). As opposed to EEG, the BOLD signal used in fMRI studies thus reflects an indirect measure of neuronal activity. Furthermore, the BOLD signal has a low temporal resolution due to the hemodynamic response function: It displays a sometimes reported initial dip, followed by a positive peak within 4 – 6 seconds after stimulus onset and dropping again, revealing an undershoot possibly lasting around 30 seconds (Buxton, Uludag et al. 2004). Usually, measures of correlation, coherence, and higher-order relations are used to identify network activations in fMRI data, as the underlying assumption is that the units of a functional network are activated simultaneously. Several analysis techniques exist to extract networks and they can be categorized into data-driven or hypothesis-driven approaches. To the former category belongs the widely used independent component analysis (ICA), whereas seed-based or region of interest (ROI) analyses are hypothesis-driven approaches. Modeling approaches as dynamic causal modeling (DCM),

psychophysiological interactions (PPIs), or structural equation modeling (SEM) mainly belong to effective connectivity analysis, but as there are several implementation techniques clear classifications in terms of functional or effective connectivity are not possible. In general, it is important to note that functional in contrast to effective connectivity is a descriptive analysis without any information about direction of information flow.

1.2.2.1 Resting state networks (RSNs)

Scarce attention was directed to intrinsic resting activity of the brain applying fMRI and positron emission tomography (PET), until Biswal et al (1995) reported coherent slow frequency fluctuations (< 1Hz) of regions forming the somatomotor network usually seen during active finger tapping, while subjects were resting (Biswal, Yetkin et al. 1995). Thereupon, many studies extended this finding to other functional systems such as the visual, auditory, language, episodic memory, the dorsal attention and central executive system among others (Lowe, Mock et al. 1998, Cordes, Haughton et al. 2000, Beckmann and Smith 2004, Hampson, Olson et al. 2004, Damoiseaux, Rombouts et al. 2006, De Luca, Beckmann et al. 2006, Fox, Corbetta et al. 2006, Hunter, Eickhoff et al. 2006, Nir, Hasson et al. 2006, Fox and Raichle 2007, Seeley, Menon et al. 2007). Another line of PET studies indicated decreased blood flow in widespread regions even when contrasting task conditions against a passive control state such as lying quietly with eyes closed (EC) or passively viewing a stimulus. Shulman et al (1997) aimed to determine some consistency across those experiments. They concluded that those decreases in blood flow were largely task independent and varied little in their location across a variety of different tasks (Shulman, Fiez et al. 1997). Based on that finding, the paper entitled "*A default mode of brain function*" claimed that the brain might be in an organized mode of brain functions at baseline including areas whose activities are shut down during attention-demanding, goal-directed activities (Raichle, MacLeod et al. 2001). Those areas mainly include the medial prefrontal cortex (mPFC), the precuneus (PrC), the anterior and posterior cingulate cortex (ACC, PCC), as well as the inferior parietal lobule (IPL) and were later known as the default mode network (DMN; see Figure 1). The DMN is assumed to maintain self-referential processing, including the retrieval and manipulation of episodic and semantic memories (Greicius, Krasnow et al. 2003). As reviewed by Broyd et al (2009), the DMN was shown to persist during altered states of consciousness such as early stages of sleep, as well as under conscious

sedation, and it is attenuated but not completely shut down during task situations (Broyd, Demanuele et al. 2009). Disruptions within the DMN in different neurologic and psychiatric disorders such as Alzheimer's disease, autism, depression, ADHD, chronic pain, and schizophrenia have been reported, suggesting a need to further understand the functional significance of the DMN (Greicius and Menon 2004, Kennedy, Redcay et al. 2006, Bluhm, Miller et al. 2007, Buckner, Andrews-Hanna et al. 2008, Greicius 2008).

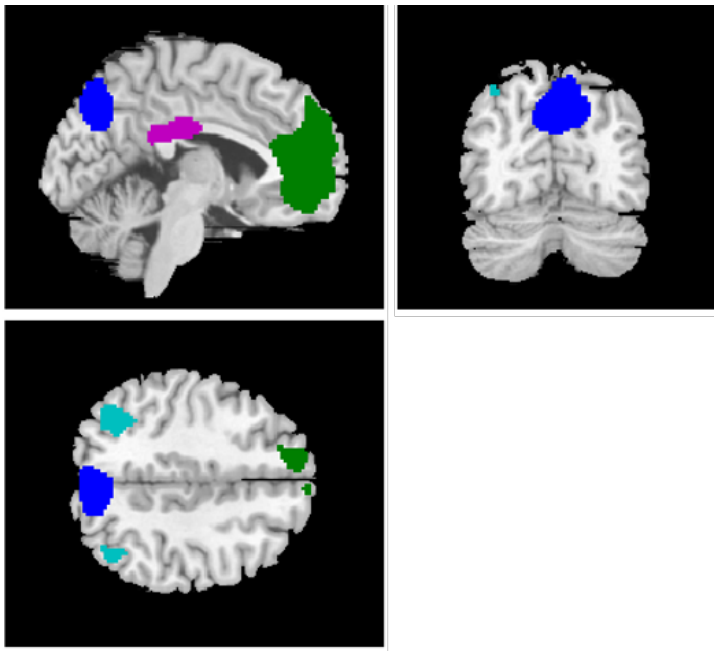

Figure 1: Often reported DMN hub regions. Dark green: mPFC = medial prefrontal cortex; light blue: IPL = inferior parietal lobule; dark blue: PrC = Precuneus; violet: PCC = posterior cingulate cortex. Templates used from the FIND Lab at Stanford University of the group headed by Michael Grecius. The toolbox XjView, a viewing program for SPM based on Matlab, was used for visualization (http://www.alivelearn.net/xjview8/)

While the DMN has probably received the most attention, it is part of roughly a dozen so-called resting state networks (RSNs) that have been identified. The terminology of RSNs refers to the resting state, however, those networks are also found during task situations. This fact led to alternative terms such as temporally coherent networks (TCNs; Calhoun, Kiehl et al. 2008) that describe both resting- as well as task-related functional networks (from now on, the term TCN will be used in this thesis).

Due to the methodological complementarity of EEG and fMRI outlined earlier (Chapters 1.2.1, 1.2.2), different features of TCNs are revealed by each method and while one technique can point out a connection between two brain regions, the other one might be "blind" to that relationship and vice versa (Figure 2 gives an overview of

all possible combinations of how EEG and fMRI capture connectivity between two fictive sources). Hence, there is a lack of knowledge how they are related to each other. To investigate their relationship, multimodal neuroimaging approaches are required.

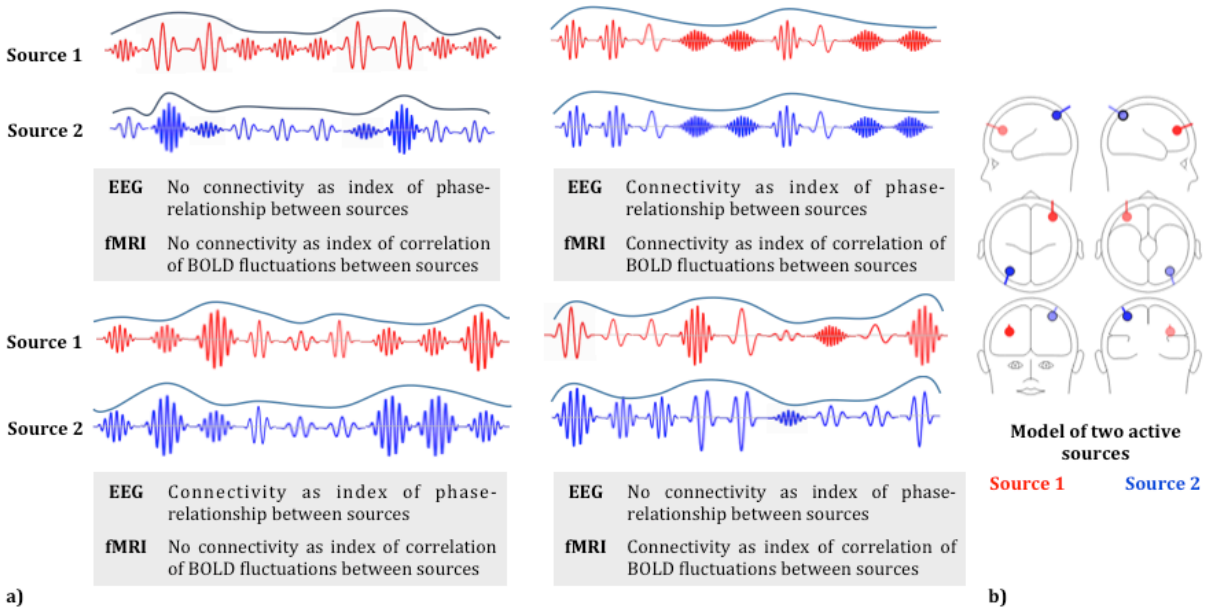

Figure 2: a) Possibilities of connectivity measured by means of EEG phase-synchronization and fMRI BOLD analyses between b) two fictive sources in the brain. Source models were created using BESA Simulator (http://www.besa.de/downloads/tools/dipole-simulator/)

1.2.3 Multimodal neuroimaging

According to Biessmann et al (Biessmann, Plis et al. 2011), some of the main advantages of multimodal imaging are summarized as follows: First, conjoint effects using complementary information gathered from multiple data sources can be revealed. Second, the understanding of neural activity measured by one single modality can be improved by multimodal methods. Finally, by means of multimodal imaging, the knowledge about pathophysiological processes in neurologic and psychiatric conditions, neurovascular and neurodegenerative diseases can be deepened and potentially used for diagnostic purposes. The simultaneous use of EEG and fMRI is one of the most common combinations enabling high spatiotemporal resolution. Using this combination of techniques, it was possible to assess the relationship between neural and hemodynamic activity, the so-called *neurovascular coupling*. Experimental studies showed that the hemodynamic response is highly correlated with LFPs, suggesting that the BOLD signal reflects input synaptic activity and local processing in a given area rather than the output spiking activity (Lauritzen 2001, Logothetis, Pauls et al. 2001, Logothetis 2002, Lauritzen and Gold 2003, Buxton, Uludag et al. 2004). Despite those

insights, the exact nature of the neurovascular coupling remains unclear (Logothetis 2008) and further investigations are still necessary in multimodal imaging.

1.2.3.1 Combined EEG-fMRI

Initially, the development of EEG-fMRI acquisition was driven by a clinical interest in relating epileptic discharges measured via surface EEG with the fMRI-BOLD signal to detect origins of the spikes with a high spatiotemporal resolution (Rosenkranz and Lemieux 2010). Since the first reported EEG-fMRI study dating back to 1993 (Ives, Warach et al. 1993), this approach has been widely applied in basic as well as clinical research (Jann, Wiest et al. 2008, Scheidegger, Wiest et al. 2013, Wiest, Estermann et al. 2013).

Most studies interested to find the hemodynamic counterparts of EEG activity (EEG-informed fMRI analyses) used amplitude (Feige, Scheffler et al. 2005, de Munck, Goncalves et al. 2007), or power (Goldman, Stern et al. 2002, Laufs, Kleinschmidt et al. 2003, Laufs, Krakow et al. 2003, Moosmann, Ritter et al. 2003) in the alpha frequency range. Consistently, negative correlations between alpha band and activity in fronto-parietal and occipital areas, and some positive associations between the thalamus (thought as generator of alpha oscillations, e.g. da Silva, van Lierop et al. 1973) and the insula were reported (e.g. Goldman, Stern et al. 2002, de Munck, Goncalves et al. 2007, Tyvaert, Levan et al. 2008). Studies including additional frequency bands found mainly alpha and beta band to be positively linked to the DMN (Laufs, Kleinschmidt et al. 2003, Mantini, Perrucci et al. 2007, Jann, Dierks et al. 2009, Jann, Kottlow et al. 2010), and negatively to the dAN (Laufs, Krakow et al. 2003, Mantini, Perrucci et al. 2007). Furthermore, reports about inverse relations of the DMN with frontal-midline (FM) theta band during rest (Scheeringa, Bastiaansen et al. 2008, Jann, Kottlow et al. 2010) and working memory (WM) tasks (Meltzer, Negishi et al. 2007, Michels, Bucher et al. 2010, Kottlow, Schlaepfer et al. 2015) were reported. Jann et al (2010) were the first who related fluctuations of EEG spectral power at each electrode to fluctuations of ten TCNs and found typical topographic EEG signatures for each TCN. As a general observation, they reported a dissociation between lower sensory and higher cognitive TCNs: On the one side, mainly positive relations of higher cognitive TCNs including self-referential processing (DMN), attention (frontoparietal control network, frontal attention network) and WM (left and right WMN) to alpha and beta band were found. On the other side, TCNs maintaining sensory processing including visual, auditory and

somatomotor processing were characterized by lower delta and theta band power increases (Jann, Kottlow et al. 2010).

Regarding measures of EEG synchronization, two studies performed voxelwise correlations of GFS values with fMRI-BOLD fluctuations. Kottlow et al (2012) found increased GFS gamma band during moments of perceiving a schematic face (as opposed to moments where pieces of the face where randomly moving). Those increments were related to the bilateral middle fusiform gyrus and left PrC (regions relevant for face perception and visual processing in general; Kottlow, Jann et al. 2012). Another study relating GFS alpha band to BOLD fluctuations found overlapping areas of lower GFS alpha (8.5 – 10.5Hz) with the dAN, whereas upper alpha (10.5 – 12.5Hz) coincided with the DMN (Jann, Dierks et al. 2009).

In schizophrenia, six studies have so far simultaneously acquired EEG-fMRI, five of which did so during tasks and only one during rest. During resting state, Razavi et al (2013) found the DMN and left WMN to be coupled with lower frequencies in patients with schizophrenia than in healthy controls (Razavi, Jann et al. 2013). Regarding task-related studies, one explored auditory evoked gamma band response (aeGBR) in subjects at high risk for psychosis and found reduction of the aeGBR related network compared to controls (Leicht, Vauth et al. 2016). Another study investigated sensory gating using a somatosensory P50 suppression paradigm and found that of all of the structures involved in the P50 suppression, only the hippocampus and thalamus showed altered sensory processing in schizophrenia patients (Bak, Rostrup et al. 2014). Foucher et al (2011) investigated if hypoactive regions observed in a WM task were sensitive to arousal as indicated by EEG low frequencies in patients. The results indicated that first, most of the regions that were hypoactive during the WM task in patients were part of regions modulated by arousal. Second, this modulation was reduced in patients compared to controls. However, other task-related and arousal sensitive regions did not show to be hypoactive in patients and patients did not show a general arousal deficit (Foucher, Luck et al. 2011). Two papers used an oddball task as an experimental manipulation. The first explored differences in neuronal correlates of the N200 elicited by deviant stimuli using an EEG-informed fMRI analysis. They reported about patients displaying differences in amplitude and temporal evolution pattern of the N200 response (Calhoun, Wu et al. 2010). The other group investigated the effect of nicotine on the P300 and its BOLD correlates and found an increase in BOLD activation related to the P300 induced by nicotine, but no group difference

between healthy controls and schizophrenia patients (Mobascher, Warbrick et al. 2012).

1.3 Schizophrenia as disconnection syndrome

With the conceptual emergence of functional connectivity in neuroscience (e.g. Friston, Frith et al. 1993), the idea of altered large-scale networks was introduced to psychiatry. Schizophrenia was referred to as a "*disconnection syndrome*" causing failures of functional integration observed both on the physiological, anatomical level of the brain as well as regarding sensorimotor and cognitive functioning (Friston and Frith 1995, Friston 1996, Friston 1998, Friston 1999, Friston 2002). A long list of studies both in functional and structural network connectivity proved evidence for this hypothesis (for reviews see Stephan, Friston et al. 2009, Pettersson-Yeo, Allen et al. 2011). Among functional connectivity studies, activation strength, spatial and temporal characteristics of TCNs during resting state (Liang, Zhou et al. 2006, Bluhm, Miller et al. 2007, Zhou, Liang et al. 2007, Jafri, Pearlson et al. 2008, Camchong, MacDonald et al. 2011, Littow, Huossa et al. 2015) as well as during different tasks (Garrity, Pearlson et al. 2007, Pomarol-Clotet, Salvador et al. 2008, Metzak, Riley et al. 2012, Brandt, Eichele et al. 2014) were found to be affected by schizophrenia. Additionally, alterations of DMN connectivity were found to correlate with symptom severity (Bluhm, Miller et al. 2007, Garrity, Pearlson et al. 2007, Camchong, MacDonald et al. 2011).

From the perspective of EEG synchronization linking single neuronal units into functional networks, findings of changed phase synchronization might reflect dysfunctional network coupling in patients. The review of Uhlhaas and Singer (2010) reported on reductions of evoked and induced beta and gamma band phase locking across electrodes and trials in a variety of sensory and higher cognitive tasks in patients with schizophrenia (Uhlhaas and Singer 2010). Among others, reduced gamma band amplitude and phase locking in visual processing (Spencer, Nestor et al. 2004), and reduced beta and gamma band phase locking in auditory processing (Hirano, Hirano et al. 2008, Mulert, Kirsch et al. 2011) were reported in schizophrenia. Furthermore, two studies using the GFS measure were performed in resting state data: The first found reduced GFS theta band in medication naïve, first episode patients during rest (Koenig, Lehmann et al. 2001). The second study investigated GFS values before and after medical treatment. They reported on a normalization of reduced GFS theta band in responders upon treatment, concluding that GFS theta rather reflects a

state-related phenomenon. On the other hand, increased GFS gamma band remained stable upon treatment and thus may refer to a trait like phenomenon (Kikuchi, Koenig et al. 2007).

To sum up, there is evidence that patients with schizophrenia suffer from altered connectivity within and between fMRI-BOLD TCNs, also visible in measures of EEG phase synchronization, during rest and task situations. The statement of Fox et al (2006) that "*the brain's intrinsic spontaneous activity may provide the context in which perception and behavior occur, shaping the manner in which we respond to external events*" reflects that rest and task-related brain activity are interdependent and is addressed in the theory of state dependent information processing (Fox, Snyder et al. 2006). I will thus elaborate on that paradigm shift in the following chapter.

1.4 State dependent information processing

In 1988, Llinas proposed that intrinsic neuronal activation of the mammalian brain forms a functionally coordinated system to which sensory input is brought into context. He also proposed that certain neurologic and psychiatric disorders might be related to alterations in this system (Llinas 1988). The theory of state dependent information processing (in short: state dependency) represents an important shift in the focus of research, namely from research on isolated stimulus-related activation (against an assumingly unrelated "noise" of background activity) to the linking of resting or prestimulus state to stimulus-evoked activity of the system.

Within the context of state dependency, inter-trial variability in healthy subjects can be explained. Studies in healthy subjects found the level of prestimulus occipital alpha power (as index of cortical excitability) accounted for the detection probability of visual stimuli presented at the detection threshold (for a review about visual processing see Britz and Michel 2011). Findings in other domains confirmed that variability of brain activity at rest or prestimulus predicts task-related responses and behavior: Such examples are found for somatosensory processing (Linkenkaer-Hansen, Nikulin et al. 2004, Fox, Snyder et al. 2006, Rossiter, Worthen et al. 2013), memory processing (Wagner, Schacter et al. 1998, Otten, Quayle et al. 2006, Sala-Llonch, Pena-Gomez et al. 2012, Haque, Wittig et al. 2015), and decision making (Pessoa and Padmala 2005). Regarding TCNs, there is a parametric modulation of the DMN depending on the amount of task difficulty (McKiernan, Kaufman et al. 2003, McKiernan, D'Angelo et al. 2006, Singh and Fawcett 2008, Vatansever, Menon et al.

2015). Reduced task-related DMN deactivation supposedly causing lapses of attention proved to be behaviorally relevant as an index of longer and more variable reaction times (Drummond, Bischoff-Grethe et al. 2005, Weissman, Roberts et al. 2006) and impaired task performance (Daselaar, Prince et al. 2004, Weissman, Roberts et al. 2006, Li, Yan et al. 2007, Eichele, Debener et al. 2008, Anticevic, Repovs et al. 2010, Soravia, Witmer et al. 2016). TCNs overlap with specific neuroanatomical systems (Damoiseaux, Rombouts et al. 2006) related to specific cognitive functions. As they co-exist, systems maintaining opposing functions should be inversely related to one another. Indeed, anti-correlations between the DMN and task-positive networks, such as the dAN (Corbetta and Shulman 2002) recruited when attention is externally oriented, were detected (McKiernan, Kaufman et al. 2003, Fox, Snyder et al. 2005, Fransson 2005, Kim 2015) and the strength of this anti-correlation was shown to be behaviorally relevant too (Kelly, Uddin et al. 2008). Some EEG-fMRI studies investigated the electrophysiological fingerprints of the DMN and revealed an inverse correlation between the DMN and frontal-midline (FM) EEG theta power during resting state (Scheeringa, Bastiaansen et al. 2008), but also the retention period of a verbal WM task (Michels, Bucher et al. 2010).

The relationship between intrinsic brain activity and task-related response or behavior is bidirectional; momentary thoughts, feelings, and action patterns can influence activation patterns in neural circuitry (Seeley, Menon et al. 2007). In that sense, altered task-related brain responses in psychiatric patients can be explained by changes in spontaneous neuronal activity. Regarding TCNs, disruptions of the balance between DMN and task demand were found in patients with schizophrenia (Pomarol-Clotet, Salvador et al. 2008, Kim, Manoach et al. 2009, Whitfield-Gabrieli, Thermenos et al. 2009), youth at high-risk for psychosis and early psychosis (Fryer, Woods et al. 2013) as well as in unaffected siblings of patients (de Leeuw, Kahn et al. 2013). As this relationship was shown to be behaviorally meaningful, it was discussed as a potential marker for efficient cognitive processing (Kelly, Uddin et al. 2008, De Pisapia, Turatto et al. 2012). On the grounds that schizophrenia patients display a variety of alterations in TCNs at rest as well as during tasks, such task-related differences could be at least partly explained by changes in TCNs at rest or prestimulus states within the context of state dependency. According to this reasoning, the objectives of the current project will be outlined in the next chapter.

1.5 Objectives

There were 3 objectives for this work: First, schizophrenia can be characterized by disruptions of large-scale neuronal networks observed both during rest and task conditions. Thus, multimodal neuroimaging such as combined EEG-fMRI can unravel complementary aspects of those networks, a methodology scarcely used in this field so far. Second, instantaneous resting brain activity can reveal significant changes of the brain's functional state that may predict, and thus potentially cause task-related alterations and thereby describe biological mechanisms of psychiatric disorders. And third, the interaction of prestimulus and task-related changes has to be assessed due to their interdependence as pointed out in the theory of state dependency. Consequently, by investigating functional networks in schizophrenia using combined EEG-fMRI and considering the resting, and pre-to-post stimulus states we intended to provide further insights into deficits of functional integration of networks in this severe mental illness.

On this account, we performed three studies. The first study included healthy subjects to establish a frame of reference for the second study. There, we looked at prestimulus and task-related network activations using a verbal WM task. In the third study, the focus was on resting state data and we used the GFS measure to reveal neuronal correlates underlying this network integration mechanism. The particular objectives and hypotheses of these three studies are outlined below.

Study 1: Using an fMRI-informed EEG analysis, this study investigated within the framework of state dependency the relationship of four TCNs (the DMN, dAN, left and right WMNs) at prestimulus with three EEG frequency bands power (theta, alpha, and beta band) during the retention period of a verbal WM task. Based on previous EEG-fMRI studies using WM paradigms, we expected to find reliable electrophysiological signatures of TCNs, even in a timely shifted manner. The same paradigm was used as in the study of Michels et al (2010) who looked at similar associations, but extracted markers of the EEG and fMRI both during the retention period of the WM task (Michels, Bucher et al. 2010). My contribution as co-author of that paper was the collection of a part of the data (N = 12 of 24 total) as well as the preprocessing. Furthermore, I wrote part of the methodology, helped in the discussion of the results and revised the manuscript.

Study 2: As this study represented an extension of study 1, we used identical methodology and analyses but comparing healthy controls to schizophrenia patients. We pursued two goals: First, to replicate results in healthy control subjects. Second,

and more importantly, we wanted to discover possible abnormalities in these associations in schizophrenia patients. As both deviations during resting state in spectral EEG as well as alterations in fMRI-BOLD TCN dynamics are well established in schizophrenia (see Chapters 1.2.1, 1.3), we expected their relationship, even at pre-to-post stimulus, to differ from controls. Our hypothesis was that a dysfunctional activation of WM functions in schizophrenia might follow from abnormalities in prestimulus resting-state activity. More specifically, we hypothesized the previously reported and WM relevant inverse association between the DMN and FM theta band to be reduced in patients.

Study 3: In this study, we performed an EEG-informed fMRI analysis to link EEG common-phase synchronization with fMRI-BOLD correlates in schizophrenia patients and healthy controls during EO resting state. We used the GFS measure for five frequency bands (delta, theta, alpha1, alpha2, and beta band) as a parametric modulator in the fMRI analysis. As schizophrenia is known to show disruptions in functional networks, we hypothesized that schizophrenia patients would demonstrate integration abnormalities in functional networks as represented by GFS.

2. EMPIRICAL CONTRIBUTION

2.1 Paper 1: Pre-stimulus BOLD-network activation modulates EEG spectral activity during working memory retention

Kottlow M, Schlaepfer A, **Baenninger A**, Michels L, Brandeis D, Koenig T

Front. Behav.Neurosci.9:111.

doi: 10.3389/fnbeh.2015.00111

frontiers in Behavioral Neuroscience

ORIGINAL RESEARCH
published: 06 May 2015
doi: 10.3389/fnbeh.2015.00111

Pre-stimulus BOLD-network activation modulates EEG spectral activity during working memory retention

Mara Kottlow[1,2,3], *Anthony Schlaepfer*[4], *Anja Baenninger*[1,3], *Lars Michels*[5], *Daniel Brandeis*[4,6,7,8] *and Thomas Koenig*[1,3]*

[1] Translational Research Center, University Hospital of Psychiatry and Psychotherapy, University Bern Psychiatric Services (UPS), Bern, Switzerland, [2] Chronobiology and Sleep Research, Institute of Pharmacology and Toxicology, University of Zurich, Zurich, Switzerland, [3] Center for Cognition, Learning and Memory, University of Bern, Bern, Switzerland, [4] Department of Child and Adolescent Psychiatry, University of Zurich, Zurich, Switzerland, [5] Institute of Neuroradiology, University Hospital Zurich, Zurich, Switzerland, [6] Department of Child and Adolescent Psychiatry and Psychotherapy, Medical Faculty, Central Institute of Mental Health, Mannheim/Heidelberg University, Mannheim, Germany, [7] Zurich Center for Integrative Human Physiology, University of Zurich, Zurich, Switzerland, [8] Neuroscience Center Zurich, University and ETH Zurich, Zurich, Switzerland

OPEN ACCESS

Edited by:
Denise Manahan-Vaughan, Ruhr University Bochum, Germany

Reviewed by:
Marian Tsanov, Ruhr University Bochum, Germany
Giulio Pergola, Università degli Studi di Bari Aldo Moro, Italy

***Correspondence:**
Thomas Koenig, Translational Research Center, University Hospital of Psychiatry and Psychotherapy, University Bern Psychiatric Services (UPS), Bolligenstrasse 111, 3000 Bern 60, Switzerland
thomas.koenig@puk.unibe.ch

Received: *14 January 2015*
Accepted: *15 April 2015*
Published: *06 May 2015*

Citation:
Kottlow M, Schlaepfer A, Baenninger A, Michels L, Brandeis D and Koenig T (2015) Pre-stimulus BOLD-network activation modulates EEG spectral activity during working memory retention. Front. Behav. Neurosci. 9:111. doi: 10.3389/fnbeh.2015.00111

Working memory (WM) processes depend on our momentary mental state and therefore exhibit considerable fluctuations. Here, we investigate the interplay of task-preparatory and task-related brain activity as represented by pre-stimulus BOLD-fluctuations and spectral EEG from the retention periods of a visual WM task. Visual WM is used to maintain sensory information in the brain enabling the performance of cognitive operations and is associated with mental health. We tested 22 subjects simultaneously with EEG and fMRI while performing a visuo-verbal Sternberg task with two different loads, allowing for the temporal separation of preparation, encoding, retention and retrieval periods. Four temporally coherent networks (TCNs)—the default mode network (DMN), the dorsal attention, the right and the left WM network—were extracted from the continuous BOLD data by means of a group ICA. Subsequently, the modulatory effect of these networks' pre-stimulus activation upon retention-related EEG activity in the theta, alpha, and beta frequencies was analyzed. The obtained results are informative in the context of state-dependent information processing. We were able to replicate two well-known load-dependent effects: the frontal-midline theta increase during the task and the decrease of pre-stimulus DMN activity. As our main finding, these two measures seem to depend on each other as the significant negative correlations at frontal-midline channels suggested. Thus, suppressed pre-stimulus DMN levels facilitated later task related frontal midline theta increases. In general, based on previous findings that neuronal coupling in different frequency bands may underlie distinct functions in WM retention, our results suggest that processes reflected by spectral oscillations during retention seem not only to be "online" synchronized with activity in different attention-related networks but are also modulated by activity in these networks during preparation intervals.

Keywords: state dependency, covariance mapping, working memory, BOLD-ICA, frontal-midline theta, temporally coherent brain networks, pre-stimulus state

Introduction

Resting state brain activity undergoes spontaneous fluctuations, and so does brain activity in response to environmental information. The paradigm of state dependent information processing aims at understanding our experiences and actions not only as a function of a perceived input but as an interaction of an input with the momentary state of the organism in general, and the brain in particular. Thus, dysfunctional responses may be understood as consequences of demand-inadequate pre-states at the moment of perception. Based on that, treatment strategies targeting those pre-states may be developed to enhance functionality.

A particularly important component of brain functionality is working memory (WM). It is a central requirement for many cognitive processes and an indicator of mental health (Klimesch et al., 2010; Van Snellenberg et al., 2015). In addition, the activation of WM related brain functions have well-known physiological EEG signatures that make it possible to quantify their recruitment as a function of pre-stimulus state. The present study aimed at understanding the EEG signatures of the recruitment of working-memory specific and other neuronal resources during a WM task as a function of the brain state preceding stimulus presentation. Thereby, this pre-state was defined by the level of activation of well-known brain networks, measured with the BOLD signal.

Numerous EEG studies on WM have used the Sternberg task (for example Jensen and Tesche, 2002; Leiberg et al., 2006; Michels et al., 2008, 2010, 2012; Maurer et al., 2015), since this task can systematically be configured for different memory loads and is moreover able to temporally separate WM into encoding, retention (maintenance) and recall phases of the WM process. These studies found load-dependent increases of spectral amplitude over broad frequency ranges. In the theta range, increases were mostly observed over medial frontal electrodes with a local maximum at the channel Afz and have been localized to the medial prefrontal cortex and the anterior cingulate cortex, regions forming part of a working memory network (WMN) (Onton et al., 2005; Meltzer et al., 2007; Michels et al., 2008, 2010, 2012; Huang et al., 2013). This frontal-midline theta effects represent sustained increases in theta power during stimulus, retention and probe phases of WM tasks and as such facilitate the maintenance of information in WM through central executive functions (Huang et al., 2013).

Further retention and load effects, however of a more phasic nature (Huang et al., 2013), have been observed in the EEG alpha range primarily over central-posterior sites (Michels et al., 2010) and over right posterior areas (Scheeringa et al., 2009). The local maxima were seen at channel Pz (Michels et al., 2008) and O2, respectively (Michels et al., 2010), and were localized to the right middle occipital gyrus with sLORETA (Michels et al., 2010). The alpha retention effect has been associated with increased demands on storage and inhibition of irrelevant stimuli (Obleser et al., 2012). The alpha load effect correlated in some studies with WM performance (Manza et al., 2014).

Also in the beta range increases with retention and to a smaller degree with load have been observed over occipital sites in a visual verbal Sternberg task (Michels et al., 2010). Thereby, beta WM load-effects seem to represent modality-dependent task relevant stimulus features, as shown by Leiberg et al. (2006) in an auditory WM Sternberg task.

Therefore, with the EEG data of our current study, we sought to replicate these existing findings on EEG load-effects during retention.

For BOLD-data, the literature reports several temporally coherent networks (TCNs; Calhoun et al., 2008) to be associated with processes related to WM (Raichle et al., 2001; Greicius et al., 2003; Dima et al., 2014; Kim, 2015). These networks consist of the task negative default mode network (DMN), and task-positive networks, among others the dorsal attention network (dAN), and the left and the right WM network. Increased connectivity between two nodes of the DMN, the posterior cingulate cortex and the medial prefrontal cortex, has been found to correlate with better WM performance (Hampson et al., 2006). The DMN also showed a load-dependent effect in earlier studies, reflected by a suppression of DMN activity during the preparation for high-load compared with low-load trials (Esposito et al., 2006). The dAN includes the frontal eye field, the superior parietal lobule, the inferior frontal junction, the medial inferior parietal sulcus, the medial dorsal superior frontal gyrus and others (Kim, 2015; Zhang et al., 2015). In contrast to the DMN activating to internally allocated attention, the dAN activates during externally allocated attention. WM processes have been associated with DMN and dAN activity in terms of a double dissociation: while DMN activity is suppressed during task preparation and execution but increases after the task, the opposite holds true for the dAN (Kim, 2015). However, no load-effects associated with the dAN are reported. Further, WM tasks were consistently found to engage a distributed network of areas together forming a WMN. This network contains regions as the dorsolateral prefrontal cortex, the anterior cingulate cortex, a posterior portion of the inferior parietal lobule (Dima et al., 2014; Koshino et al., 2014) and according to some studies the pre-supplementary motor area (Van Snellenberg et al., 2015). The WMN can be further divided into a right and a left lateralized prefronto-parietal network, the lWMN, and the rWMN (Jann et al., 2010; Visintin et al., 2015). The lWMN was found to be activated already in task preparation, whereas both WMNs are active during the execution of WM tasks (Visintin et al., 2015). Right-hemispheric dominance has been associated with verbal WM load (Dima et al., 2014).

When analyzed simultaneously, combined EEG-fMRI studies have shown a link between the TCNs and EEG spectral activity for resting state (Jann et al., 2010) as well as for task conditions (Scheeringa et al., 2009; Michels et al., 2010). During rest as well as during task, the correlations of BOLD and theta power resulted in negative values in areas of the DMN (Meltzer et al., 2007; Scheeringa et al., 2008, 2009; Jann et al., 2010; Michels et al., 2010, 2012). Between load-dependent posterior alpha increases and BOLD, negative correlations during WM retention were found

Abbreviations: CBA, cardio ballistic artifact; dAN, dorsal attention network; DMN, default mode network; ICA, independent component analysis; lWMN, left WMN; RT, reaction time; rWMN, right WMN; TCT, Topographic consistency tests; TCNs, temporally coherent networks; WM, working memory; WMN, working memory network; 3T, 3 Tesla.

in the parietal-occipital midline (Meltzer et al., 2007) as well as in the primary visual cortex and the middle temporal gyrus (Tuladhar et al., 2007). Resting state beta power showed only positive correlations with BOLD responses during resting state in simultaneous EEG/fMRI studies (Michels et al., 2010), primarily in the middle PFC and other regions of the DMN (Laufs et al., 2003).

None of these studies has investigated the effect of pre-stimulus TCN activation upon EEG signatures of WM specific recruitment of brain resources during retention. Thus, in this study we followed a mainly exploratory approach. Nevertheless, one hypothesis can be derived from the literature: Based on studies showing increased pre-stimulus DMN activity leading to deteriorated task performance (Esposito et al., 2006; Li et al., 2007), and the findings on load-dependent increases in theta-power during WM tasks (Onton et al., 2005; Meltzer et al., 2007; Michels et al., 2008, 2010, 2012; Huang et al., 2013), we expected load-dependent decreases in pre-stimulus DMN activity to be predictive of load-dependent EEG theta power increases during the task.

Material and Methods

Subjects

Data from a total of 24 subjects measured with simultaneous EEG/fMRI during a visual Sternberg task in two different scanners were taken for the BOLD- independent component analysis (ICA) and EEG analyses. Subjects were recruited via university message boards and had normal or corrected-to-normal vision, met the standard fMRI inclusion criteria and gave their written informed consent for participation in the study. None of the subjects suffered from neurological or psychiatric disorders or used psychoactive medication or drugs. The subjects refrained from caffeine and nicotine for four minimum 2 h before the measurement. The study was approved by the local ethics committee of Bern and Zurich, respectively. For the covariance mapping, two subjects had to be excluded because of residual scan artifacts in the EEG data, resulting in 22 subjects for the covariance mapping analysis (age 27.68 years, SD 7.24; 12 f). Of these subjects, 10 had been tested in a Siemens scanner at the Inselspital Bern, 12 in a Philips scanner at the Psychiatric University Clinic Zurich by using the same measurement parameters (see Sections MRI and EEG Data).

Task

We used a modified Sternberg visual WM task adapted from Michels et al. (2010) allowing for the temporal separation of preparation, encoding, retention and retrieval periods (Sternberg, 1966). Similar versions have been used by Jensen and Tesche (2002), Michels et al. (2008, 2012) and Maurer et al. (2015). During the task, 64 trials (32 per condition) were presented, each consisting of the sequential presentation of a visual stimulus (duration 2.5 s), a retention period (duration 3.5 s), a visual probe (duration 2.0 s), and a fixation cross (random duration between 1.8 and 2.5 s).

The trials were presented in four large blocks each composed of two high- and two low-load sub-blocks. Each sub-block contained four trials of the same load. Before and after each of the four large blocks, a longer baseline condition of 24.5 s consisting of a fixation cross was presented.

For the stimulus, either two (low load) or five (high load) consonants were presented in an array of 3 × 3 items with the remaining positions being plus signs (+). The positions of the consonants excluding the center one were counterbalanced across trials. The stimuli were presented in black font on a white background surrounded by a red frame. Luminance was kept constant. One trial included a stimulus array presented for 2.5 s, followed by the retention period consisting of a centered fixation cross (+) for 3.5 s. The probe consisted of the same array of crosses with the probe letter being presented always in the middle and was presented for 2 s. The probe requested a Yes/No response (forced choice) depending on whether the letter was part of the stimulus set or not. Responses were given with the index and middle finger of the right hand, and response button assignment ("right/left") was counterbalanced across subjects. The inter-stimulus interval between trials consisted also of a fixation cross and was of a random duration in the range of 1.8–2.5 s (mean 2 s) to minimize preparatory activity. A centered fixation star (*) was projected for 24.5 s as a baseline condition five times interspersed. After every block, a short fixation identical to the inter-stimulus interval appeared for 2.5 s. Full task performance summed up to 13 min. A schematic illustration of the task design is given in **Figure 1**. To become familiar with the task, subjects were given a short practice version of the task outside the scanner.

Subjects viewed the stimuli via goggles (VisualStimDigital MR-compatible video goggles; Resonance Technology Inc., Northridge, CA, USA) while lying inside the scanner. Responses were made via a fiber-optics response button box. In Bern, an in-house MR-compatible response box was used for the task, in Zurich a 4 Button Curve Right Fiber Optic Response Pad

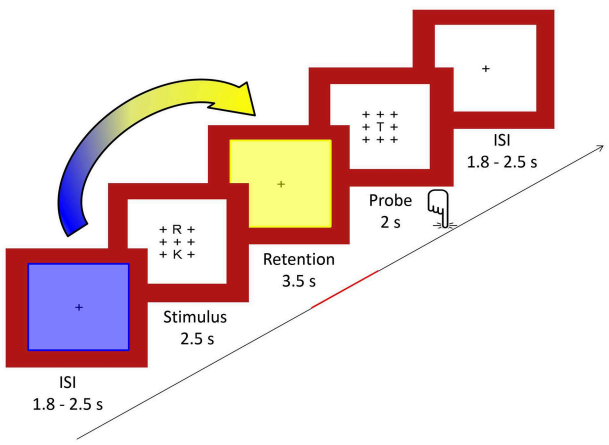

FIGURE 1 | In the Sternberg WM task, sets of either two or five consonants were presented for 2.5 s (stimulus) and had to be retained in memory for 3.5 s (retention). Subsequently, a probe letter was shown for 2 s (retrieval). Subjects indicated by button press whether the probe had been part of the stimulus. As indicated by the arrow, we computed covariance mappings between pre-stimulus percent TCN-activity fluctuations (period marked in blue) and EEG spectral fluctuations from the last 2.5 s of the retention period (period marked in yellow).

(Current Designs, Inc., Philadelphia PA, USA). Stimulus delivery and response registration was controlled by Presentation (Version 170011414, Neurobehavioral Systems Inc., Albany, CA, USA) in Zurich, and by E-Prime (Version 2.0.10.553) in Bern.

Accuracy in terms of percent correct answers and reaction time (RT) was computed from the responses in the low and high WM load conditions, and the differences between the conditions were tested using *t*-tests.

MRI Data

Data were acquired at two different measuring sites and with different 3.0 Tesla (3T) scanners: measuring site (a) was at the University Hospital of Psychiatry in Bern (3T Siemens Magnetom Trio MR Scanner; Siemens 12-channels head coil; Siemens, Erlangen, Germany), measuring site (b) was at the University Hospital of Psychiatry in Zurich (3T Philips Achieva whole-body system; Philips SENSE Head coil 32-elements; Philips Medical Systems, Best, the Netherlands).

The functional T2*-weighted MR images were acquired with an echo planar imaging sequence. The characteristics of the sequence were: 250 volumes for the resting state and 406 volumes for the Sternberg WM task, 35 slices, voxel size of $3 \times 3 \times 3\,mm^3$, matrix size 64×64, FOV $192 \times 192\,mm^2$, TR/TE 1960 ms/30 ms. This sequence was optimized for simultaneous EEG/fMRI measurements and hold as similar as possible among measuring sites.

Structural data was acquired with an T1-weighted ADNI-sequence to minimize differences among measuring sites. The ADNI sequence had the following parameters: 176 sagittal slices, slice thickness 1.0 mm, voxel size $1 \times 1 \times 1\,mm^3$, FOV $256 \times 256\,mm^2$, TR/TE 2300 ms/2.98 ms.

For the preprocessing of the functional MRI data, SPM8 (Welcome Department of Imaging Neuroscience, London, http://www.fil.ion.ucl.ac.uk/spm) was used. After slice timing the data was motion corrected to the mean image. The anatomical T1 was coregistered to the mean image followed by the segmentation into six tissue probability maps. Finally, data was normalized and smoothed using a 6 mm FHWM Gaussian kernel.

ICA-approach

BOLD data was parceled into 20 independent components by means of a group ICA implemented in the GIFT toolbox (Calhoun et al., 2008). The independent components were visually compared to networks described in the literature and to templates provided by the GIFT toolbox by means of a spatial similarity tool in order to identify templates for the DMN as a task negative network and the dAN, the lWMN, and the rWMN as task positive networks, driven by our hypothesis introduced above. The four selected templates were back-projected onto the continuous BOLD data of each subject to obtain individual time courses for each TCN and subject. These time courses were deconvolved by the hemodynamic response function and normalized (z-transformed, over time-points). The dynamics of a TCN consist of the percent strength of the respective TCN in the fMRI volume in the middle of each pre-stimulus period (3500 ms before retention onset) in each subject. TCN dynamics were temporally correlated with EEG theta spectral power from the retention intervals (trials of correct responses only). This so-called covariance mapping yielded the spatial distribution of the theta EEG fluctuations during retention associated with the dynamics of the respective TCN in the pre-stimulus interval. In addition, in a time window from −4.3 to 5.5 s in reference to the retention periods, z-transformed TCN dynamics were interpolated on a 0.1 s time-scale and averaged across trials for each subject and load condition. These mean TCN dynamics were then compared moment by moment against zero using two-tailed single one-sample *t*-tests. Similarly, the load conditions were compared using paired *t*-tests. Since the data-window chosen had included a maximum of five MR volumes, these tests were thresholded at a p-value<0.01, which corresponds to a Bonferroni-correction with a factor 5.

EEG Data

At both measuring sites, continuous EEG was recorded simultaneously during fMRI-acquisition with a sampling rate of 5 kHz synchronized to the scanner clock and TR to minimize gradient residuals (Mandelkow et al., 2006) using MR-compatible equipment (BrainAmp DC-amplifiers by Brain Products GmbH, Gilching, Germany; EEG caps by EASYCAP GmbH, Herrsching, Germany). Data was recorded with a 0.1 Hz highpass and a 250 Hz lowpass filter and a resolution of 0.5 μV applied to scalp channels. In addition to the scalp channels, an electrooculogram and an electrocardiogram have been measured. Electrode impedances were kept below 20 kΩ. The electrodes were connected to BrainAmp MR-compatible amplifiers (Brain Products GmbH, Gilching). Fz was used as the recording reference, and the EEG was band-pass filtered at 0.1–250 Hz with a sampling rate of 5 kHz. For patient safety, the EEG amplifiers were battery powered and connected through optical wires to the data acquisition PC.

The Zurich data set has been acquired with 60 scalp channels. A lowpass filter of 1000 Hz and a resolution of 10 μV was applied to the ECG channels. The scalp electrodes covered the 10–20-system plus the channels OI1/2. O1'/2' and Fp1'/2' were placed 15% more laterally to Oz/FPz for a more even coverage. The Bern data set has been acquired using 92 scalp channels at the position of the international 10–10 system.

Artifact Correction and Other Preprocessing

For the joint analysis of both data sets, a common electrode subset consisting of 66 channels (AF3, AF4, AFz, C1-6, CP1-6, CPz, Cz, F3-8, Fz, Fc1-6, FCz, Fp1, Fp2, Fpz, FT7-10, Iz, O1, O2, Oz, OI1, OI2, P3-8, Pz, PO1-4, PO7-10, T7, T8, TP7-10) has been created for analyses. A resting state EEG with the eyes closed was recorded outside the scanner and was later used for artifact correction. The start of each volume was automatically marked in the EEG data. The EEG data were preprocessed using Brain Vision Analyzer 2.0.4.368 (Brain Products GmbH, Gilching). The aim of the EEG data preprocessing was to remove scan and artifact and cardio ballistic artifacts (CBA) as well as ocular movement artifacts from the EEG. In a first step, a sliding average MR pulse artifact was computed and subtracted from the individual pulse artifacts for the removal of the scan artifact (Allen et al., 1998). Then, the CBA was removed with a similar averaging method,

described in Michels et al. (2010). In a second step, the correction of residual scan and CB artifacts was done with a concatenated ICA procedure previously applied by our group for resting state and task data (Jann et al., 2010; Kottlow et al., 2012): An extended ICA (Bell and Sejnowski, 1995; Lee et al., 1999a,b; Jung et al., 2001) was used to decompose the measured signal into components that appear to be brain activity and components that appear to be artifacts (Jung et al., 2000a,b). To improve the decomposition, the ICA was computed for a dataset that included both the task EEG inside the scanner and the resting EEG outside the scanner, providing a basis for learning the EEG uncontaminated from MR pulse artifacts. To maintain computational feasibility, the EEG was filtered at 1–49 Hz and down-sampled to a sampling rate of 500 Hz. For the objective identification of artifact components, the loadings of all ICA factors were segmented into 2-s epochs and frequency transformed. The average spectral power across epochs of each factor was compared between the measurement outside and inside the scanner. The factors in which the power inside the scanner considerably exceeded the power outside the scanner were identified as MR-related artifacts and removed. Components representing ocular artifacts were identified by their topographic signature. After removal of these specific factors, the EEG obtained inside the scanner was reconstructed from the remaining factors. Still residing artifacts were manually marked, the ECG and EOG channels were removed altogether from the EEG and the data were recomputed to average reference. For all further quantitative analyses the data were down-sampled to 250 Hz and divided into artifact free segments containing the last 2.5 s of the retention period separately for the correctly answered trials of each load condition. From this data, the time-varying EEG frequency spectral amplitude was obtained using a continuous complex Gabor transformation in the frequency range from 2 to 20 Hz, with an envelope that had its half-max at about the latency of a full cycle of the oscillation. These frequency transformed single trial epochs served as basis for all subsequent analyses. For statistics, the values were pooled into three frequency bands, namely Theta (3–7 Hz), Alpha (8–12 Hz), and Beta (13–20 Hz).

Replication of the Load Effect

For the replication of the load-dependent frontal-midline theta effect reported in the literature (Michels et al., 2010), the single epochs of each subject were averaged for each load condition across trials in 5 time bins of 0.5 s duration. In analogy to Michels et al. (2010) a relative load effect computed as the ratio of high load to low load. This relative load effect was compared against the expected constant value of 1.0 using a one-factorial within subject TANOVA for each of the time bin and frequency band. Adjacent time bins where the TANOVA yielded significant effects ($p < 0.05$) were averaged and displayed as t-maps. The same was done in the alpha and beta frequency bands. Since there were a-priori hypotheses about the existence and topographies of load effects, no corrections for multiple testing were applied, but significant results were tested for compatibility with previous studies based on *t*-tests at electrodes reported in these studies.

Covariance Mapping

As schematically shown in **Figure 1**, we established the predictive value of pre-stimulus TCN activation upon the EEG during the retention period using a so-called covariance mapping, which is based on a linear regression analysis of a predictor (in this case pre-stimulus TCN activation) upon fluctuations of multichannel EEG patterns (in this case the spectral amplitudes during the retention period). Computational details have been described elsewhere (Koenig et al., 2008). Since these covariance maps were established within subjects, we had to test for the stability of the obtained results across subjects. This was done using a permutation test (the so-called topographic consistency test, or TCT) that tests whether in a series of EEG spatial distributions (in our case the individual covariance maps) have something in common that is unlikely to have resulted by chance alone (Koenig and Melie-García, 2010). These TCTs were applied to each TCN, frequency band and load level. In order to minimize the number of tests, we collapsed the data within the entire time period. Since there was no previous study that would provide empirical hypotheses on the outcome of these tests, the resulting *p*-values were thresholded according to a false discovery rate of 5%.

If, within a frequency band, a set of significant TCTs indicated the presence of consistent covariance maps for more than one TCN and/or load-level, we furthermore aimed to clarify if these covariance maps had a spatial distribution that was particular or common for the different TCNs and/or load-levels. This was achieved by computing TANOVAs including those covariance maps that met the above TCT criterion, with TCN and/or load as within subject factors. Significant effects of TCN and/or load-level where further explored by computing t-maps for the relevant contrasts. The labels of the electrodes with the highest/lowest *t*-values were retained and reported to describe the obtained maps, but not used for statistical inference, since this has already been established using the preceding tests.

Results

Accuracy

Accuracy as measured by percent correct answers did not differ significantly between the two load conditions ($p = 0.61$). RT was significantly higher for high load compared to low load conditions ($p < 0.01$; mean RT low load 0.82 s ($\pm$ 0.32), mean RT high load 1.02 s ($\pm$ 0.38).

EEG

As shown in **Figure 2**, the replication analysis yielded significant load effects in all frequency bands. In the theta band, the TANOVA yielded a significant load effect within the first second of the analysis period (*p* always below 0.05). In the subsequent *post-hoc t*-map analysis in the average of this period, the strongest load effects were seen at frontal-midline electrodes, with a maximal *t*-value at electrode Fz ($t = 3.44$, $p = 0.0025$, $df = 21$). This findings replicate earlier results for WM retention as described by Michels et al. (2010). The same time windows also displayed significant load effects in the alpha band (TANOVA *p*-values always below 0.01), the corresponding *t*-map was dominated by a midline parietal negativity (*t*-min $= -4.98$, $p < 0.0001$,

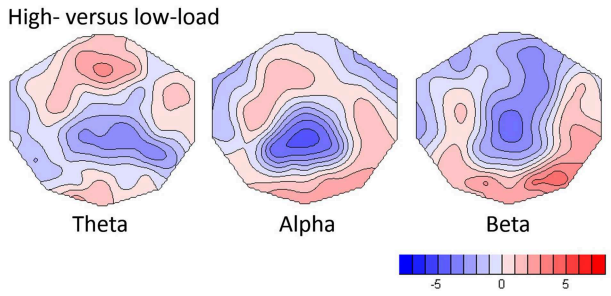

FIGURE 2 | T-maps showing load-dependent effects for theta, alpha and beta frequency bands. For the computation, the differences between high- and low-load conditions were normalized by the low load and *t*-tests against one were computed.

df = 21, at electrode Pz) and an occipital positivity which was maximal at electrode O2 ($t = 2.94$, df = 21, $p = 0.023$). In the beta band the first 1.5 s of the analysis period yielded significant TANOVA results, the *t*-map of the contrast computed in this interval showed a negativity with a central parietal midline minimum (t-min = −4.90, $p < 0.0001$, df = 21, at CPz) and a right occipital maximum (t-max = 4.16, $p < 0.0005$, df = 21, at O2).

BOLD-TCN Activity during the Pre-Stimulus Interval

The four TCNs as obtained by the group ICA of the continuous BOLD data are shown in **Figure 3**. The peak MNI coordinates and localized regions of the TCNs can be found in the supplementary material. The most prominent regions however are the bilateral precuneus, the posterior cingulate gyrus and the medial frontal gyrus for the DMN, the superior parietal lobuli, the right middle inferior gyrus including the frontal eye field, the right inferior and superior frontal gyrus for the dAN and the middle frontal gyri including the dorsolateral prefrontal corteces and the pre-supplementary motor areas, the inferior parietal lobuli as well as the anterior cingulate cortex for the WMNs. Additionally, in **Figure 3** the TCN activity over the average task trial for both loads is shown, including information when these dynamics were significantly different from the mean. DMN activity was significantly decreased during task preparation (pre-stimulus), encoding (stimulus) and retention in high-load conditions. dAN activity was significantly increased during task-preparation, and decreased during the retention and probe period, these dynamics were significantly larger in the high-load condition. The activity pattern over the task for the lWMN and the rWMN were similar to each other, and showed a significant increase of activation only for the high-load condition during the retention (lWMN only) and probe (lWMN and rWMN).

Covariance Mapping of Pre-stimulus TCN Activity and Retention EEG Frequency Power

Covariance maps relating the pre-stimulus TCN percent activity fluctuations over trials with the dynamics of EEG spectral wavelet activity of the retention period were computed separately for both WM loads and all four TCNs. This resulted in covariance maps for each of the four pre-stimulus TCNs, each of the three frequency band and both load conditions for each subject (totally 24). To test whether these covariance maps were consistent across subjects, TCTs were calculated for each category with the covariance maps of all subjects, resulting in a total of 24 TCTs. Among these, nine TCTs reached significance when permitting an overall false discovery rate of 5% (theta load 5: DMN, alpha load 2: DMN, dAN, lWMN, rWMN, alpha load 5: dAN, beta load 2: dAN, lMWN, rWMN).

Tests of the Obtained Covariance Maps for Topographic Differences as Function of TCNs and Load Levels

In the theta band, the TCT indicated significant covariance maps only for the DMN, and only in the high-load condition. Since in theta band no other TCN showed significant covariance maps, no further analyses were conducted. The t-map (against zero) of the theta-covariance maps of the DMN in the high-load condition is shown in **Figure 4**, and had a negative maximum at electrode AFz ($t = -2.701$).

In the alpha band, there were significant TCT results for all TCNs in the low-load condition, and for the dAN the high-load condition. To further assess if the covariance maps differed between the four TCNs, a TANOVA across the four covariance maps of the low-load condition was computed. This TANOVA was significant ($p = 0.0002$). Since the covariance maps of the left- and right WMN were visually very similar, we compared them in a separate TANOVA, which was, as expected, not significant ($p = 0.400$). On the other side, the TANOVA comparing the DMN, the dAN, and the combined left- and right-WMN remained significant ($p = 0.0002$) as well as other sub-comparisons (DMN–dAN $p = 0.0002$, DMN–WM $p = 0.0054$, dAN–WM $p = 0.0096$), such that we concluded that the covariance maps of the DMN, the dAN and either WMN with the alpha band can be distinguished, whereas there is no evidence to distinguish the covariance maps of the lWM and the rWM with alpha. In addition, since for the dAN, there were significant covariance maps for the load and high-load conditions, these maps were also compared; the result of this TANOVA indicated no evidence for a difference ($p = 0.894$). Accordingly, t-maps were computed for what the analyses indicated to be the smallest discrete fingerprints of pre-stimulus TCN activation, which were found for the DMN in the low-load condition (with a positive maximum at electrode P7; $t = 5.85$), for the combined left- and right WM also in the low-load condition (positive maximum at Pz, $t = 2.68$), and for the dAN, but combining the low and high load conditions (negative maximum at P8, $t = -4.76$) (**Figure 4**).

The analysis of the beta-band yielded significant TCT results for the three task-positive networks, but only in the low-load condition. A subsequent TANOVA on these three covariance maps indicated that these maps were significantly different ($p = 0.0146$). The resulting t-maps are again shown in **Figure 4**.

Discussion

The present study investigated fMRI network dynamics and EEG spectral changes during the execution of a WM task with two load levels. Specifically, complementing earlier studies reporting

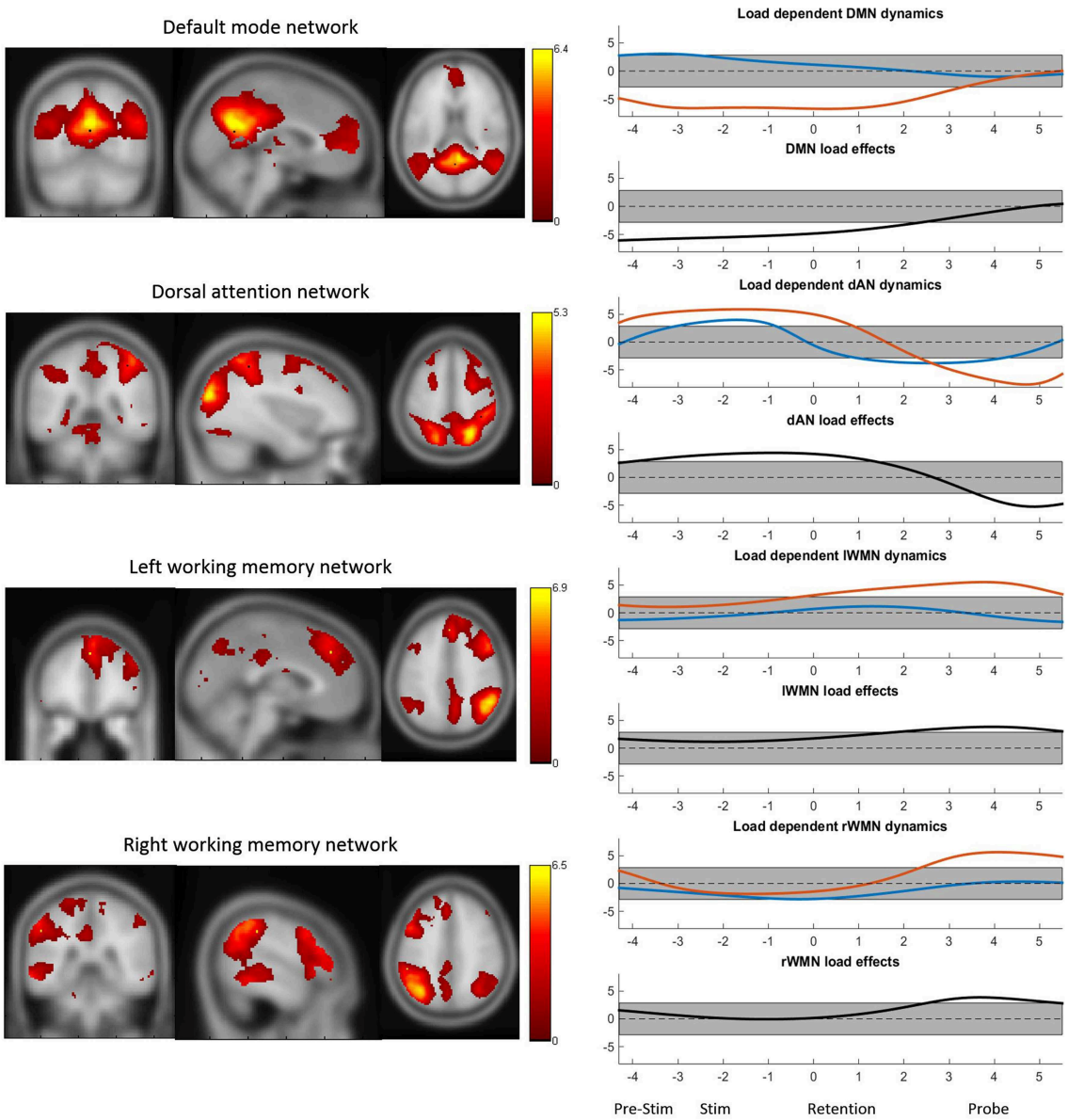

FIGURE 3 | The four TCNs and their activity over the task for high- and low-load conditions. The plots on the right show the t-statistics (across subjects) of the z-transformed TCN percent activity over the mean task conditions for low-load (blue) and high-load (red) conditions and *t*-test between high- vs. low-load conditions. Y-axes represent *t*-values and the gray bar represents the significance-threshold. The x-axis represents the time in seconds: −4 to −2.2: pre-stimulus; −2.5 to 0: stimulus; 0 to 3.5: retention; 3.5 to 5.5: probe; 5.5 to 5.8 and −4 to −2.5: pre-stimulus. 0 marks the beginning of the retention period.

load-dependent effects during WM retention in the EEG (Onton et al., 2005; Meltzer et al., 2007; Michels et al., 2008, 2010, 2012; Scheeringa et al., 2009; Huang et al., 2013) and during task preparation in the DMN (Esposito et al., 2006; Manelis and Reder, 2014), we investigated here the relationship among pre-stimulus and task related brain activity.

As a first result, the data replicated a series of findings obtained in similar studies and therefore validates both these results and the findings obtained here. In particular, in the EEG, we found an expected load effect during the retention period in the form of an increase of frontal midline theta in the high-load condition, which is in agreement with a large body of literature linking frontal midline theta to WM, and showing that this link is load dependent (Onton et al., 2005; Meltzer et al., 2007; Michels et al., 2008, 2010, 2012; Scheeringa et al., 2009; Huang et al., 2013).

As also previously reported (Michels et al., 2010), we furthermore found increased alpha and beta power in the high-load condition, maximal at electrode O2. The interpretation of load-related power increases in the alpha range is still under debate: while some argue that this reflects a top-down suppression of

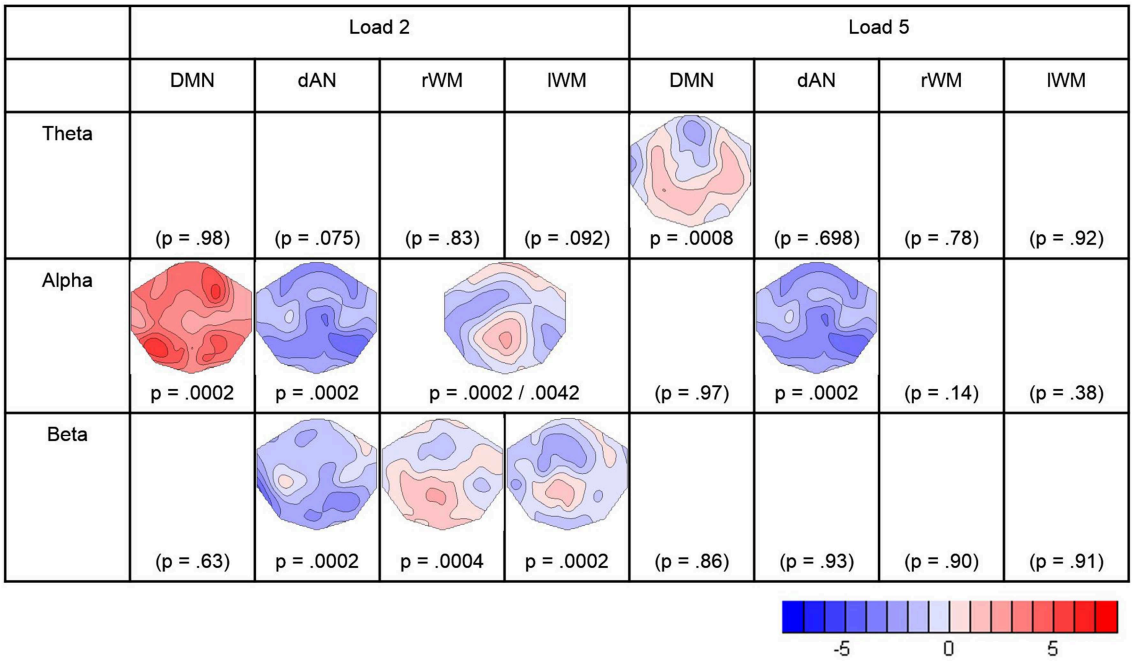

FIGURE 4 | Result of the TCTs (*p*-values) for each frequency-band and TCN, and t-maps of the significant covariance maps. Blue indicates negative *t*-values representing negative correlations between the pre-stimulus TCN activity and the retention frequency band power. Red indicates positive *t*-values representing positive correlations. The figure contains the results surviving the adjustment for a FDR of 5%.

irrelevant information during the task (Klimesch et al., 2010; Huang et al., 2013; Roux and Uhlhaas, 2014), others explain this effect with the active participation in attentional processes through the retention of relevant items (Nenert et al., 2012; Manza et al., 2014). Some assign both inhibition of task-irrelevant cortical areas and an active role in conscious attention to the alpha increase during WM (Palva and Palva, 2007). On the other hand, we found load-related alpha and beta decreases at midline centro-parietal electrodes, whereas the paper by Michels et al. (2010) had shown this only for the beta band.

Also the results obtained in the analysis of the event-related dynamics of the TCNs yielded effects that where in agreement with previous studies: DMN activity showed a load-dependent decrease already during task preparation, as previously shown by Manelis and Reder (2014). Beyond that, the mean time courses of the investigated task-positive TCNs over a trial also matched the behavior of these networks described in the literature: the dynamics of the dAN where opposite to the one of the DMN during high-load conditions (Kim, 2015), both WMNs were active during the executing of the WM task, that is the (late) retention and probe phase (Visintin et al., 2015). However, contrary to the findings of Visintin et al. (2015) in our data the lWMN was not yet active in the pre-stimulus period. And both, not only the rWMN (Dima et al., 2014) should a load-effect during the WM task. Further, although many studies reported negative correlations between the DMN and the WMN during resting state and task performance there is evidence that during task preparation both DMN core regions and WMN regions are co-activated (Koshino et al., 2014). This is apparently the case in the low-load conditions of our data.

The principal aim and novelty of our study was the attempt to establish whether and how varying levels of pre-stimulus TCN activation would affect the recruitment of neuronal resources during task execution, as indexed by retention EEG spectral amplitude. The study is thus endorsing the concept of state dependent information processing. This concept assumes that responses to environmental information depend on an interaction of the input with the momentary brain state. Accordingly, part of the variance observed in these responses, and eventually also dysfunctional responses, may be explained by normal variance or abnormal features of the brain state before and at the time of perception.

In our task design, task difficulty was varied pseudo-randomly in blocks of four trials and was thus partly predictable for the subject. Therefore, we could separate anticipatory and random variations of brain state, whereas anticipatory effects were defined as load-dependent mean pre-stimulus effects, while random variations were defined as trial by trial deviations of a TCN from a mean.

As a first result, we found an inverse relation of pre-stimulus DMN activation with frontal midline theta during the retention period, which is in-line with the well-known theta load effect and the findings on pre-stimulus DMN fluctuations indicative of WM functions (Esposito et al., 2006; Hampson et al., 2006; Manelis and Reder, 2014). Previous studies have already established a relation of frontal midline theta and simultaneous

DMN activation during the retention period (Michels et al., 2010). Our result extend this finding by showing that DMN activation preceding task execution and quantified prior to any percept to be kept in mind was already predictive for the later recruitment of WM resources. It is thus not that processes related to DMN activation and processes related to WM processes are merely anti-correlated, but that, in the high load condition, pre-stimulus DMN activation "sets the stage" for later WM processes to develop. When task demand was low, these WM processes seemed to be unaffected by pre-stimulus DMN activation.

The predictive power of pre-stimulus DMN upon frontal midline theta during retention in the high load condition supports other findings showing fluctuations of intrinsically organized brain dynamics have effects on cognitive processes and can predict fluctuations in the performance of tasks requiring executive control. A recent study from Nozawa et al. (2014) correlated fluctuations of pre-stimulus TCN activity with reactions times from a color-word Stroop task and was able to show that pre-stimulus DMN fluctuations predicted RT fluctuations, thus constituting "cognitive readiness." The pre-stimulus TCN-DMN dynamics accordingly may represent a useful measure for anticipatory and preparatory processes, which often cannot be controlled in cognitive experiments. Interestingly, the topography of the pre-stimulus DMN informed theta-band covariance map was also similar to the one found by Jann et al. (2010) through a covariance mapping of resting state DMN with resting state theta power, in the absence of any explicit task. This suggests that frontal midline theta is modulated by DMN activity under very different conditions including rest. Still, the time-lagged relationship between pre-stimulus and task seems not to be a general mechanism, as in our study, the coupling was only significantly present during high-load conditions.

In addition, in the low-load condition, the level of pre-stimulus DMN activation was predictive for alpha increases, which were widespread, but had occipital maxima. As reported in the literature, occipital alpha typically showed positive correlations with DMN activity under resting conditions (Nishida et al., 2015). The result, in conjunction with the finding that the low-load condition on average did not produce a significant suppression of DMN activity, may thus suggest that DMN fluctuations were relatively unaffected by the stimulus and may have extended from the pre-stimulus period into the retention period, such that the encountered alpha band effect in the retention period and pre-stimulus DMN fluctuations represent common, but temporally extended processes.

The task-positive networks had significant covariance maps only in the alpha and beta band. Prestimulus dAN was predictive for a widespread suppression of alpha in the retention period, independent of load level. Since both load-levels also showed an increase of dAN activity before the task, this might indicate that a strong activation of attentional systems prior to stimulus processing might also increase the amount of resources recruited during the retention period, as indicated by alpha-suppression. In addition, in the low-load condition, pre-stimulus activation of left and right WM networks induced an increase of alpha at midline parietal electrodes which was opposite to the alpha band effect of high-load at these electrodes. One may thus speculate that randomly occurring processes engaging WM functions in the pre-stimulus period had a negative impact on task related WM processes during retention.

In the beta band, we found, at least for task-positive networks, a correspondence in significance and topography with the covariance maps of the alpha band. As argued previously (Nishida et al., 2015), in combined EEG-fMRI studies, alpha and low beta-band fMRI correlates were often found to be similar, such that the interpretation of these findings may follow those of the alpha band.

In general, based on previous findings that neuronal coupling in different frequency bands may underlie distinct functions in WM retention (Palva et al., 2010) our results suggest that processes reflected by spectral oscillations during retention seem not only to be momentary EEG counterparts of activity in different attention-related networks but are also affected by activity in these areas during the pre-stimulus or preparation intervals. Thus, the proper functioning of the brain already in the preparatory state before a stimulus seems to be a necessary prerequisite for successful WM processing. Future research will have to further investigate these mechanisms. However, the finding of this interdependence may be important for the development of treatment options in cases of WM deficits.

Author Contributions

MK wrote the manuscript. TK, LM, and DB drafted the work and advised the analyses. MK, AB, AS, DB, and TK drafted the experimental design. MK and LM set up the task design, AS and AB acquired and preprocessed the data. TK, MK, and AS wrote scripts for data analysis. MK and TK analyzed and interpreted the data. DB contributed to the interpretation of the data and revised the work for intellectual content. MK, TK, and AB created the figures. TK revised all versions of the manuscript. MK, AB, AS, LM, DB, and TK approved the final version and agreed on all aspects regarding the submitted work.

Acknowledgments

This study was supported by the Swiss National Foundation Sinergia Grant CRSII3_136249. We would like to thank the rest of the team, Prof. Dr. Peter Achermann, Prof. Dr. Lutz Jaencke, Carina Klein, Laura Tueshaus and Laura Díaz-Hernàndez for their conceptual and practical help. We also thank Dr. Kay Jann and Dr. Joshua Balsters for their help with the BOLD-ICA and Dr. Andrea Federspiel and Dr. Philipp Staempfli for their technical help with the MRI measurements.

Supplementary Material

The Supplementary Material for this article can be found online at: http://journal.frontiersin.org/article/10.3389/fnbeh.2015.00111/abstract

References

Allen, P. J., Polizzi, G., Krakow, K., Fish, D. R., and Lemieux, L. (1998). Identification of EEG events in the MR scanner: the problem of pulse artifact and a method for its subtraction. *Neuroimage* 8, 229–239. doi: 10.1006/nimg.1998.0361

Bell, A. J., and Sejnowski, T. J. (1995). An information maximization approach to blind separation and blind deconvolution. *Neural Comput.* 7, 1129–1159. doi: 10.1162/neco.1995.7.6.1129

Calhoun, V. D., Kiehl, K. A., and Pearlson, G. (2008). Modulation of temporally coherent brain networks estimated using ICA at rest and during cognitive tasks. *Hum. Brain Mapp.* 29, 828–838. doi: 10.1002/hbm.20581

Dima, D., Jogia, J., and Frangou, S. (2014). Dynamic causal modeling of load-dependent modulation of effective connectivity within the verbal working memory network. *Hum. Brain Mapp.* 35, 3025–3035. doi: 10.1002/hbm.22382

Esposito, F., Bertolino, A., Scarabino, T., Latorre, V., Blasi, G., Popolizio, T., et al. (2006). Independent component model of the default-mode brain function: assessing the impact of active thinking. *Brain Res. Bull.* 70, 263–269. doi: 10.1016/j.brainresbull.2006.06.012

Greicius, M. D., Krasnow, B., Reiss, A. L., and Menon, V. (2003). Functional connectivity in the resting brain: a network analysis of the default mode hypothesis. *Proc. Natl. Acad. Sci. U.S.A.* 100, 253–258. doi: 10.1073/pnas.0135058100

Hampson, M., Driesen, N. R., Skudlarski, P., Gore, J. C., and Constable, R. T. (2006). Brain connectivity related to working memory performance. *J. Neurosci.* 26, 13338–13343. doi: 10.1523/JNEUROSCI.3408-06.2006

Huang, L.-Y., She, H.-C., Chou, W.-C., Chuang, M.-H., Duann, J.-R., and Jung, T.-P. (2013). Brain oscillation and connectivity during a chemistry visual working memory task. *International Journal of Psychophyiology* 90, 172–179. doi: 10.1016/j.ijpsycho.2013.07.001

Jann, K., Kottlow, M., Dierks, T., Boesch, C., and Koenig, T. (2010). Topographic electrophysiological signatures of FMRI Resting State Networks. *PLoS ONE* 5:e12945. doi: 10.1371/journal.pone.0012945

Jensen, O., and Tesche, C. D. (2002). Frontal theta activity in humans increases with memory load in a working memory task. *Eur. J. Neurosci.* 15, 1395–1399. doi: 10.1046/j.1460-9568.2002.01975.x

Jung, T. P., Makeig, S., Humphries, C., Lee, T. W., McKeown, M. J., Iragui, V., et al. (2000a). Removing electroencephalographic artifacts by blind source separation. *Psychophysiology* 37, 163–178. doi: 10.1111/1469-8986.3720163

Jung, T. P., Makeig, S., McKeown, M. J., Bell, A. J., Lee, T. W., and Sejnowski, T. J. (2001). Imaging brain dynamics using independent component analysis. *Proc. IEEE Inst. Electr. Electron. Eng.* 89, 1107–1122. doi: 10.1109/5.939827

Jung, T. P., Makeig, S., Westerfield, M., Townsend, J., Courchesne, E., and Sejnowski, T. J. (2000b). Removal of eye activity artifacts from visual event-related potentials in normal and clinical subjects. *Clin. Neurophysiol.* 111, 1745–1758. doi: 10.1016/S1388-2457(00)00386-2

Kim, H. (2015). Encoding and retrieval along the long axis of the hippocampus and their relationships with dorsal attention and default mode networks: the HERNET model. *Hippocampus* 25, 500–510. doi: 10.1002/hipo.22387

Klimesch, W., Freunberger, R., and Sauseng, P. (2010). Oscillatory mechanisms of process binding in memory. *Neurosci. Biobehav. Rev.* 34, 1002–1014. doi: 10.1016/j.neubiorev.2009.10.004

Koenig, T., and Melie-García, L. (2010). A method to determine the presence of averaged event-related fields using randomization tests. *Brain Topogr.* 23, 233–242. doi: 10.1007/s10548-010-0142-1

Koenig, T., Melie-García, L., Stein, M., Strik, W., and Lehmann, C. (2008). Establishing correlations of scalp field maps with other experimental variables using covariance analysis and resampling methods. *Clin. Neurophysiol.* 119, 1262–1270. doi: 10.1016/j.clinph.2007.12.023

Koshino, H., Minamoto, T., Yaoi, K., Osaka, M., and Osaka, N. (2014). Coactivation of the default mode network regions and working memory network regions during task preparation. *Sci. Rep.* 4:5954. doi: 10.1038/srep05954

Kottlow, M., Jann, K., Dierks, T., and Koenig, T. (2012). Increased phase synchronization during continuous face integration measured simultaneously with EEG and fMRI. *Clin. Neurophysiol.* 123, 1536–1548. doi: 10.1016/j.clinph.2011.12.019

Laufs, H., Krakow, K., Sterzer, P., Eger, E., Beyerle, A., Salek-Haddadi, A., et al. (2003). Electroencephalographic signatures of attentional and cognitive default modes in spontaneous brain activity fluctuations at rest. *Proc. Natl. Acad. Sci. U.S.A.* 100, 11053–11058. doi: 10.1073/pnas.1831638100

Lee, T. W., Girolami, M., and Sejnowski, T. J. (1999a). Independent component analysis using an extended infomax algorithm for mixed subgaussian and supergaussian sources. *Neural Comput.* 11, 417–441. doi: 10.1162/089976699300016719

Lee, T. W., Lewicki, M. S., Girolami, M., and Sejnowski, T. J. (1999b). Blind source separation of more sources than mixtures using overcomplete representations. *IEEE Signal Process. Lett.* 6, 87–90. doi: 10.1109/97.752062

Leiberg, S., Lutzenberger, W., and Kaiser, J. (2006). Effects of memory load on cortical oscillatory activity during auditory pattern working memory. *Brain Res.* 1120, 131–140. doi: 10.1016/j.brainres.2006.08.066

Li, C.-S. R., Yan, P., Bergquist, K. L., and Sinha, R. (2007). Greater activation of the "default" brain regions predicts stop signal errors. *Neuroimage* 38, 640–648. doi: 10.1016/j.neuroimage.2007.07.021

Mandelkow, H., Halder, P., Boesiger, P., and Brandeis, D. (2006). Synchronization facilitates removal of MRI artefacts from concurrent EEG recordings and increases usable bandwidth. *Neuroimage* 32, 1120–1126. doi: 10.1016/j.neuroimage.2006.04.231

Manelis, A., and Reder, L. M. (2014). Effective connectivity among the working memory regions during preparation for and during performance of the n-back task. *Front. Hum. Neurosci.* 8:593. doi: 10.3389/fnhum.2014.00593

Manza, P., Hau, C. L., and Leung, H. C. (2014). Alpha power gates relevant information during working memory updating. *J. Neurosci.* 34, 5998–6002. doi: 10.1523/JNEUROSCI.4641-13.2014

Maurer, U., Brem, S., Liechti, M., Maurizio, S., Michels, L., and Brandeis, D. (2015). Frontal midline theta reflects individual task performance in a working memory task. *Brain Topogr.* 28, 127–134. doi: 10.1007/s10548-014-0361-y

Meltzer, J. A., Negishi, M., Mayes, L. C., and Constable, R. T. (2007). Individual differences in EEG theta and alpha dynamics during working memory correlate with fMRI responses across subjects. *Clin. Neurophysiol.* 118, 2419–2436. doi: 10.1016/j.clinph.2007.07.023

Michels, L., Bucher, K., Lüchinger, R., Klaver, P., Martin, E., Jeanmonod, D., et al. (2010). Simultaneous EEG-fMRI during working memory task: modulations in low and high frequency bands. *PLoS ONE* 5:e10298. doi: 10.1371/journal.pone.0010298

Michels, L., Lüchinger, R., Koenig, T., Martin, E., and Brandeis, D. (2012). Developmental changes of BOLD signal correlations with global human EEG power and synchronization during working memory. *PLoS ONE* 7:e39447. doi: 10.1371/journal.pone.0039447

Michels, L., Moazami-Goudarzi, M., Jeanmonod, D., and Sarnthein, J. (2008). EEG alpha distinguishes between cuneal and precuneal activation in working memory. *Neuroimage* 40, 1296–1310. doi: 10.1016/j.neuroimage.2007.12.048

Nenert, R., Viswanathan, S., Dubuc, D. M., and Visscher, K. M. (2012). Modulations of ongoing alpha oscillations predict successful short-term visual memory encoding. *Front. Hum. Neurosci.* 6:127. doi: 10.3389/fnhum.2012.00127

Nishida, K., Razavi, N., Jann, K., Yoshimura, M., Dierks, T., Kinoshita, T., et al. (2015). Integrating different aspects of resting brain activity: a review of electroencephalographic signatures in resting state networks derived from functional magnetic resonance imaging. *Neuropsychobiology* 71, 6–16. doi: 10.1159/000363342

Nozawa, T., Sugiura, M., Yokoyama, R., Ihara, M., Kotozaki, Y., Miyauchi, C. M., et al. (2014). Ongoing activity in temporally coherent networks predicts intra-subject fluctuation of response time to sporadic executive control demands. *PLoS ONE* 9:e99166. doi: 10.1371/journal.pone.0099166

Obleser, J., Wöstmann, M., Hellbernd, N., Wilsch, A., and Maess, B. (2012). Adverse listening conditions and memory load drive a common α oscillatory network. *J. Neurosci.* 32, 12376–12383. doi: 10.1523/JNEUROSCI.4908-11.2012

Onton, J., Delorme, A., and Makeig, S. (2005). Frontal midline EEG dynamics during working memory. *Neuroimage* 27, 341–356. doi: 10.1016/j.neuroimage.2005.04.014

Palva, J. M., Monto, S., Kulashekhar, S., and Palva, S. (2010). Neuronal synchrony reveals working memory networks and predicts individual memory capacity. *Proc. Natl. Acad. Sci. U.S.A.* 107, 7580–7585. doi: 10.1073/pnas.0913113107

Palva, S., and Palva, J. M. (2007). New vistas for alpha-frequency band oscillations. *Trends Neurosci.* 30, 150–158. doi: 10.1016/j.tins.2007.02.001

Raichle, M. E., MacLeod, A. M., Snyder, A. Z., Powers, W. J., Gusnard, D. A., and Shulman, G. L. (2001). A default mode of brain

function. *Proc. Natl. Acad. Sci. U.S.A.* 98, 676–682. doi: 10.1073/pnas.98.2.676

Roux, F., and Uhlhaas, P. J. (2014). Working memory and neural oscillations: alpha-gamma versus theta-gamma codes for distinct WM information? *Trends Cogn. Sci.* 18, 16–25. doi: 10.1016/j.tics.2013.10.010

Scheeringa, R., Bastiaansen, M. C. M., Petersson, K. M., Oostenveld, R., Norris, D. G., and Hagoort, P. (2008). Frontal theta EEG activity correlates negatively with the default mode network in resting state. *Int. J. Psychophyiol.* 67, 242–251. doi: 10.1016/j.ijpsycho.2007.05.017

Scheeringa, R., Petersson, K. M., Oostenveld, R., Norris, D. G., Hagoort, P., and Bastiaansen, M. C. M. (2009). Trial-by-trial coupling between EEG and BOLD identifies networks related to alpha and theta EEG power increases during working memory maintenance. *Neuroimage* 44, 1224–1238. doi: 10.1016/j.neuroimage.2008.08.041

Sternberg, S. (1966). High-speed scanning in human memory. *Science* 153, 652–654. doi: 10.1126/science.153.3736.652

Tuladhar, A. M., ter Huurne, N., Schoffelen, J. M., Maris, E., Oostenveld, R., and Jensen, O. (2007). Parieto-occipital sources account for the increase in alpha activity with working memory load. *Hum Brain Mapp.* 28, 785–792. doi: 10.1002/hbm.20306

Van Snellenberg, J. X., Slifstein, M., Read, C., Weber, J., Thompson, J. L., Wager, T. D., et al. (2015). Dynamic shifts in brain network activation during supracapacity working memory task performance. *Hum. Brain Mapp.* 36, 1245–1264. doi: 10.1002/hbm.22699

Visintin, E., De Panfilis, C., Antonucci, C., Capecci, C., Marchesi, C., and Sambataro, F. (2015). Parsing the intrinsic networks underlying attention: a resting state study. *Behav. Brain Res.* 278, 315–322. doi: 10.1016/j.bbr.2014.10.002

Zhang, Z., Zheng, H., Liang, K., Wang, H., Kong, S., Hu, J., et al. (2015). Functional degeneration in dorsal and ventral attention systems in amnestic mild cognitive impairment and Alzheimer's disease: an fMRI study. *Neurosci. Lett.* 585, 160–165. doi: 10.1016/j.neulet.2014.11.050

Conflict of Interest Statement: The authors declare that the research was conducted in the absence of any commercial or financial relationships that could be construed as a potential conflict of interest.

2.1.1 Supplemental material of Paper 1

Table S1: Regions of the identified four TCNs that formed the basis for the subsequent analyses. The extraction of the max values and the labeling of the coordinates was done with the "write Tailairach table" utility included in the gift toolbox. This procedure applies a localization based on the Talairach Daemon. The threshold for the beta-values was set at 3.5, distance between contiguous voxels was 4mm. Only positive regions are listed.

TCN	Region	Random effects: Max Value (x,y,z)
DMN	Precuneus	9.2 (-20, -66, 49)/11.6 (30, -72, 35)
	Superior Parietal Lobule	9.4 (-24, -55, 60)/11.4 (22, -59, 56)
	Middle Temporal Gyrus	8.6 (-34, -76, 24)/11.4 (38, -76, 24)
	Superior Occipital Gyrus	8.9 (-32, -78, 28)/10.8 (38, -76, 28)
	Angular Gyrus	6.3 (-34, -74, 31)/10.0 (36, -72, 31)
	Middle Occipital Gyrus	8.9 (-32, -82, 21)/9.3 (34, -81, 21)
	Inferior Parietal Lobule	6.4 (-34, -50, 56)/8.7 (44, -36, 53)
	Postcentral Gyrus	5.9 (-18, -51, 63)/8.2 (44, -34, 50)
	Cuneus	7.6 (-28, -80, 32)/7.5 (30, -80, 32)
	Middle Frontal Gyrus	4.6 (-26, 3, 55)/6.7 (30, 9, 60)
	Inferior Temporal Gyrus	6.5 (-53, -64, -2)/5.1 (48, -70, -2)
	Superior Frontal Gyrus	5.0 (-24, 15, 58)/6.4 (26, 7, 55)
	Inferior Frontal Gyrus	4.1 (-53, 13, 21)/5.6 (48, 9, 22)
	Paracentral Lobule	3.7 (0, -38, 50)/5.4 (4, -46, 59)
	Superior Temporal Gyrus	3.9 (-46, 6, -5)/4.7 (48, -61, 18)
	Fusiform Gyrus	4.3 (-44, -67, -12)/4.5 (48, -57, -12)
	Precentral Gyrus	4.5 (-55, -4, 39)/4.0 (59, -17, 40)
	Culmen	4.4 (-16, -37, -12)/3.8 (2, -45, -8)
	Insula	4.2 (-42, 4, -4)
	Cingulate Gyrus	4.0 (6, -37, 41)
	Medial Frontal Gyrus	3.9 (-20, 3, 51)
	Inferior Occipital Gyrus	3.9 (-42, -70, -3)
	Thalamus	3.9 (16, -29, 12)
dAN	Precuneus	8.5 (-20, -66, 49)/11.0 (30, -72, 35)
	Middle Temporal Gyrus	8.4 (-30, -75, 20)/10.7 (38, -77, 22)
	Superior Occipital Gyrus	8.0 (-28, -80, 28)/10.4 (38, -76, 26)
	Superior Parietal Lobule	8.6 (-24, -57, 58)/10.2 (24, -57, 58)
	Angular Gyrus	5.9 (-34, -76, 31)/9.6 (38, -76, 30)

	Middle Occitipital Gyrus	8.2 (-32, -79, 21)/7.8 (36, -83, 19)
	Cuneus	8.0 (-26, -76, 31)/7.9 (32, -80, 33)
	Inferior Parietal Lobule	6.7 (-30, -50, 54)/7.9 (34, -50, 56)
	Postcentral Gyrus	4.5 (-6, -53, 65)/7.3 (44, -34, 50)
	Middle Frontal Gyrus	5.5 (26, 0, 48)
	Inferior Frontal Gyrus	5.2 (48, 9, 24)
	Superior Frontal Gyrus	5.1 (26, 7, 55)
	Inferior Temporal Gyrus	4.5 (-53, -58, -4)/4.9 (51, -61, -9)
	Precentral Gyrus	3.6 (-53, -2, 41)/4.2 (59, -17, 41)
	Fusiform Gyrus	4.1 (50, -61, -12)
	Superior Temporal Gyrus	3.9 (48, -61, 18)
rWMN	Inferior Parietal Lobule	6.3 (-48, -52, 43)/16.6 (46, -54, 47)
	Superior Parietal Lobule	4.3 (-38, -56, 51)/16.4 (42, -58, 49)
	Supramarginal Gyrus	4.4 (-46, -51, 36)/14.7 (51, -49, 37)
	Middle Frontal Gyrus	4.9 (-44, 50, -1)/13.3 (46, 21, 39)
	Angular Gyrus	3.6 (-48, -55, 36)/12.6 (48, -55, 36)
	Precentral Gyrus	11.9 (48, 21, 36)
	Superior Frontal Gyrus	6.1 (-2, 33, 48)/11.7 (36, 22, 49)
	Medial Frontal Gyrus	7.1 (-2, 35, 42)/10.2 (4, 35, 39)
	Middle Temporal Gyrus	4.3 (-63, -27, -5)/9.9 (63, -26, -7)
	Postcentral Gyrus	9.3 (55, -36, 50)
	Inferior Frontal Gyrus	3.8 (-48, 47, 0)/9.3 (40, 54, 1)
	Precuneus	3.6 (0, -70, 46)/8.9 (36, -66, 42)
	Superior Temporal Gyrus	7.9 (48, -48, 21)
	Cingulate Gyrus	3.6 (-2, -26, 31)/6.9 (10, -45, 37)
	Declive	6.6 (-10, -79, -20)/-999.0 (0, 0, 0)
	Anterior Cingulate	5.6 (8, 41, 13)
	Inferior Temporal Gyrus	4.8 (59, -14, -16)
	Insula	4.1 (48, -40, 20)
	Uvula	3.9 (-14, -71, -23)
	Cuneus	3.7 (10, -66, 31)
lWMN	Inferior Parietal Lobule	14.9 (-38, -62, 44)/7.1 (34, -58, 40)
	Superior Parietal Lobule	14.6 (-36, -62, 49)/6.3 (40, -58, 51)

	Precuneus	13.0 (-34, -64, 40)/5.9 (32, -62, 40)
	Inferior Frontal Gyrus	11.5 (-46, 43, 5)/5.5 (53, 38, 13)
	Angular Gyrus	11.1 (-46, -56, 36)/5.4 (34, -58, 36)
	Supramarginal Gyrus	10.7 (-46, -53, 36)/5.1 (38, -49, 37)
	Middle Frontal Gyrus	10.6 (-46, 44, -4)/5.3 (50, 36, 18)
	Middle Temporal Gyrus	9.8 (-61, -37, -5)/5.1 (65, -35, -5)
	Superior Temporal Gyrus	9.1 (-46, -57, 29)/3.9 (63, -2, 7)
	Precentral Gyrus	8.0 (-44, 17, 34)/3.5 (61, -1, 11)
	Superior Frontal Gyrus	7.6 (-34, 14, 51)
	Inferior Temporal Gyrus	7.1 (-51, -53, -11)
	Medial Frontal Gyrus	6.6 (-4, 29, 41)
	Fusiform Gyrus	6.4 (-48, -55, -11)
	Uvula	5.3 (32, -63, -24)
	Cingulate Gyrus	5.0 (-2, -33, 33)/3.8 (2, -33, 33)
	Postcentral Gyrus	4.7 (-51, -31, 49)/4.2 (53, -34, 51)
	Superior Occipital Gyrus	4.5 (-38, -74, 28)
	Culmen	4.2 (28, -61, -24)
	Cuneus	4.0 (0, -90, 17)
	Insula	3.6 (-40, 17, -1)

2.2 Paper 2: Inefficient Preparatory fMRI-BOLD Network Activations Predict Working Memory Dysfunctions in Patients with Schizophrenia

Baenninger A, Diaz Hernandez L, Rieger K, Ford JM, Kottlow M, Koenig T

Front. Psychiatry 7:29.

doi: 10.3389/fpsyt.2016.00029

frontiers in Psychiatry

ORIGINAL RESEARCH
published: 18 March 2016
doi: 10.3389/fpsyt.2016.00029

Inefficient Preparatory fMRI-BOLD Network Activations Predict Working Memory Dysfunctions in Patients with Schizophrenia

Anja Baenninger[1,2], Laura Diaz Hernandez[1,3], Kathryn Rieger[3], Judith M. Ford[2,4], Mara Kottlow[1,3] and Thomas Koenig[1,3]*

[1] Translational Research Center, University Hospital of Psychiatry and Psychotherapy, University of Bern, Bern, Switzerland, [2] San Francisco VA Medical Center, San Francisco, CA, USA, [3] Center for Cognition, Learning and Memory, University of Bern, Bern, Switzerland, [4] Department of Psychiatry, University of California San Francisco, San Francisco, CA, USA

OPEN ACCESS

Edited by:
Thomas W. Weickert, University of New South Wales, Australia

Reviewed by:
Lars Michels, University Hospital Zurich, Switzerland
Jacqueline Ann Rushby, University of New South Wales, Australia

***Correspondence:**
Anja Baenninger
anja.baenninger@puk.unibe.ch

Specialty section:
This article was submitted to Schizophrenia, a section of the journal Frontiers in Psychiatry

Received: *17 October 2015*
Accepted: *22 February 2016*
Published: *18 March 2016*

Citation:
Baenninger A, Diaz Hernandez L, Rieger K, Ford JM, Kottlow M and Koenig T (2016) Inefficient Preparatory fMRI-BOLD Network Activations Predict Working Memory Dysfunctions in Patients with Schizophrenia. Front. Psychiatry 7:29. doi: 10.3389/fpsyt.2016.00029

Patients with schizophrenia show abnormal dynamics and structure of temporally coherent networks (TCNs) assessed using fMRI, which undergo adaptive shifts in preparation for a cognitively demanding task. During working memory (WM) tasks, patients with schizophrenia show persistent deficits in TCNs as well as EEG indices of WM. Studying their temporal relationship during WM tasks might provide novel insights into WM performance deficits seen in schizophrenia. Simultaneous EEG-fMRI data were acquired during the performance of a verbal Sternberg WM task with two load levels (load 2 and load 5) in 17 patients with schizophrenia and 17 matched healthy controls. Using covariance mapping, we investigated the relationship of the activity in the TCNs before the memoranda were encoded and EEG spectral power during the retention interval. We assessed four TCNs – default mode network (DMN), dorsal attention network (dAN), left and right working memory networks (WMNs) – and three EEG bands – theta, alpha, and beta. In healthy controls, there was a load-dependent inverse relation between DMN and frontal midline theta power and an anti-correlation between DMN and dAN. Both effects were not significantly detectable in patients. In addition, healthy controls showed a left-lateralized load-dependent recruitment of the WMNs. Activation of the WMNs was bilateral in patients, suggesting more resources were recruited for successful performance on the WM task. Our findings support the notion of schizophrenia patients showing deviations in their neurophysiological responses before the retention of relevant information in a verbal WM task. Thus, treatment strategies as neurofeedback targeting prestates could be beneficial as task performance relies on the preparatory state of the brain.

Keywords: schizophrenia, working memory, temporally coherent networks, state-dependent information processing, simultaneous EEG-fMRI, covariance mapping

INTRODUCTION

Deficits in working memory (WM) – defined as a system for temporary storage and manipulation of visual and phonological information (1) – represent a core feature in schizophrenia (2–5). There are studies discussing cognitive deficits in schizophrenia patients being mainly found in one specific domain, as for example in verbal episodic memory (6). The most consistent finding across studies, however, seems to be a generalized impairment across neuropsychological measures including verbal and spatial WM tests (5, 7, 8). These WM deficits are highly treatment resistant (9) and are indirectly related to poor functional outcome (10, 11). Although earlier fMRI studies reported on the dorsolateral prefrontal cortex (dlPFC) as the critical brain structure contributing to faulty WM in schizophrenia (12–16), later studies found that larger functional networks were recruited for successful performance (17–19).

The concept of fMRI-BOLD temporally coherent networks (TCNs) refers to a set of brain regions being temporally coactivated and describes both resting-state and task-related networks (20). Both resting-state networks (21–25) and task-related networks (18, 19, 26, 27) are affected by schizophrenia, as revealed by connectivity between or within the networks, their activation strength, or their spatial and temporal characteristics. Alterations in the most studied TCN, the default mode network (DMN), were related to severity of positive (26) and both positive and negative symptoms (22) during an oddball task and resting state, respectively. During WM tasks, the amount of DMN deactivation was linearly related to task demands (28), a balance that is behaviorally relevant in healthy subjects (29, 30). A disruption of the balance between DMN and task demands has been reported in patients with schizophrenia (31, 32), youth at high-risk for psychosis and early psychosis (33) as well as in unaffected siblings (34). According to the theory of state-dependent information processing (35), the brain's state before a memory trial begins affects the subsequent neuronal response to internal or external stimuli such that greater DMN activation before stimulus presentation was linked to more errors in a flanker task (36) as well as in a stop signal task (37).

Measuring EEG and fMRI simultaneously has become an established tool for basic as well as clinical research since the first pilot study proved its feasibility (38). With the combination of these complementary methods, well-localized hemodynamic activity from fMRI can be related to neural activity from the EEG (39). A combined EEG-fMRI study with healthy subjects revealed the DMN being negatively correlated with frontal theta power in a resting condition (40), consistent with enhanced frontal EEG theta power in tasks requiring WM and focused attention (41–44). The same inverse association between frontal theta power and DMN was observed during the retention period of a verbal Sternberg WM task (45). This was replicated and extended in a recent study using the same WM paradigm within the framework of state dependency: four prestimulus fMRI-BOLD TCNs modulated three EEG frequencies during the subsequent retention interval when memoranda had to be held in WM (46). Importantly, their analysis provided temporal information about the relationship: prestimulus DMN activity modulated poststimulus frontal theta power. There is evidence from EEG studies during WM tasks that in schizophrenia, frontal midline (FM) theta power is reduced (47, 48), but no study has investigated the temporal relationship between DMN activity and neural activity during retention as reflected in FM theta.

The role of EEG alpha power linked to WM is somewhat controversial with reports of both load-dependent increases and decreases at different scalp sites from posterior, central to parietal areas (44, 46, 49–51). Greater WM loads are related to increased EEG power in the beta band at occipital (45, 46) and temporal sites (52, 53).

During rest, several TCNs are linked to specific EEG frequencies. A study of Jann and colleagues concluded that TCNs representing higher cognitive functions including self-referential, attention, and memory processes as the DMN and left and right working memory networks (WMNs) among others were positively related to higher frequencies (alpha and beta band) and had unique topographic frequency distributions (54). Applying the same method, a shift of the EEG spectral correlates of TCN fluctuations toward lower frequencies was detected for the DMN (from beta toward theta and alpha band) and the left WMN (from alpha and beta toward theta band) in schizophrenia patients (55). This finding further supports the notion that specific topographical associations of TCNs with frequencies are functionally relevant and aberrant in this patient population.

The goals of this study were to further extend previous results of Kottlow et al. (46) to schizophrenia. Exploring WM in a state-dependent manner may yield novel insights into deviations of cognitive functioning in this severe mental illness. Therefore, we investigated the effect of four prestimulus TCNs – the DMN, the dorsal attention network (dAN), the left and right WMNs – upon three EEG frequency bands (theta, alpha, and beta) during WM retention in patients compared to controls. First of all, we aimed at replicating findings in healthy controls to the previous study. Second and more importantly, we wanted to know if we could find evidence for a putative link between the well-known resting-state abnormalities, as seen both in spectral EEG deviations [e.g., Ref. (56)] and differences in fMRI-BOLD TCN dynamics [e.g., Ref. (32)], and the task-induced activation of WM-related brain functions, measured through changes in FM theta. In other words, we wanted to know if it is possible to find support for the hypothesis that a dysfunctional activation of WM functions in schizophrenia may follow from abnormalities in prestimulus resting-state activity. Thus, we expected the previously reported and WM relevant inverse association between the DMN and FM theta band to be reduced in patients.

MATERIALS AND METHODS

The preprocessing and analysis methods are identical to those used by Kottlow et al. (46). As the output data are multidimensional including the different TCNs, frequency bands, number of electrodes, load levels, as well as the two groups, we had to deal with the problem of multiple testing. By means of two analysis methods that eliminate the problem of multiple testing across electrodes, namely, the topographic consistency test (TCT) and the topographic analysis of variance (TANOVA), we reduced

this problem (see Relative EEG Load Effects for further details). In addition, the findings of the mentioned paper were used to *a priori* limit the number of hypotheses that we considered.

Subjects

We included 17 patients (14 males, 3 females; mean age: 34.62 ± SD: 8.79 years) and 17 age and gender matched healthy control subjects (14 males, 3 females; mean age: 31.62 ± SD: 7.06 years) in the study. Data from nine of these controls were included in Kottlow et al. Healthy control subjects were recruited *via* word of mouth.

All subjects satisfied standard inclusion criteria for participation in MRI studies, were right-handed, and had normal or corrected-to-normal vision. All refrained from caffeine and nicotine at least 4 h and alcohol 14 h prior to the experiment.

Patients were recruited at the University Hospital of Psychiatry in Bern, Switzerland. They were diagnosed according to the ICD-10 and DSM-IV either with schizophrenia (F20.0–F20.3; 295.1–295.4/295.6; $N = 9$) or acute and transient psychotic disorder (F23.0–F23.2; 297.1/298.8; $N = 8$). Patients medicated with the atypical antipsychotic medication clozapine were excluded due to its adverse effects on the EEG (57). Other exclusion criteria included comorbidities for other psychiatric disorders, substance abuse (except for nicotine and caffeine), and neurological or other severe medical conditions. Sixteen of the 17 patients received antipsychotics (typical = 1; atypical = 15), 1 received antidepressants, 2 received mood stabilizers, and 2 received tranquilizers. Healthy controls had no history of psychiatric and neurologic disorders and abuse or dependence on psychoactive medication or drugs other than nicotine and caffeine.

Study procedures were approved by the local ethics committee of the canton of Bern, Switzerland (KEK no. 192/05). All subjects gave their written informed consent prior to examination and were aware that they could drop out at any time point and without cause and for patients without treatment consequences. Patients indicating poor understanding of the study were excluded. Treating psychiatrists confirmed the patient's ability to give informed consent. Participation was unpaid. The characteristics of the subjects and clinical variables are given in **Table 1**.

Task and Procedures

The study was conducted on 2 or 3 separate days. On the first day, the neurophysiological measurements were held between 8 a.m. and 12 a.m. at the Inselspital of Bern, Switzerland. Within a week, cognitive performance was assessed by means of four subtests of the Wechsler adult intelligence scale (WAIS III; similarities, digit span, the block design test, and the digit symbol-coding test). Additionally, a clinical-diagnostic interview was performed with patients during the same day as the cognitive assessment or on a third day close to the other assessment days.

The procedures for the neurophysiological measurements were as follows: first, the EEG cap was placed followed by 8 min resting-state acquisition consisting of alternating blocks of 2 min eyes open and closed outside of the scanner. Before going into the MR scanner, subjects performed a short practice version of the WM task. Subjects were placed carefully in the scanner for the simultaneous EEG-fMRI measurements consisting of another 8 min resting state and then the performance of the WM task. After removal of the EEG cap, the anatomical sequences were executed.

In the scanner, stimuli were presented *via* goggles (VisualStimDigital MR-compatible video goggles; Resonance Technology Inc., Northridge, CA, USA). The visual angle of the stimuli was 60° with a resolution of 800 × 600 pixels and 60 Hz refresh rate. An in-house fabricated MR compatible response box was used. Stimuli were delivered and responses registered using E-Prime (Version 2.0.10.553, Psychology Software Tools, Inc.).

To assess verbal WM processes, a version of the Sternberg Item Recognition Paradigm [SIRP; Ref. (58)] adapted from Michels et al. (45) was used. This paradigm allows the temporal separation of the encoding of memory items (*encoding phase*), retaining them (*retention period*), and their retrieval (*probe period*). Either two (*load 2*) or five (*load 5*) consonants were presented in an array of 3 × 3 items with the remaining positions being plus signs (+). The positions of the consonants were counterbalanced across trials, with the center one being excluded. This array was presented in black font on a white background surrounded by a red frame. One trial included a stimulus array presented for 2.5 s, followed by the retention period consisting of a centered fixation cross (+) for 3.5 s. Then, in the probe period, one consonant was presented in the center for 2 s. There was a variable duration (range: 1.8–2.5 s, mean: 2 s) inter-stimulus interval (ISI) before the next trial with the centered fixation cross. Subjects had to indicate by bottom press whether the probe letter was presented before or not (the use of the right index and middle finger to indicate "yes" or "no" answers was counterbalanced between subjects). The task included 8 blocks per load condition comprising 4 trials each, resulting in 32 trials per load condition. Between blocks, the fixation cross was displayed for 2.5 s. Five times throughout the task, a centered fixation star (*) was projected during 24.5 s of rest. Task duration was 13 min. **Figure 1** illustrates the experimental design for one trial, and **Figure 2** the task design.

EEG Acquisition and Preprocessing

The EEG was measured using a 96-channel MR compatible system from Brain Products (Gilching, Germany; Input range: 16.3 mV, resolution: 16 bit). Ninety-two electrodes were mounted in an elastic cap according to the international 10–10 system. Additionally, two channels each were used to measure the electrocardiogram (ECG; below the clavicles) and the electrooculogram (EOG; below the eyes). Electrode Fz was used as recording reference. Three BrainAmp MR compatible amplifiers were connected to 32 channels each and connected to the acquisition computer *via* fiber cables for safety reasons. The EEG was online bandpass filtered between 0.1 and 250 Hz and sampled with 5 kHz. We aimed at keeping electrode impedances below 20 kΩ while restricting the duration of entire EEG preparation to 1 h in order to avoid tiring the subjects. Across subjects, 90% of all electrodes had impedances below 25 kΩ, 5% were higher than 30 kΩ of which only 14.7% of subjects shared common electrodes and mean impedance was 17.5 kΩ. To avoid aliasing artifacts, the clock of the recording computer was synchronized to the clock of the MR system (10 kHz refresh rate), and each MR scan volume was automatically marked in the EEG data.

TABLE 1 | Descriptive and clinical variables of subjects.

	Patients ($N = 17$)		Controls ($N = 17$)		*T*-tests
	(m/f)	%	(m/f)	%	
Gender	14/3	82.4/17.6	14/3	82.4/17.6	
	Mean	**SD**	**Mean**	**SD**	***p* (df = 32)**
Age (years)	34.62	8.79	31.62	7.09	0.281
WAIS III (*t*-values)	43.47	7.12	55.88	5.18	<0.001
Duration of illness (months)	66.66	67.86			
Number of episodes	3.88	3.44			
CPZE	344.17	236.28			
DPZE	0.2	0.7			
PANSS positive	12.65	4.47			
PANSS negative	12.82	7.76			
PANSS total	52.12	22.94			

WAIS III, Wechsler adult intelligence scale (four subtests: similarities, digit span, the block design test, and the digit symbol-coding test); CPZE, chlorpromazine equivalence dosage; DPZE, diazepam equivalence dosage; PANSS, positive and negative syndrome scale.

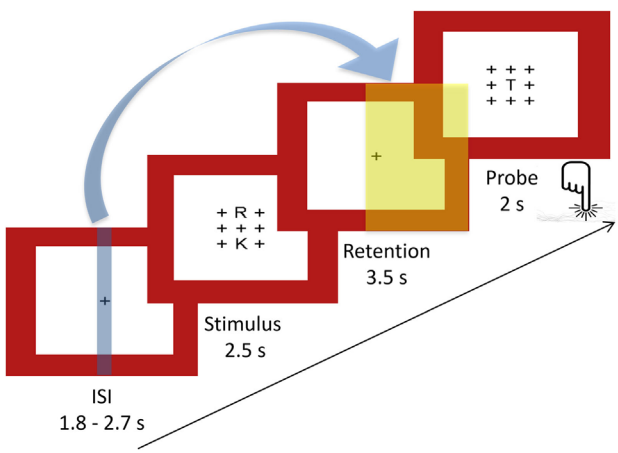

FIGURE 1 | Sternberg WM task: experimental design of a single trial. Indicated with the blue arrow and the blue and yellow plains are the time points of fMRI (blue) and EEG (yellow) markers extracted for the covariance mapping (ISI, inter-stimulus interval, mean: 2 s).

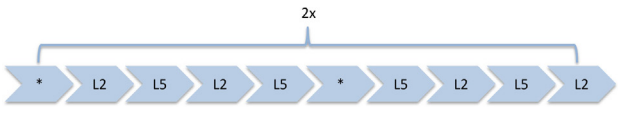

FIGURE 2 | Sternberg WM task: task design. Four blocks of each load (load 2 = L2, load 5 = L5) alternating among baseline conditions (*). Each block contains four trials per load and was followed by a fixation of 2.5 s added to the ISI (+).

Preprocessing was performed using Vision Analyzer (Version 2.0.4.368; Brain Products, Gilching, Germany). Methods used for artifact removal are in accordance with previously published papers (46, 54, 55, 59) and briefly summarized in the following section. The EEG was corrected for artifacts including scan-pulse and cardio-ballistic artifact, using average artifact subtraction with a sliding window (60). Thereafter, for each subject, EEG files from outside and inside of the scanner were down-sampled to 500 Hz and concatenated. The resulting file was then bandpass filtered (1–49 Hz and a notch filter) and bad channels were disabled (in controls: one subject had four disabled channels, one subject had two, two had one channel; in patients: one had five disabled channels, five had one channel). Using an ICA-based approach, the EEG was further cleaned from remaining cardio-ballistic, scan-pulse, and eye movement artifacts. Components loading for artifacts were identified using visual inspection of their temporal dynamics, topographic maps, and the comparison of their power spectra inside versus outside of the scanner. The EEG of each subject was reconstructed from the remaining factors, and epochs containing residual scanner or movement artifacts were marked by visual inspection thereafter. Disabled channels were interpolated using a spherical spline interpolation. Furthermore, the ECG and EOG channels were removed, and the EEG was recalculated to average reference. Finally, the file was separated again into the resting state and verbal WM task.

MRI Data Acquisition and Preprocessing

The recordings were performed in a 3-T Siemens Magnetom Trio MR Scanner (Siemens, Erlangen, Germany) with a 12-channel head coil. The functional T2*-weighted MR images were acquired with an echo planar imaging (EPI) sequence. The characteristics of the sequence were 250 and 406 volumes for the resting state and the Sternberg WM task, respectively, 35 slices, 3 mm × 3 mm × 3 mm, matrix size 64 × 64, FOV 192 mm × 192 mm, TR/TE = 1960 ms/30 ms.

The structural T1-weighted sequence (ADNI) had following parameters: 176 sagittal slices, slice thickness 1.0 mm, voxel size 1 mm × 1 mm × 1 mm, FOV 256 mm × 256 mm, TR/TE = 2300 ms/2.98 ms.

Preprocessing of the functional MRI data was done in SPM8 (Welcome Department of Imaging Neuroscience, London).[1] First, slice time correction was performed, and the data were

[1]http://www.fil.ion.ucl.ac.uk/spm

motion corrected to the mean image. Then, the anatomical T1 was coregistered to the mean image, followed by its segmentation into six tissue probability maps. Finally, the data were normalized and smoothed using an FWHM kernel of 6 mm × 6 mm × 6 mm.

TCN Extraction

To obtain the temporal dynamics of the TCNs from our fMRI data, we applied a spatial–temporal regression implemented in the GIFT toolbox (61).[2] As templates to reconstruct single subject's components, we applied the four components of interest (DMN, dAN, left and right WMNs) from the group-ICA on 24 healthy subjects from the previous study (46). First, the fMRI-BOLD time series of each subject were preprocessed applying the variance normalization option of the toolbox for comparability reasons. Then, the four components of interest were back projected onto the subject's time series. The resulting time courses were *z*-transformed and represent the percent signal strength of each TCN at each volume acquired over whole WM task duration (406 volumes total) of each subject.

Evolution of TCNs over Average Task Trials

Based on previous findings, we expected the DMN and dAN to show opposing dynamics in healthy controls and that these dynamics would be relevant for performance (46, 62–65). To reveal whether differences in performance between patients and healthy controls could be related to the relative pre- or post-stimulus network activations of the DMN and dAN, their mean dynamics where extracted from the time courses of these TCNs of the prestimulus period (−4.3 until −2.5 s before retention onset) and the retention period (0 until 3.5 s). These mean dynamics were then compared for each time point with a three-factorial ANOVA (2 × 2 × 2) with the factors network, load, and group. To check whether pre- to postdifferences could be ascribed only to the higher load condition (load 5), another ANOVA was performed including the factors pre–post, network and group for load 5 only (2 × 2 × 2 factorial design). Furthermore, separate ANOVAs were conducted for the prestimulus and retention periods for each TCN for the factors of load and group ($2 \times 4 = 8$ ANOVAs with a 2 × 2 factorial design). Using in-house Matlab scripts, we additionally plotted the TCN dynamics. Therefore, in a time window from −4.3 to 5.5 in reference to the retention period each TCN time course was interpolated on a 0.1-s time scale using the Matlab spline interpolation and averaged across trials for each group and load condition. The five baseline periods were disregarded from that time window. Using *t*-test statistics, these averaged dynamics were compared every 0.1 s against 0 within (two-tailed one-sample *t*-tests) and between (two-tailed unpaired samples *t*-tests) load levels and groups.

Spectral Power Differences during Resting State

To check for spectral power differences during the resting-state condition with eyes closed, the cleaned resting-state EEG file was segmented into the eyes closed condition only, resulting in 4 min of continuous EEG. Then, the EEG was segmented into equally sized segments (2.048 s) and a fast Fourier transformation (resolution: 0.48828 Hz, hanning window: 10%) was performed. Afterwards, frequency bins were collapsed into the three frequency bands theta (3–7 Hz), alpha (8–12 Hz), and beta (13–20 Hz). For each subject, the average across all segments and the global spectral power across all channels were calculated. Finally, patients and controls were compared with frequency bin wise *t*-tests.

Relative EEG Load Effects

Similar to Kottlow et al. (46), relative load effects defined as ratio of high versus low load were calculated. Therefore, the cleaned EEG data were segmented from 1 to 3.5 s within the retention period for correctly answered trials for each load separately. For each frequency band (theta, alpha, and beta), relative load effects were computed. Furthermore, the software package Ragu,[3] which is based on randomization statistics was used to check the spatial stability of the load effects for each frequency across subjects per group with the TCT [for a detailed description of the methods, see Ref. (66)]. As this test is run across all electrodes at once, the problem of multiple testing is being reduced. Where significant TCTs resulted for the same frequency bands per group, topographic analyses of variance (TANOVAs) were run in Ragu to check for significant topographical differences between groups. With this analysis too, the problem of multiple tests is decreased due to the comparison of topographies as a whole, not single electrodes. Other comparisons are not meaningful due to the lack of consistency across subjects.

Covariance Mapping

As the aim of the study was to explore state dependency within a WM task incorporating both fMRI and EEG measures at different time points, we used a method suitable for multivariate datasets, the so-called covariance mapping. Hereby, EEG scalp topographies representing the channel-wise covariance of a single EEG parameter (such as power at a specific frequency) with another continuous external variable (such as reaction times, but also a single fMRI parameter) are calculated [for further details, see Ref. (67)]. Positive covariance means both variables fluctuate in the same direction together whereas negative values point toward an inverse relationship between the two. We here examined the lagged coupling of the relative signal strengths from four fMRI TCNs at prestimulus with the amplitude of three EEG frequency bands during the retention period of a WM task. Therefore, the cleaned EEG data of the WM task were divided into segments containing the last 2.5 s of the WM retention period for correctly answered trials separately for each load condition and each subject. To extract spectral amplitude of frequencies, a continuous complex Gabor transformation spanning frequencies from 2 to 20 Hz with an envelope having its half maximum at the latency of a full cycle of the oscillation was applied. The single trial epochs were pooled into the previously used frequency bands theta (3–7 Hz), alpha (8–12 Hz), and beta (13–20 Hz). Covariance maps were

[2] http://mialab.mrn.org/software/gift/

[3] http://www.thomaskoenig.ch/Ragu.htm

calculated relating the level of every TCN before stimulus presentation (−3.5 s before retention onset) with the EEG frequency band data (the last 2.5 s within the retention period) for both load levels and every subject separately. Thus, 24 covariance maps were obtained per subject (4 TCN × 3 Frequency bands × 2 loads).

The subsequent analyses were performed again with the software package Ragu. First, TCTs were run on the covariance maps averaged over the whole time window (1.0–3.5 s within the retention period) for each TCN and frequency band across subjects per group. We further explored differences in covariance maps between groups if both groups showed significant TCTs for the same conditions according to the procedure for the relative load effects. For covariance maps that were significantly consistent within both groups, TANOVAs were computed to check whether the topographies of the covariance maps were significantly different between groups and load levels. Significant effects were then visualized using *t*-maps. To explore whether covariance maps were affected by medication (chlorpromazine equivalence dosage = CPZE), the severity of symptoms (PANSS positive, negative, and total scores), or cognitive performance (*t*-values of summed WAIS III subtests), for every TCN, we ran TANCOVAs with each of these variables as covariates.

Finally, based on the existing literature, we expected that control subjects would show a focal inverse relationship of theta at frontal electrodes [Fz: Ref. (40, 45) or AFz: Ref. (46)] with DMN activation in the prestimulus interval (46) selectively for the high-load condition. We therefore tested in a FM theta analysis the covariance of these specific electrodes (Fz and AFz) for load and group differences.

Figure 3 provides an overview of all analyses steps applied on the EEG and fMRI data separately as well as their joint analyses.

RESULTS

Behavioral Data

For an overview of the results see **Table 2**. We performed two ANOVAs for reaction times and accuracies (2 × 2 factorial design with factors load and group). The ANOVA for reaction times resulted in a significant main effect load ($p \leq 0.001$) and group ($p = 0.023$), but no significant interaction effect ($p = 0.708$). The ANOVA run for accuracies (percent correctly answered trials) yielded a significant main effect load ($p = 0.001$) and interaction of load by group ($p = 0.017$), but scarcely no significant main effect group ($p = 0.056$). To further explore this result, independent sampled *t*-tests were run to check for differences in accuracy between groups for each load level separately. It resulted that the significant interaction from the ANOVA was driven by a significant effect of load 5 only (load 2: $t = 0.585$, df = 32, $p = 0.563$; load 5: $t = 2.588$, df = 32, $p = 0.014$). The performance across both loads ranged in controls from 81.25 to 100% and in patients from 62.5 to 100%, indicating that all subjects were able to perform the task above chance level.

Evolution of TCNs

The mean activations of pre–post (prestimulus and retention period) for the DMN and dAN for both loads are shown in **Figure 4**. The three-factorial ANOVA for the prestimulus interval revealed a nearly significant interaction of TCN by group ($p = 0.053$), whereas no significant effect arose for the retention period. Further analysis indicated that healthy controls showed the anti-correlation of the two networks known in the literature (46, 62, 63, 68), the DMN was significantly lower than the overall mean level (one-sample *t*-test, $p = 0.0058$) as opposed to a significantly enhanced dAN (one-sample *t*-test, $p = 0.029$). In patients, no systematic deviations from the mean could be observed. In addition, significant performance differences were limited to load 5. The respective ANOVA (2 × 2 × 2 factorial design with factors network, pre–post and group for load 5) supported this finding by a significant interaction effect of the factors pre–post and group ($p = 0.028$). The ANOVAs run separately for each network at prestimulus and retention period with factors load and group revealed a significant main effect of load ($p < 0.001$) for the DMN and a main effect of group ($p = 0.023$) for the dAN at prestimulus period. In the retention period, a significant load effect ($p = 0.013$) and a group effect ($p = 0.021$) resulted for the WMN on the right.

The time resolved event-related TCN dynamics are represented in **Figure 5**. For healthy controls, the fluctuations of their four TCNs were comparable to those seen in the preceding study (46). Main findings were the significant load-dependent decrease of the DMN from prestimulus until the retention period, while the dAN displayed a different pattern with higher activation in the prestimulus period decreasing in the middle of the retention period thereafter. A stronger recruitment of the WMN on the left was present over the entire trial period in the more challenging condition. This was not the case for the WMN on the right, which was even suppressed during encoding of the memoranda and the first second of the retention period.

In patients, a reduced suppression of the DMN for trials at load 5 was seen. The group effect reached significance from the beginning until 2.2 s of the retention period (*p*-values: ≤0.048 and ≥0.031). The evolution of the dAN was comparable to the one in control subjects apart from a reduced activation level for higher load trials during prestimulus as well as for lower load trials in the probe period (significant group effect from 1.4 s until the end of the 2-s probe period, *p*-values: ≤0.049 and ≥0.048). Comparing the evolution of left and right WMNs, patients did not show the lateralization effect seen in controls for the more difficult WM condition: their WMN on the left was not as activated as in controls (in spite of showing the same evolution pattern), whereas the WMN on the right grew stronger toward the end of the stimulus and over the whole retention period (group effect with maximum *p*-value of .02). Finally, there was a group by load interaction in the left WMN during stimulus period (*p*-values: ≤0.045 and ≥0.0162), which could be explained by controls having greater left WMN recruitment at load 5 and smaller at load 2 than patients during encoding the memoranda.

Spectral Power Differences during Resting State

Regarding the preprocessing of the EEG data *via* ICA, there was no significant difference in the number of removed components between groups (controls: mean = 20.5, SD = 2.7; patients:

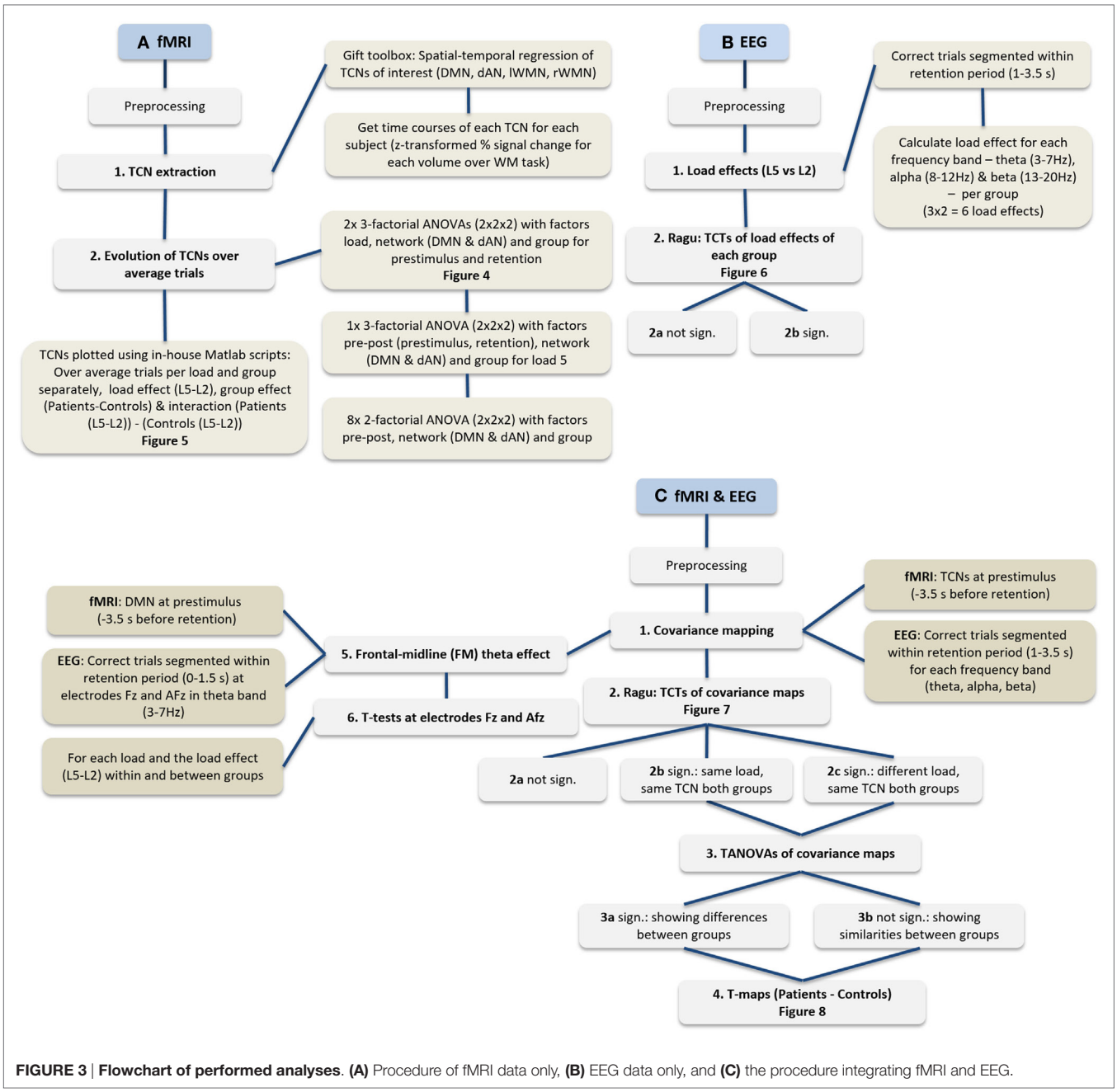

FIGURE 3 | Flowchart of performed analyses. (A) Procedure of fMRI data only, **(B)** EEG data only, and **(C)** the procedure integrating fMRI and EEG.

TABLE 2 | Behavioral results of the WM task.

	Patients (*N* = 17; 14 = m, 3 = f)		Controls (*N* = 17; 14 = m, 3 = f)	
	Mean	**SD**	**Mean**	**SD**
RT all (ms)	1162.16	186.48	975.98	224.20
RT L2 (ms)	1018.7	196.4	852.07	205.28
RT L5 (ms)	1283.25	225.62	1099.02	267.03
Acc all (%)	89.43	9.6	94.76	4.97
Acc L2 (%)	94.12	8.26	95.59	6.26
Acc L5 (%)	84.93	13.18	93.93	5.68

Means and SDs of reaction times (RTs) and accuracies (Acc) for each load level (L2, L5) separately and merged (All) for each group.

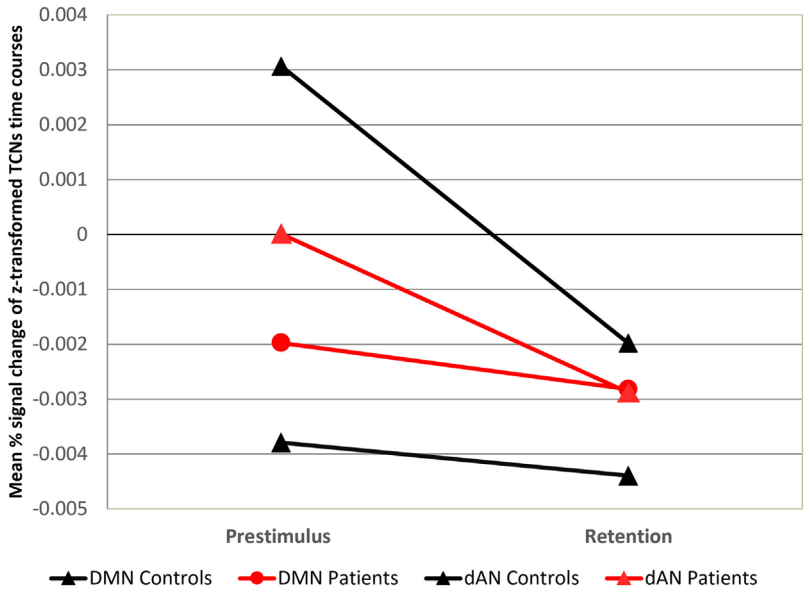

FIGURE 4 | **Mean DMN and dAN from pre- to poststimulus in the WM task**. Mean DMN and dAN dynamics at prestimulus and retention intervals for each load and group. *X*-axis: time points (prestimulus and retention period), *Y*-axis: mean percent signal change of variance normalized, and *z*-transformed TCNs.

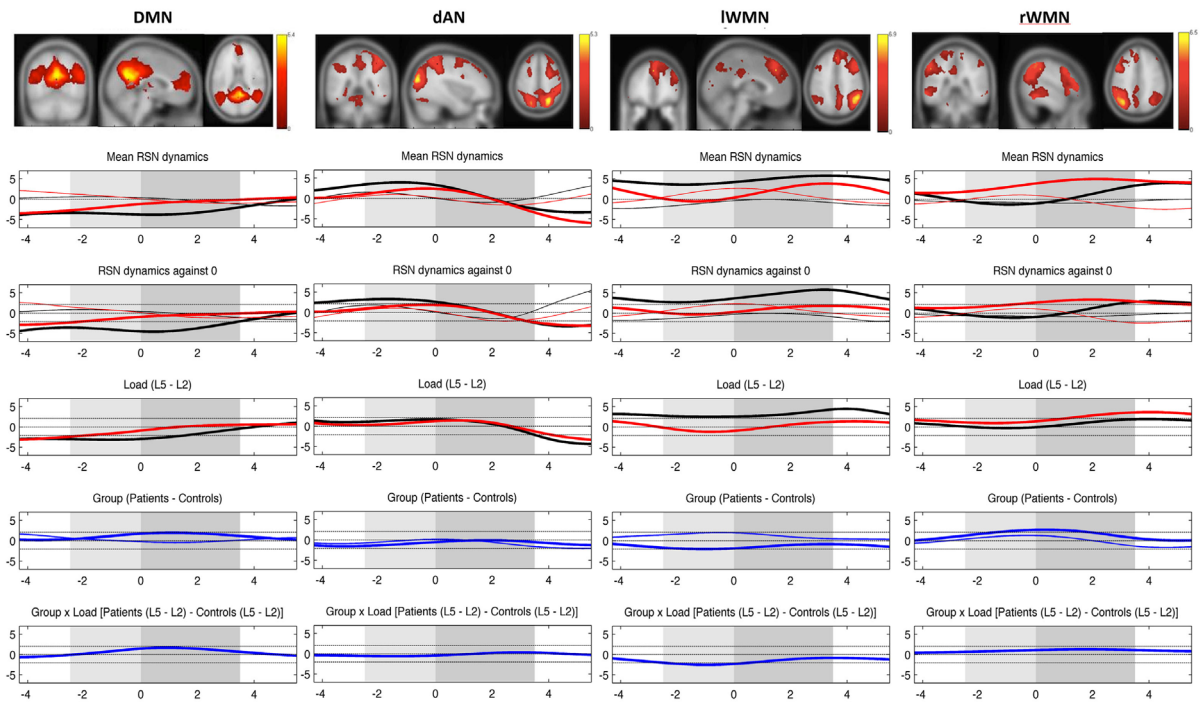

FIGURE 5 | **Mean evolution of TCNs over average trials**. Upper plot shows the templates for each TCN from the study of Kottlow et al. with the three orthogonal slices through areas of maximum activation (only positive values; for detailed information about included regions, see Table S1 in Supplementary Material). Lower plots display the mean network evolutions over average trials for each load (thin line = load 2; thick line = load 5) and each group (black line = controls; red line = patients). Dashed lines indicate significance of the *t*-tests (two-sided, $p = 0.05$): (1) mean evolutions, (2) mean evolutions against 0, (3) load effect, (4) group effect (blue thin line = load 2; blue thick line = load 5), and (5) interaction of group by load. *X*-axis: time over trial [prestimulus: −4 to −2.5 s; stimulus (light gray block): −2.5 to 0 s; retention (dark gray block): 0–3.5 s; probe: 3.5–5.5 s], *Y*-axis: percent signal change of variance normalized, and *z*-transformed TCNs' time courses.

mean = 18.4, SD = 3.4 out of 64 components, $t = 1.994$, df = 32, $p = 0.055$).

The comparison of the power spectra between the groups resulted in a significant elevation of theta (4.7–6.6 Hz, $t > 2.0369$, $p = 0.05$, double-sided) as well as beta (15.1–16.5 and 18.1–20 Hz, $t > 2.0369$, $p = 0.05$, double-sided) band in patients compared to controls (Figure S1 in Supplementary Material).

Relative EEG Load Effects

Topographic consistency tests were done in Ragu to check the stability of load effects for each frequency band and group (3 frequency bands × 2 groups = 6 TCTs). In controls, all three TCTs of their load effects revealed significantly consistent topographies (p-values: theta = 0.0002, alpha = 0.0002, and beta = 0.0002). In patients, however, none of the load effects had significant topographic consistency (p-values: theta = 0.986, alpha = 0.983, and beta = 0.995). **Figure 6** shows that controls had positive load effects in all frequency bands that included frontal and left temporo-parietal sites and had a local maximum at the expected position Fz in the theta band (maximum t-value at P9 = 5.25, t-value at Fz = 3.33). No TANOVA could be performed, as there was no significant effect in patients to be compared to the topography of controls.

Covariance Maps

For the analysis of the covariance maps, the data of 16 patients and 16 matched controls were analyzed as 1 patient lacked enough clean EEG segments (16 good segments out of 64). Healthy controls showed a higher number of consistent covariance maps than patients over all TCNs and frequency bands (out of 24 total TCTs, 8 were significant in patients and 9 in controls, see **Figure 7**). Highlighted in the figure are these maps, which were compared further between groups (being referred to cases 2b and 2c in **Figure 3C**). Coupling between the DMN at prestimulus and theta frequency during retention in high-load trials was significantly different in the two groups representing case 3a in **Figure 3C** (TANOVA: $p = 0.015$; t-min = −3.9, $p = 0.119$ at TP7; t-max = 1.6, $p = 0.00046$ at PO8, see **Figure 8**). Patients showed in general a rather left lateralized and a much more extended inverse coupling than controls.

Looking at the dAN with theta band, patients' covariance map of load 2 resembled controls map of load 5. Their topographies seemed visually similar with mainly negative covariance at frontal, central, and parietal electrodes, which was further confirmed by the TANOVA not yielding a significant difference between the groups (TANOVA: $p = 0.31$, case 3b in **Figure 3C**.). For the dAN with alpha frequency, both load conditions had significant TCTs for both groups and they visually all looked very similar having extended negative couplings matching again Kottlow et al. (see **Figure 7**, case 3b in **Figure 3C**). We assessed load, group, and group by load interactions with the TANOVA and found no significant effects, suggesting that there was no specific topographic coupling of the dAN with alpha for load or group. Finally, we found significant TCTs of the right WMN with alpha for patients at load 5 and controls at load 2. Similar to the dAN with theta, the TANOVA revealed no significant effects (TANOVA: $p = 0.57$, case 3b in **Figure 3C**), thus both covariance maps resembled each other. The maps demonstrated again mainly inverse but also some positive association at centro-parietal areas.

None of the computed TANCOVAs including covariates as medication, severity of symptoms, and cognitive performance was significant, and we therefore have no reason to believe that our covariance maps were influenced by any of these factors.

In controls, the planned FM theta analysis indicated the expected inverse relation of prestimulus DMN level with frontal theta specifically for the high-load condition. However, this effect was only significant in the mean of the first 1.5 s of the retention

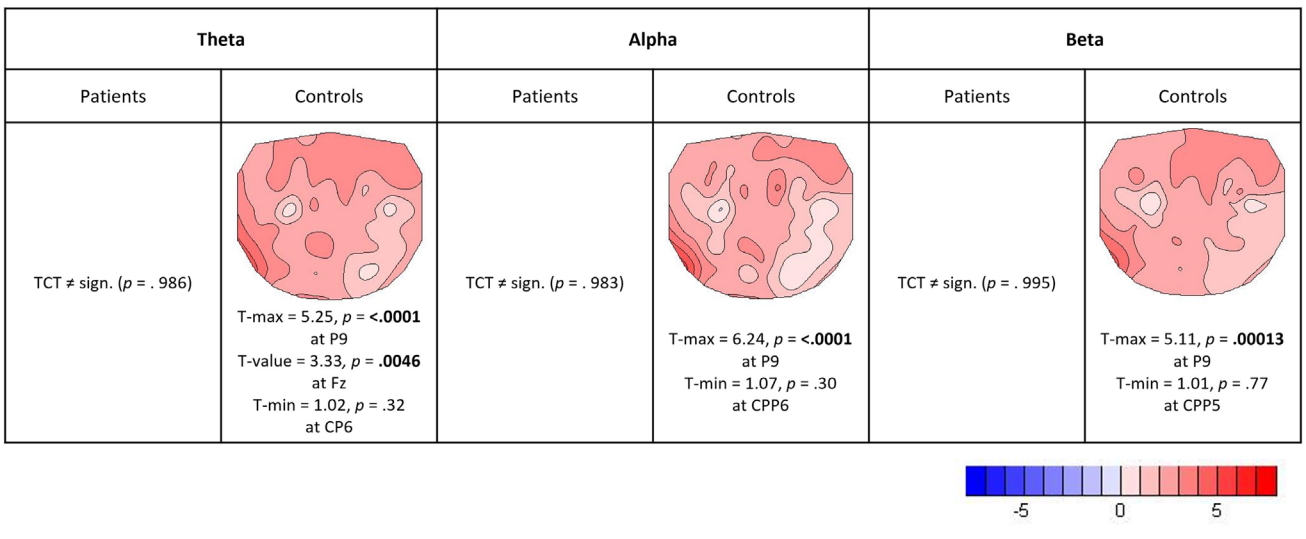

FIGURE 6 | Relative load effects (load 5 versus load 2). *T*-maps with maximum and minimum *t*-values and their significance level (two-sided, $p = 0.05$) are indicated for those frequency bands and groups where the TCT reached significance.

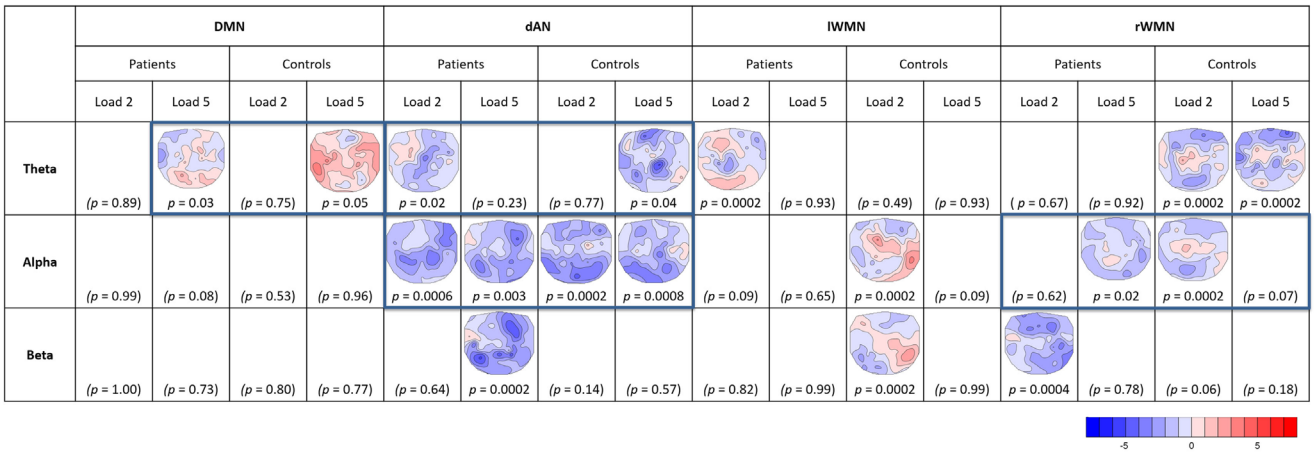

FIGURE 7 | **Overview of significant TCTs of covariance maps**. For each TCN (DMN, dAN, left and right WMNs), frequency band (theta, alpha, and beta), and load (L2, L5) per group (patients, controls). *T*-maps of significant TCTs (two-sided, $p = 0.05$) are indicated (blue = negative, red = positive covariance). Framed maps were further compared between groups.

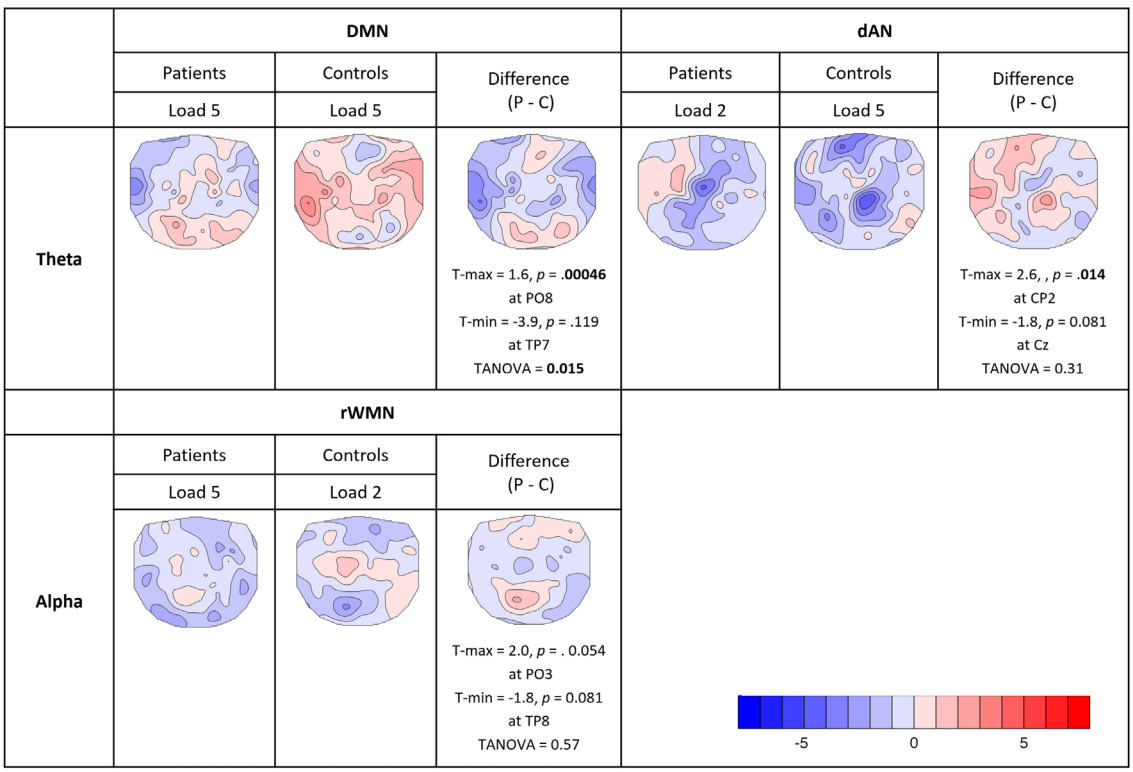

FIGURE 8 | **Comparison of consistent covariance maps between groups**. Where the TCTs were significant for both groups within the same TCNs and frequency bands, TANOVAs were run to check for significant spatial differences or similarities. Displayed in the figure are *t*-maps for each group and their difference (patients – controls) showing electrodes with maximum and minimum *t*-values, the significance levels (two-sided, $p = 0.05$) and the results of the TANOVAs.

period. Namely, theta covariance during load 5 at Fz was more negative than 0 ($t = -1.76$, df = 15, $p = 0.049$, single-sided), and significantly more negative for the load 5 compared to the load 2 condition ($t = -2.72$, df = 15, $p = 0.016$). In patients, no consistent covariance was found during load 5 ($t = 0.22$, df = 15, $p = 0.83$), and no difference between loads was found ($t = 0.73$, df = 15, $p = 0.48$). The load-dependent effects in FM theta covariance (load 5 – load 2) were significantly different between groups

($t = 2.25$, df $= 30$, $p = 0.032$). At electrode AFz, these effects were far weaker and not significant. We note that while in the mean, a negative covariance of prestimulus DMN activation and FM theta during retention was present over the entire analysis period, the effect was only significant in a time window before the analysis period we had initially chosen. Since this analysis period was primarily chosen based on previous literature that had not considered such pre- to poststimulus interactions, we reanalyzed the data of the study by Kottlow et al. (46) that first reported this type of interactions. The reanalysis of this data showed that the described effect could also be found in the early time period as reported here. We therefore felt it was more appropriate to adjust the analysis window rather than rejecting the result due to the difference in timing.

DISCUSSION

To expand the current understanding of the neurophysiology underlying WM deficits in schizophrenia, we explored the modulatory effect of prestimulus fMRI-BOLD networks on EEG spectral power during the subsequent memory retention interval.

Overall, we found consistent and specific topographies of the relative EEG load effects as well as a coupling of prestimulus TCNs with EEG oscillatory frequencies during the retention period. We replicated earlier findings reported by Kottlow et al. (46). Namely, healthy subjects showed similar dynamics of the TCNs, and we mainly saw load effects pointing toward significant changes for more difficult trials. Thus, we can argue that the WM task of load 2 recruits few cognitive resources resulting in little change captured by the neurophysiological measures. Consequently, the prestimulus neurophysiological state of the brain relates to subsequent processing of information in a demand-dependent manner and may therefore support or interfere with cognitive functioning.

Regarding the patient data, our resting-state analysis replicated established reports on increased power in slow frequencies as theta and also higher frequency beta band (55, 56, 69–72).

In general, subjects were significantly slower to respond to more difficult trials. In agreement with existing literature, patients had significantly prolonged reaction times for the execution of the WM task (14, 31, 33). Interestingly, there is a recent publication that could link reaction time to prestimulus theta band activity in an identical WM task in healthy subjects (73).

The accuracy level significantly dropped for the higher load level over all subjects and patients were significantly less accurate in responding to load 5 trials compared to control subjects (84 versus 94%). However, the overall high behavioral accuracy (mean patients: 89.43%, mean controls: 94.76%) indicated that the higher load condition was still within the range of WM capacities in patients. According to studies including even higher load conditions in a similar WM paradigm (18, 33, 74), we would expect that just a small increment of the difficulty level would have led to further substantial drops in patients' performance.

Our results in controls also demonstrated the known theta band load effects during the retention period and deviations in the patient data. In patients, no evidence for consistent load effects in any of the three investigated frequency bands was found. The lack of the classical theta band load effect in patients with schizophrenia is consistent with WM dysfunction reported in the literature. That alpha band was not affected by load in patients and may reflect counter-veiling roles of alpha oscillations to inhibit irrelevant brain regions while supporting demands on attention (75). Finally, beta band power seems to be less affected by load than alpha and theta. The increase in left parietal beta power is opposite to other studies that showed increased power in occipital (45, 46) and temporal regions (52, 53). It is consistent, however, with an early report of beta power at parietal areas being involved in cognitive tasks (76). The analysis of the load effects therefore indicates that in patients there was substantially less load-dependent modulation of WM functions suggesting that independent of load, patients were closer to their WM capacity limits.

Healthy controls showed the expected anti-correlation of the DMN and dAN. This is in agreement with their attributed functional role of external versus internal orientation of attention, respectively (62, 63, 68). Furthermore, better performance in cognitive tasks, indexed by shorter and less variable reaction times, was linked to higher anti-correlations of the DMN and dAN leading to the discussion of anti-correlation between dAN and DMN being a possible marker for efficient cognitive processing (64, 65). This finding could be refined by relating WM performance in healthy subjects to higher anti-correlations of two hub regions of these networks, namely, the medial prefrontal cortex (mPFC) of the DMN and the dlPFC of the dAN at resting state (77). In addition, the significant prestimulus effects, namely, a reduction of the DMN and an increased activation of the dAN during the high-load condition imply that control subjects allocated their processing resources accordingly to task difficulty.

On the other hand, patient data gave evidence of a reduced anti-correlation of the DMN and dAN from prestimulus until the end of the WM retention at load 5, supporting the hypothesis of a deviant orientation of attention to internal versus external events. In particular, in patients, there was a reduced activation of the dAN during the prestimulus period and reduced suppression of the DMN during the retention period. Findings of altered activation of the dlPFC, a hub region of the dAN that is crucially involved in WM performance were frequently reported in schizophrenia. However, depending on the study, both under- as well as over-activations of the dlPFC have been discovered (12–16). As reported in the introduction, deviations in the form of reduced DMN suppression during WM tasks in schizophrenia are also well established and could be extended to youth at high-risk as well as unaffected siblings (31–34). Consequently, these results suggest that in patients there is a less coherent pattern of task-dependent preparatory processes.

Additionally, we found a missing lateralization effect regarding the recruitment of WMNs at higher load in patients. In controls, we observed a higher involvement of the left WMN over the whole trial duration. Patients in contrast showed less activation of the left WMN and a significantly higher involvement of right WMN during the retention period. In accordance with a study revealing relevance of left hemispheric WMN for

verbal compared to right for spatial WM tasks in healthy subjects and its absence in patients (78), this finding could be interpreted either as inefficient inhibition of the task-irrelevant hemisphere or might be a compensation effect. The interpretation of this finding is hampered by controversial reports about hemispheric dominance in the literature. Although some studies seem to support left-sided dominance for verbal and right for spatial and object information (79), others showed bilateral involvement of the dlPFC as part of the WMNs (80) or even right hemispheric dominance, but left-sided being more commonly reported (81). These differences might be related to specifics of the WM tasks as well as methodologies of TCN extractions and definitions. It thus remains a question for future research to address.

Coming to the central aim of the present study, namely, the interaction of prestimulus TCN dynamics with task-related EEG spectral changes, the previous findings could be at least partly accounted for by the results from the covariance analyses. These covariance analyses can be considered as a biological fingerprint of the mechanisms that link preparatory activity captured by systematic prestimulus dynamics of specific TCNs to poststimulus, content-related processes.

First, in controls, the activation level of prestimulus DMN was negatively related to FM EEG theta during WM retention in a load-dependent manner. In patients, we found no FM effect for more difficult trials. Based on a previous finding that the stronger the inverse relationship between DMN and FM theta the better WM performance (82), we argue that a decreased effect in patients impacts their WM performance. In controls, the covariance map of the DMN with theta band at higher WM load resembled the one from the preceding study of Kottlow et al. (46). Therefore, we can argue that their map gave evidence that there are mechanisms through which prestimulus task dependent and therefore adaptive changes of TCN dynamics enhance task execution. The fact that the covariance map of the DMN was significantly different in patients and did not resemble a reversed EEG load effect indicates that such pre- to poststimulus processes did not affect the same poststimulus processes as in controls. This is especially interesting considering that the DMN activity did not differ significantly between groups in the prestimulus period, suggesting they were equally prepared for the task, but could not rally the necessary increase in theta band activity. During resting state, the study of Razavi et al. (55) found that for the DMN, the covariance maps of patients in the theta and alpha band were similar to the ones of controls in the beta band, indicating that the functional coupling of the DMN is changed in patients. Furthermore, as mentioned earlier there is the evidence of heightened theta power at rest in this patient population, which might partly explain the disclosed differences too. As our reported findings refer to task-related activations, it remains to be solved how the different coupling of the DMN with theta band can be explained. However, this finding demonstrates a difference in the functional state of the DMN in schizophrenia patients and might explain alterations in their cognitive processing.

Second, besides the reduced activation of patients' dAN before encoding memoranda of five items, the coupling of the dAN with theta at lower load resembled the one at higher load in controls. This may be explained by the hypothesis that the retention of five items for controls and two items for patients depended on similar prestimulus attentional processes. The absence of such a link in controls at load 2 may then indicate that such attentional processes were irrelevant, whereas patients at load 5 were at their capacity limits and we observed a ceiling effect. The results of their performance showed the same pattern with the accuracy for patients at lower load (94.12%) being close to the one for controls at higher load (93.93%). The finding is in line with the left-shifted inverted *U*-shaped relationship between dlPFC activation and WM load in schizophrenia (74, 83, 84): higher activation levels are found in the dlPFC in patients at lower WM loads as well as reduced activity with increasing error rates at higher memory loads. Consequently, the WM system of patients seems to reach its capacity limits earlier (12, 13, 18, 74). This effect has been found not only in the dlPFC but also in the right parietal and left cingulate regions (83).

To conclude, the reported findings favor the view that in patients with schizophrenia is not only the balance of up- and downregulation of functional brain networks altered but also the relationship between pre-encoding activation and EEG power later during the retention interval. Despite only including trials with correct performance, we argue that the data presented here might at least partly explain well-known deficits in cognitive tasks such as WM. Furthermore, the findings of altered power spectra in patients during resting state indicates that these impairments might be of more generalized nature than only during a WM task as here investigated. Future studies should address the question of these impairments being rather state or trait markers. This work provides new insights regarding WM processing in schizophrenia and might motivate possible treatment strategies such as neurofeedback (85, 86) targeting preparatory brain states as for example the dAN, which showed a lack of anticipatory activation patterns in patients as an important factor for cognitive functioning in this disorder. Still, the specificity of these findings to WM performance needs to be proven.

One limitation of the study is the restriction of data due to the lack of both consistent load effects and covariance maps across groups. However, this is a meaningful outcome as patients showed less topographic consistencies both of relative EEG load effects and of their coupling of TCNs with EEG driving frequencies than healthy controls. The few consistent covariance maps for TCNs with beta band for both groups were in line with the finding of weaker load-dependent beta band effects, which might implicate that beta band was not crucially involved for successful WM performance. Somehow conflicting was the result of the right WMN coupled with alpha band at load 5 in patients being similar to load 2 in controls. The topography of the covariance map is comparable to previous studies at rest and during WM, but we might only speculate about the possible reason for the finding of coupling at higher load with alpha in patients resembling the one at lower load in controls. Therefore, we suggest that this finding should be taken cautiously and needs further evaluations. Other aspects for further investigations is the sensitivity of the time windows being crucial for successful WM performance, as we found different time windows to be critically different between controls and patients with schizophrenia, and the extension of

the selection of TCN templates to be investigated. Finally, even though we took the medication dosage as covariate into account in our analyses, there is a study indicating that atypical medication other than clozapine, which has been excluded here, can lead to EEG abnormalities in patients and that these abnormalities are not correlated to the chlorpromazine equivalence dosage (87). However, the analyses of EEG correlates of TCN fluctuations and the analyses of the load effects are mathematically independent of constant changes in EEG spectral power. So, if one assumes that drug-induced EEG effects do not significantly interact with the experimental task, medication is not expected to play a significant role.

AUTHOR CONTRIBUTIONS

AB and TK wrote the manuscript; AB, LDH, and KR performed the measurements; AB, MK, and TK conceived and implemented experimental procedures and scripts for analyses; AB, TK, and JMF critically revised the manuscript.

ACKNOWLEDGMENTS

The Swiss National Science Foundation Sinergia Grant CRSII3_136249 and DocMobility Grant #P1BEP3_158984 supported this work. We thank the rest of the Sinergia team for their conceptual and practical help: Prof. Dr. Peter Achermann, Prof. Dr. Daniel Brandeis, Prof. Dr. Lutz Jaencke, Dr. Carina Klein, Anthony Schlaepfer, and Laura Tueshaus. Furthermore, we appreciate the technical help of Dr. Kay Jann and Prof. Dr. Andrea Federspiel regarding MRI measurements; the MTRA team of the Inselspital for assistance in performing the MRIs; Dr. Nadja Razavi and Dr. med. Alex Wopfner for their introduction and support in conducting clinical-diagnostic interviews; as well as Dr. Ulrich Raub for patients recruitment; and finally, we thank the participants of the study.

SUPPLEMENTARY MATERIAL

The Supplementary Material for this article can be found online at http://journal.frontiersin.org/article/10.3389/fpsyt.2016.00029

REFERENCES

1. Baddeley A. Working memory. *Science* (1992) **255**:556–9. doi:10.1126/science.1736359
2. Weinberger DR, Egan MF, Bertolino A, Callicott JH, Mattay VS, Lipska BK, et al. Prefrontal neurons and the genetics of schizophrenia. *Biol Psychiatry* (2001) **50**:825–44. doi:10.1016/S0006-3223(01)01252-5
3. Gold JM. Cognitive deficits as treatment targets in schizophrenia. *Schizophr Res* (2004) **72**:21–8. doi:10.1016/j.schres.2004.09.008
4. Green MF. Cognitive impairment and functional outcome in schizophrenia and bipolar disorder. *J Clin Psychiatry* (2006) **67**:e12. doi:10.4088/JCP.1006e12
5. Schaefer J, Giangrande E, Weinberger DR, Dickinson D. The global cognitive impairment in schizophrenia: consistent over decades and around the world. *Schizophr Res* (2013) **150**:42–50. doi:10.1016/j.schres.2013.07.009
6. Reichenberg A, Harvey PD. Neuropsychological impairments in schizophrenia: integration of performance-based and brain imaging findings. *Psychol Bull* (2007) **133**:833–58. doi:10.1037/0033-2909.133.5.833
7. Hyde TM, Nawroz S, Goldberg TE, Bigelow LB, Strong D, Ostrem JL, et al. Is there cognitive decline in schizophrenia? A cross-sectional study. *Br J Psychiatry* (1994) **164**:494–500. doi:10.1192/bjp.164.4.494
8. Hill SK, Schuepbach D, Herbener ES, Keshavan MS, Sweeney JA. Pretreatment and longitudinal studies of neuropsychological deficits in antipsychotic-naive patients with schizophrenia. *Schizophr Res* (2004) **68**:49–63. doi:10.1016/S0920-9964(03)00213-5
9. Goldberg TE, Weinberger DR. Effects of neuroleptic medications on the cognition of patients with schizophrenia: a review of recent studies. *J Clin Psychiatry* (1996) **57**(Suppl 9):62–5.
10. Couture SM, Granholm EL, Fish SC. A path model investigation of neurocognition, theory of mind, social competence, negative symptoms and real-world functioning in schizophrenia. *Schizophr Res* (2011) **125**:152–60. doi:10.1016/j.schres.2010.09.020
11. Mancuso F, Horan WP, Kern RS, Green MF. Social cognition in psychosis: multidimensional structure, clinical correlates, and relationship with functional outcome. *Schizophr Res* (2011) **125**:143–51. doi:10.1016/j.schres.2010.11.007
12. Manoach DS, Press DZ, Thangaraj V, Searl MM, Goff DC, Halpern E, et al. Schizophrenic subjects activate dorsolateral prefrontal cortex during a working memory task, as measured by fMRI. *Biol Psychiatry* (1999) **45**:1128–37. doi:10.1016/S0006-3223(98)00318-7
13. Manoach DS, Gollub RL, Benson ES, Searl MM, Goff DC, Halpern E, et al. Schizophrenic subjects show aberrant fMRI activation of dorsolateral prefrontal cortex and basal ganglia during working memory performance. *Biol Psychiatry* (2000) **48**:99–109. doi:10.1016/S0006-3223(00)00227-4
14. Johnson MR, Morris NA, Astur RS, Calhoun VD, Mathalon DH, Kiehl KA, et al. A functional magnetic resonance imaging study of working memory abnormalities in schizophrenia. *Biol Psychiatry* (2006) **60**:11–21. doi:10.1016/j.biopsych.2005.11.012
15. Potkin SG, Turner JA, Brown GG, McCarthy G, Greve DN, Glover GH, et al. Working memory and DLPFC inefficiency in schizophrenia: the FBIRN study. *Schizophr Bull* (2009) **35**:19–31. doi:10.1093/schbul/sbn162
16. Quide Y, Morris RW, Shepherd AM, Rowland JE, Green MJ. Task-related fronto-striatal functional connectivity during working memory performance in schizophrenia. *Schizophr Res* (2013) **150**:468–75. doi:10.1016/j.schres.2013.08.009
17. Glahn DC, Ragland JD, Abramoff A, Barrett J, Laird AR, Bearden CE, et al. Beyond hypofrontality: a quantitative meta-analysis of functional neuroimaging studies of working memory in schizophrenia. *Hum Brain Mapp* (2005) **25**:60–9. doi:10.1002/hbm.20138
18. Metzak PD, Riley JD, Wang L, Whitman JC, Ngan ET, Woodward TS. Decreased efficiency of task-positive and task-negative networks during working memory in schizophrenia. *Schizophr Bull* (2012) **38**:803–13. doi:10.1093/schbul/sbq154
19. Brandt CL, Eichele T, Melle I, Sundet K, Server A, Agartz I, et al. Working memory networks and activation patterns in schizophrenia and bipolar disorder: comparison with healthy controls. *Br J Psychiatry* (2014) **204**:290–8. doi:10.1192/bjp.bp.113.129254
20. Calhoun VD, Kiehl KA, Pearlson GD. Modulation of temporally coherent brain networks estimated using ICA at rest and during cognitive tasks. *Hum Brain Mapp* (2008) **29**:828–38. doi:10.1002/hbm.20581
21. Liang M, Zhou Y, Jiang T, Liu Z, Tian L, Liu H, et al. Widespread functional disconnectivity in schizophrenia with resting-state functional magnetic resonance imaging. *Neuroreport* (2006) **17**:209–13. doi:10.1097/01.wnr.0000198434.06518.b8
22. Bluhm RL, Miller J, Lanius RA, Osuch EA, Boksman K, Neufeld RW, et al. Spontaneous low-frequency fluctuations in the BOLD signal in schizophrenic patients: anomalies in the default network. *Schizophr Bull* (2007) **33**:1004–12. doi:10.1093/schbul/sbm052
23. Zhou Y, Liang M, Tian L, Wang K, Hao Y, Liu H, et al. Functional disintegration in paranoid schizophrenia using resting-state fMRI. *Schizophr Res* (2007) **97**:194–205. doi:10.1016/j.schres.2007.05.029
24. Jafri MJ, Pearlson GD, Stevens M, Calhoun VD. A method for functional network connectivity among spatially independent resting-state components in schizophrenia. *Neuroimage* (2008) **39**:1666–81. doi:10.1016/j.neuroimage.2007.11.001
25. Littow H, Huossa V, Karjalainen S, Jaaskelainen E, Haapea M, Miettunen J, et al. Aberrant functional connectivity in the default mode and central executive networks in subjects with schizophrenia – a whole-brain resting-state ICA study. *Front Psychiatry* (2015) **6**:26. doi:10.3389/fpsyt.2015.00026

26. Garrity AG, Pearlson GD, McKiernan K, Lloyd D, Kiehl KA, Calhoun VD. Aberrant "default mode" functional connectivity in schizophrenia. *Am J Psychiatry* (2007) **164**:450–7. doi:10.1176/appi.ajp.164.3.450
27. Pomarol-Clotet E, Salvador R, Sarro S, Gomar J, Vila F, Martinez A, et al. Failure to deactivate in the prefrontal cortex in schizophrenia: dysfunction of the default mode network? *Psychol Med* (2008) **38**:1185–93. doi:10.1017/S0033291708003565
28. McKiernan KA, Kaufman JN, Kucera-Thompson J, Binder JR. A parametric manipulation of factors affecting task-induced deactivation in functional neuroimaging. *J Cogn Neurosci* (2003) **15**:394–408. doi:10.1162/089892903321593117
29. Daselaar SM, Prince SE, Cabeza R. When less means more: deactivations during encoding that predict subsequent memory. *Neuroimage* (2004) **23**:921–7. doi:10.1016/j.neuroimage.2004.07.031
30. Anticevic A, Repovs G, Shulman GL, Barch DM. When less is more: TPJ and default network deactivation during encoding predicts working memory performance. *Neuroimage* (2010) **49**:2638–48. doi:10.1016/j.neuroimage.2009.11.008
31. Kim DI, Manoach DS, Mathalon DH, Turner JA, Mannell M, Brown GG, et al. Dysregulation of working memory and default-mode networks in schizophrenia using independent component analysis, an fBIRN and MCIC study. *Hum Brain Mapp* (2009) **30**:3795–811. doi:10.1002/hbm.20807
32. Whitfield-Gabrieli S, Thermenos HW, Milanovic S, Tsuang MT, Faraone SV, McCarley RW, et al. Hyperactivity and hyperconnectivity of the default network in schizophrenia and in first-degree relatives of persons with schizophrenia. *Proc Natl Acad Sci U S A* (2009) **106**:1279–84. doi:10.1073/pnas.0809141106
33. Fryer SL, Woods SW, Kiehl KA, Calhoun VD, Pearlson GD, Roach BJ, et al. Deficient suppression of default mode regions during working memory in individuals with early psychosis and at clinical high-risk for psychosis. *Front Psychiatry* (2013) **4**:92. doi:10.3389/fpsyt.2013.00092
34. de Leeuw M, Kahn RS, Zandbelt BB, Widschwendter CG, Vink M. Working memory and default mode network abnormalities in unaffected siblings of schizophrenia patients. *Schizophr Res* (2013) **150**:555–62. doi:10.1016/j.schres.2013.08.016
35. Koukkou M, Lehmann D. Dreaming: the functional state-shift hypothesis. A neuropsychophysiological model. *Br J Psychiatry* (1983) **142**:221–31. doi:10.1192/bjp.142.3.221
36. Eichele T, Debener S, Calhoun VD, Specht K, Engel AK, Hugdahl K, et al. Prediction of human errors by maladaptive changes in event-related brain networks. *Proc Natl Acad Sci U S A* (2008) **105**:6173–8. doi:10.1073/pnas.0708965105
37. Li CS, Yan P, Bergquist KL, Sinha R. Greater activation of the "default" brain regions predicts stop signal errors. *Neuroimage* (2007) **38**:640–8. doi:10.1016/j.neuroimage.2007.07.021
38. Ives JR, Warach S, Schmitt F, Edelman RR, Schomer DL. Monitoring the patient's EEG during echo planar MRI. *Electroencephalogr Clin Neurophysiol* (1993) **87**:417–20. doi:10.1016/0013-4694(93)91206-G
39. Vitali P, Di Perri C, Vaudano AE, Meletti S, Villani F. Integration of multimodal neuroimaging methods: a rationale for clinical applications of simultaneous EEG-fMRI. *Funct Neurol* (2015) **30**:9–20. doi:10.11138/FNeur/2015.30.1.009
40. Scheeringa R, Bastiaansen MC, Petersson KM, Oostenveld R, Norris DG, Hagoort P. Frontal theta EEG activity correlates negatively with the default mode network in resting state. *Int J Psychophysiol* (2008) **67**:242–51. doi:10.1016/j.ijpsycho.2007.05.017
41. Gevins A, Smith ME, McEvoy L, Yu D. High-resolution EEG mapping of cortical activation related to working memory: effects of task difficulty, type of processing, and practice. *Cereb Cortex* (1997) **7**:374–85. doi:10.1093/cercor/7.4.374
42. Jensen O, Tesche CD. Frontal theta activity in humans increases with memory load in a working memory task. *Eur J Neurosci* (2002) **15**:1395–9. doi:10.1046/j.1460-9568.2002.01975.x
43. Onton J, Delorme A, Makeig S. Frontal midline EEG dynamics during working memory. *Neuroimage* (2005) **27**:341–56. doi:10.1016/j.neuroimage.2005.04.014
44. Khader PH, Jost K, Ranganath C, Rosler F. Theta and alpha oscillations during working-memory maintenance predict successful long-term memory encoding. *Neurosci Lett* (2010) **468**:339–43. doi:10.1016/j.neulet.2009.11.028
45. Michels L, Bucher K, Luchinger R, Klaver P, Martin E, Jeanmonod D, et al. Simultaneous EEG-fMRI during a working memory task: modulations in low and high frequency bands. *PLoS One* (2010) **5**:e10298. doi:10.1371/journal.pone.0010298
46. Kottlow M, Schlaepfer A, Baenninger A, Michels L, Brandeis D, Koenig T. Prestimulus BOLD-network activation modulates EEG spectral activity during working memory retention. *Front Behav Neurosci* (2015) **9**:111. doi:10.3389/fnbeh.2015.00111
47. Schmiedt C, Brand A, Hildebrandt H, Basar-Eroglu C. Event-related theta oscillations during working memory tasks in patients with schizophrenia and healthy controls. *Brain Res Cogn Brain Res* (2005) **25**:936–47. doi:10.1016/j.cogbrainres.2005.09.015
48. Haenschel C, Bittner RA, Waltz J, Haertling F, Wibral M, Singer W, et al. Cortical oscillatory activity is critical for working memory as revealed by deficits in early-onset schizophrenia. *J Neurosci* (2009) **29**:9481–9. doi:10.1523/JNEUROSCI.1428-09.2009
49. Jensen O, Gelfand J, Kounios J, Lisman JE. Oscillations in the alpha band (9-12 Hz) increase with memory load during retention in a short-term memory task. *Cereb Cortex* (2002) **12**:877–82. doi:10.1093/cercor/12.8.877
50. Schack B, Klimesch W. Frequency characteristics of evoked and oscillatory electroencephalic activity in a human memory scanning task. *Neurosci Lett* (2002) **331**:107–10. doi:10.1016/S0304-3940(02)00846-7
51. Michels L, Moazami-Goudarzi M, Jeanmonod D, Sarnthein J. EEG alpha distinguishes between cuneal and precuneal activation in working memory. *Neuroimage* (2008) **40**:1296–310. doi:10.1016/j.neuroimage.2007.12.048
52. Leiberg S, Lutzenberger W, Kaiser J. Effects of memory load on cortical oscillatory activity during auditory pattern working memory. *Brain Res* (2006) **1120**:131–40. doi:10.1016/j.brainres.2006.08.066
53. Stokic M, Milovanovic D, Ljubisavljevic MR, Nenadovic V, Cukic M. Memory load effect in auditory-verbal short-term memory task: EEG fractal and spectral analysis. *Exp Brain Res* (2015) **233**(10):3023–38. doi:10.1007/s00221-015-4372-z
54. Jann K, Kottlow M, Dierks T, Boesch C, Koenig T. Topographic electrophysiological signatures of fMRI resting state networks. *PLoS One* (2010) **5**:e12945. doi:10.1371/journal.pone.0012945
55. Razavi N, Jann K, Koenig T, Kottlow M, Hauf M, Strik W, et al. Shifted coupling of EEG driving frequencies and fMRI resting state networks in schizophrenia spectrum disorders. *PLoS One* (2013) **8**:e76604. doi:10.1371/journal.pone.0076604
56. Boutros NN, Arfken C, Galderisi S, Warrick J, Pratt G, Iacono W. The status of spectral EEG abnormality as a diagnostic test for schizophrenia. *Schizophr Res* (2008) **99**:225–37. doi:10.1016/j.schres.2007.11.020
57. Treves IA, Neufeld MY. EEG abnormalities in clozapine-treated schizophrenic patients. *Eur Neuropsychopharmacol* (1996) **6**:93–4. doi:10.1016/0924-977X(95)00057-V
58. Sternberg S. High-speed scanning in human memory. *Science* (1966) **153**:652–4. doi:10.1126/science.153.3736.652
59. Kottlow M, Jann K, Dierks T, Koenig T. Increased phase synchronization during continuous face integration measured simultaneously with EEG and fMRI. *Clin Neurophysiol* (2012) **123**:1536–48. doi:10.1016/j.clinph.2011.12.019
60. Allen PJ, Josephs O, Turner R. A method for removing imaging artifact from continuous EEG recorded during functional MRI. *Neuroimage* (2000) **12**:230–9. doi:10.1006/nimg.2000.0599
61. Calhoun VD, Adali T, Pearlson GD, Pekar JJ. A method for making group inferences from functional MRI data using independent component analysis. *Hum Brain Mapp* (2001) **14**:140–51. doi:10.1002/hbm.1048
62. Fox MD, Snyder AZ, Vincent JL, Corbetta M, Van Essen DC, Raichle ME. The human brain is intrinsically organized into dynamic, anticorrelated functional networks. *Proc Natl Acad Sci U S A* (2005) **102**:9673–8. doi:10.1073/pnas.0504136102
63. Fransson P. Spontaneous low-frequency BOLD signal fluctuations: an fMRI investigation of the resting-state default mode of brain function hypothesis. *Hum Brain Mapp* (2005) **26**:15–29. doi:10.1002/hbm.20113
64. Kelly AM, Uddin LQ, Biswal BB, Castellanos FX, Milham MP. Competition between functional brain networks mediates behavioral variability. *Neuroimage* (2008) **39**:527–37. doi:10.1016/j.neuroimage.2007.08.008
65. De Pisapia N, Turatto M, Lin P, Jovicich J, Caramazza A. Unconscious priming instructions modulate activity in default and executive networks of the human brain. *Cereb Cortex* (2012) **22**:639–49. doi:10.1093/cercor/bhr146

66. Koenig T, Kottlow M, Stein M, Melie-Garcia L. Ragu: a free tool for the analysis of EEG and MEG event-related scalp field data using global randomization statistics. *Comput Intell Neurosci* (2011) **2011**:938925. doi:10.1155/2011/938925
67. Koenig T, Melie-Garcia L, Stein M, Strik W, Lehmann C. Establishing correlations of scalp field maps with other experimental variables using covariance analysis and resampling methods. *Clin Neurophysiol* (2008) **119**:1262–70. doi:10.1016/j.clinph.2007.12.023
68. Kim H. Encoding and retrieval along the long axis of the hippocampus and their relationships with dorsal attention and default mode networks: the HERNET model. *Hippocampus* (2015) **25**:500–10. doi:10.1002/hipo.22387
69. Itil TM. Qualitative and quantitative EEG-findings in schizophrenia. *EEG EMG Z Elektroenzephalogr Elektromyogr Verwandte Geb* (1978) **9**:1–13.
70. Galderisi S, Mucci A, Mignone ML, Maj M, Kemali D. CEEG mapping in drug-free schizophrenics. Differences from healthy subjects and changes induced by haloperidol treatment. *Schizophr Res* (1991) **6**:15–23. doi:10.1016/0920-9964(91)90016-K
71. Sponheim SR, Clementz BA, Iacono WG, Beiser M. Clinical and biological concomitants of resting state EEG power abnormalities in schizophrenia. *Biol Psychiatry* (2000) **48**:1088–97. doi:10.1016/S0006-3223(00)00907-0
72. Galderisi S, Mucci A, Volpe U, Boutros N. Evidence-based medicine and electrophysiology in schizophrenia. *Clin EEG Neurosci* (2009) **40**:62–77. doi:10.1177/155005940904000206
73. Klein C, Diaz Hernandez L, Koenig T, Kottlow M, Elmer S, Jancke L. The influence of pre-stimulus EEG activity on reaction time during a verbal sternberg task is related to musical expertise. *Brain Topogr* (2016) **29**:67–81. doi:10.1007/s10548-015-0433-7
74. Cairo TA, Woodward TS, Ngan ET. Decreased encoding efficiency in schizophrenia. *Biol Psychiatry* (2006) **59**:740–6. doi:10.1016/j.biopsych.2005.08.009
75. Nenert R, Viswanathan S, Dubuc DM, Visscher KM. Modulations of ongoing alpha oscillations predict successful short-term visual memory encoding. *Front Hum Neurosci* (2012) **6**:127. doi:10.3389/fnhum.2012.00127
76. Ray WJ, Cole HW. EEG alpha activity reflects attentional demands, and beta activity reflects emotional and cognitive processes. *Science* (1985) **228**:750–2. doi:10.1126/science.3992243
77. Keller JB, Hedden T, Thompson TW, Anteraper SA, Gabrieli JD, Whitfield-Gabrieli S. Resting-state anticorrelations between medial and lateral prefrontal cortex: association with working memory, aging, and individual differences. *Cortex* (2015) **64**:271–80. doi:10.1016/j.cortex.2014.12.001
78. Walter H, Wunderlich AP, Blankenhorn M, Schafer S, Tomczak R, Spitzer M, et al. No hypofrontality, but absence of prefrontal lateralization comparing verbal and spatial working memory in schizophrenia. *Schizophr Res* (2003) **61**:175–84. doi:10.1016/S0920-9964(02)00225-6
79. Fletcher PC, Henson RN. Frontal lobes and human memory: insights from functional neuroimaging. *Brain* (2001) **124**:849–81. doi:10.1093/brain/124.5.849
80. Wager TD, Smith EE. Neuroimaging studies of working memory: a meta-analysis. *Cogn Affect Behav Neurosci* (2003) **3**:255–74. doi:10.3758/CABN.3.4.255
81. Nee DE, Brown JW, Askren MK, Berman MG, Demiralp E, Krawitz A, et al. A meta-analysis of executive components of working memory. *Cereb Cortex* (2013) **23**:264–82. doi:10.1093/cercor/bhs007
82. White TP, Jansen M, Doege K, Mullinger KJ, Park SB, Liddle EB, et al. Theta power during encoding predicts subsequent-memory performance and default mode network deactivation. *Hum Brain Mapp* (2013) **34**:2929–43. doi:10.1002/hbm.22114
83. Callicott JH, Bertolino A, Mattay VS, Langheim FJ, Duyn J, Coppola R, et al. Physiological dysfunction of the dorsolateral prefrontal cortex in schizophrenia revisited. *Cereb Cortex* (2000) **10**:1078–92. doi:10.1093/cercor/10.11.1078
84. Callicott JH, Mattay VS, Verchinski BA, Marenco S, Egan MF, Weinberger DR. Complexity of prefrontal cortical dysfunction in schizophrenia: more than up or down. *Am J Psychiatry* (2003) **160**:2209–15. doi:10.1176/appi.ajp.160.12.2209
85. Diaz Hernandez L, Rieger K, Baenninger A, Brandeis D, Koenig T. Towards using microstate-neurofeedback for the treatment of psychotic symptoms in schizophrenia. A feasibility study in healthy participants. *Brain Topogr* (2015) **29**(2):308–21. doi:10.1007/s10548-015-0460-4
86. Zhang Q, Zhang G, Yao L, Zhao X. Impact of real-time fMRI working memory feedback training on the interactions between three core brain networks. *Front Behav Neurosci* (2015) **9**:244. doi:10.3389/fnbeh.2015.00244
87. Centorrino F, Price BH, Tuttle M, Bahk WM, Hennen J, Albert MJ, et al. EEG abnormalities during treatment with typical and atypical antipsychotics. *Am J Psychiatry* (2002) **159**:109–15. doi:10.1176/appi.ajp.159.1.109

Conflict of Interest Statement: The authors declare that the research was conducted in the absence of any commercial or financial relationships that could be construed as a potential conflict of interest.

2.2.1 Supplemental material of Paper 2

Supplementary Material

Inefficient preparatory fMRI-BOLD network activations predict working memory dysfunctions in patients with schizophrenia

Anja Baenninger*, Laura Diaz Hernandez, Kathryn Rieger, Judith M. Ford, Mara Kottlow, Thomas Koenig

*** Correspondence:** Anja Baenninger: anja.baenninger@puk.unibe.ch

1.1 Supplementary Tables

Supplementary Table 1. Regions of the four template TCNs from Kottlow et al. Using the "write Talairach table" option based on the Talairach Daemon of the gift toolbox, max values and labeling of the coordinates were extracted. A threshold of 3.5 was applied for beta-values and the distance between contiguous voxels was set to 4mm. Only positive regions are listed.

TCN	Region	Random effects: Max Value (x,y,z)
DMN	Precuneus	9.2 (-20, -66, 49) / 11.6 (30, -72, 35)
	Superior Parietal Lobule	9.4 (-24, -55, 60) / 11.4 (22, -59, 56)
	Middle Temporal Gyrus	8.6 (-34, -76, 24) / 11.4 (38, -76, 24)
	Superior Occipital Gyrus	8.9 (-32, -78, 28) / 10.8 (38, -76, 28)
	Angular Gyrus	6.3 (-34, -74, 31) / 10.0 (36, -72, 31)
	Middle Occipital Gyrus	8.9 (-32, -82, 21) / 9.3 (34, -81, 21)
	Inferior Parietal Lobule	6.4 (-34, -50, 56) / 8.7 (44, -36, 53)
	Postcentral Gyrus	5.9 (-18, -51, 63) / 8.2 (44, -34, 50)
	Cuneus	7.6 (-28, -80, 32) / 7.5 (30, -80, 32)

	Middle Frontal Gyrus	4.6 (-26, 3, 55) / 6.7 (30, 9, 60)
	Inferior Temporal Gyrus	6.5 (-53, -64, -2) / 5.1 (48, -70, -2)
	Superior Frontal Gyrus	5.0 (-24, 15, 58) / 6.4 (26, 7, 55)
	Inferior Frontal Gyrus	4.1 (-53, 13, 21) / 5.6 (48, 9, 22)
	Paracentral Lobule	3.7 (0, -38, 50) / 5.4 (4, -46, 59)
	Superior Temporal Gyrus	3.9 (-46, 6, -5) / 4.7 (48, -61, 18)
	Fusiform Gyrus	4.3 (-44, -67, -12) / 4.5 (48, -57, -12)
	Precentral Gyrus	4.5 (-55, -4, 39) / 4.0 (59, -17, 40)
	Culmen	4.4 (-16, -37, -12)/3.8 (2, -45, -8)
	Insula	4.2 (-42, 4, -4)
	Cingulate Gyrus	4.0 (6, -37, 41)
	Medial Frontal Gyrus	3.9 (-20, 3, 51)
	Inferior Occipital Gyrus	3.9 (-42, -70, -3)
	Thalamus	3.9 (16, -29, 12)
dAN	Precuneus	8.5 (-20, -66, 49) / 11.0 (30, -72, 35)
	Middle Temporal Gyrus	8.4 (-30, -75, 20) / 10.7 (38, -77, 22)
	Superior Occipital Gyrus	8.0 (-28, -80, 28) / 10.4 (38, -76, 26)
	Superior Parietal Lobule	8.6 (-24, -57, 58) / 10.2 (24, -57, 58)
	Angular Gyrus	5.9 (-34, -76, 31) / 9.6 (38, -76, 30)
	Middle Occitipital Gyrus	8.2 (-32, -79, 21) / 7.8 (36, -83, 19)

	Cuneus	8.0 (-26, -76, 31) / 7.9 (32, -80, 33)
	Inferior Parietal Lobule	6.7 (-30, -50, 54) / 7.9 (34, -50, 56)
	Postcentral Gyrus	4.5 (-6, -53, 65) / 7.3 (44, -34, 50)
	Middle Frontal Gyrus	5.5 (26, 0, 48)
	Inferior Frontal Gyrus	5.2 (48, 9, 24)
	Superior Frontal Gyrus	5.1 (26, 7, 55)
	Inferior Temporal Gyrus	4.5 (-53, -58, -4) / 4.9 (51, -61, -9)
	Precentral Gyrus	3.6 (-53, -2, 41) / 4.2 (59, -17, 41)
	Fusiform Gyrus	4.1 (50, -61, -12)
	Superior Temporal Gyrus	3.9 (48, -61, 18)
rWMN	Inferior Parietal Lobule	6.3 (-48, -52, 43) / 16.6 (46, -54, 47)
	Superior Parietal Lobule	4.3 (-38, -56, 51) / 16.4 (42, -58, 49)
	Supramarginal Gyrus	4.4 (-46, -51, 36) / 14.7 (51, -49, 37)
	Middle Frontal Gyrus	4.9 (-44, 50, -1) / 13.3 (46, 21, 39)
	Angular Gyrus	3.6 (-48, -55, 36) / 12.6 (48, -55, 36)
	Precentral Gyrus	11.9 (48, 21, 36)
	Superior Frontal Gyrus	6.1 (-2, 33, 48) / 11.7 (36, 22, 49)
	Medial Frontal Gyrus	7.1 (-2, 35, 42) / 10.2 (4, 35, 39)
	Middle Temporal Gyrus	4.3 (-63, -27, -5) / 9.9 (63, -26, -7)
	Postcentral Gyrus	9.3 (55, -36, 50)
	Inferior Frontal Gyrus	3.8 (-48, 47, 0) / 9.3 (40, 54, 1)

	Precuneus	3.6 (0, -70, 46) / 8.9 (36, -66, 42)
	Superior Temporal Gyrus	7.9 (48, -48, 21)
	Cingulate Gyrus	3.6 (-2, -26, 31) / 6.9 (10, -45, 37)
	Declive	6.6 (-10, -79, -20) / -999.0 (0, 0, 0)
	Anterior Cingulate	5.6 (8, 41, 13)
	Inferior Temporal Gyrus	4.8 (59, -14, -16)
	Insula	4.1 (48, -40, 20)
	Uvula	3.9 (-14, -71, -23)
	Cuneus	3.7 (10, -66, 31)
lWMN	Inferior Parietal Lobule	14.9 (-38, -62, 44) / 7.1 (34, -58, 40)
	Superior Parietal Lobule	14.6 (-36, -62, 49) / 6.3 (40, -58, 51)
	Precuneus	13.0 (-34, -64, 40) / 5.9 (32, -62, 40)
	Inferior Frontal Gyrus	11.5 (-46, 43, 5) / 5.5 (53, 38, 13)
	Angular Gyrus	11.1 (-46, -56, 36) / 5.4 (34, -58, 36)
	Supramarginal Gyrus	10.7 (-46, -53, 36) / 5.1 (38, -49, 37)
	Middle Frontal Gyrus	10.6 (-46, 44, -4) / 5.3 (50, 36, 18)
	Middle Temporal Gyrus	9.8 (-61, -37, -5) / 5.1 (65, -35, -5)
	Superior Temporal Gyrus	9.1 (-46, -57, 29) / 3.9 (63, -2, 7)
	Precentral Gyrus	8.0 (-44, 17, 34) / 3.5 (61, -1, 11)
	Superior Frontal Gyrus	7.6 (-34, 14, 51)

	Inferior Temporal Gyrus	7.1 (-51, -53, -11)
	Medial Frontal Gyrus	6.6 (-4, 29, 41)
	Fusiform Gyrus	6.4 (-48, -55, -11)
	Uvula	5.3 (32, -63, -24)
	Cingulate Gyrus	5.0 (-2, -33, 33) / 3.8 (2, -33, 33)
	Postcentral Gyrus	4.7 (-51, -31, 49) / 4.2 (53, -34, 51)
	Superior Occipital Gyrus	4.5 (-38, -74, 28)
	Culmen	4.2 (28, -61, -24)
	Cuneus	4.0 (0, -90, 17)
	Insula	3.6 (-40, 17, -1)

Supplementary Figure 1: Difference of spectral power in three frequency bands (theta, alpha, beta) comparing patients with controls during the resting state condition with eyes closed. Indicated with the dashed black line is the critical threshold for the significant t-value (2.0369; df = 32, p = .05, double-sided).

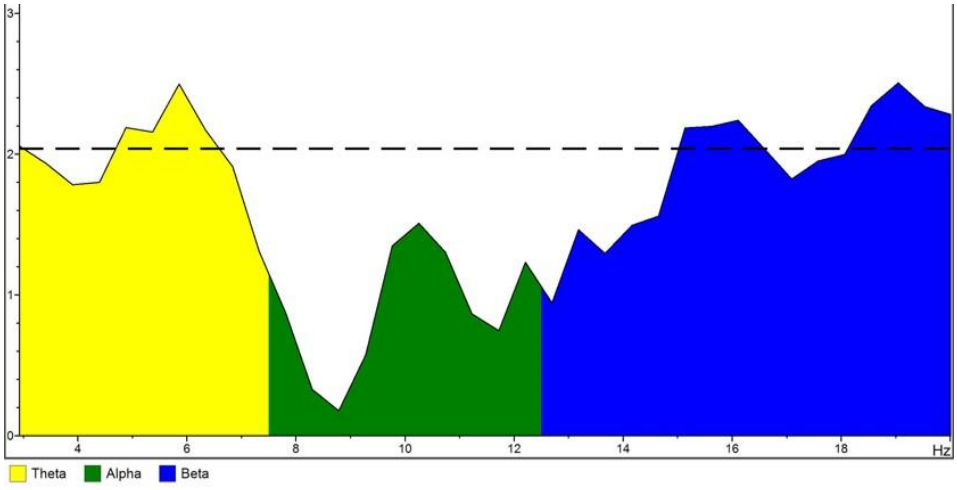

2.3 Paper 3: Delta EEG synchronization linked to DMN activity in schizophrenia

Baenninger A, Palzes VA, Roach BJ, Mathalon DH , Ford JM, Koenig T

Submitted at NeuroImage: Clinical

Delta EEG synchronization linked to DMN activity in schizophrenia

Anja Baenninger[1,2], Vanessa A Palzes[3], Brian J Roach[3], Daniel H Mathalon[3,4] , Judith M Ford[3,4], Thomas Koenig[1,2]

Affiliations:
[1]Translational Research Center, University Hospital of Psychiatry and Psychotherapy, University of Bern, Switzerland
[2]Center for Cognition, Learning and Memory, University of Bern, Bern, Switzerland
[3]San Francisco VA Medical Center, San Francisco, CA, USA
[4]Department of Psychiatry, University of California San Francisco, CA, USA

Corresponding author:
Thomas Koenig, Translational Research Center, University Hospital of Psychiatry, University of Bern, Bolligenstrasse 111, 3000 Bern 60, Switzerland.
Email: thomas.koenig@puk.unibe.ch

Author contributions:
AB, JMF, TK, VAP wrote the manuscript; AB, VAP performed the measurements; AB, BJR, VAP, TK conceived and implemented experimental procedures and scripts for analyses; BJR, VAP and DHM critically revised the manuscript

Conflict of interest:
All authors hereby declare that there is no actual or potential conflict of interest including financial, personal or other relationships with other people or organizations, which would inappropriately influence our work.

Abstract

Common-phase synchronization of neuronal oscillations is a mechanism by which distributed brain regions can be integrated into transiently stable networks. Based on the hypothesis that schizophrenia is characterized by deficits in functional integration within neuronal networks, this study aimed to explore whether schizophrenia patients exhibit differences in brain regions involved in integrative mechanisms. With that objective, an EEG-informed fMRI analysis on eyes-open resting state data of patients and healthy controls from two study sites was performed. Global field synchronization (GFS) was chosen as an EEG measure indicating common-phase synchronization across electrodes. Several brain clusters appeared to be differently coupled in patients compared to controls: The extrastriate visual cortex was inversely related to GFS alpha1 (8.5 – 10.5Hz) band in healthy controls, while patients had a tendency towards a positive relationship. Most extensive findings were that brain areas belonging to the default mode network (DMN) were negatively associated to GFS delta (1 – 3.5Hz) and beta (13 – 30Hz) bands in patients, whereas controls showed an opposite pattern in those regions. Taken together, the GFS measure might be useful to detect additional aspects of deficient functional network integration in schizophrenia.

Key words (max 6): schizophrenia, functional network integration, global field synchronization (GFS), EEG-informed fMRI analysis (or EEG-fMRI study), eyes-open (EO) resting state, delta band

1. Introduction

For the last decade, neuroimaging data have been accumulating to provide support for anatomical and functional disconnectivity in schizophrenia suggested by Friston and Frith (Friston and Frith 1995, Friston 1996, Friston 1998) (for comprehensive reviews see Stephan, Friston et al. 2009, Pettersson-Yeo, Allen et al. 2011). The term “disconnection” refers to a failure of functional integration within the brain, and “functional integration” refers to the interaction of functionally specialized systems (i.e., populations of neurons, cortical areas and sub-areas; Friston 2002). Functional integration is necessary to adaptively integrate sensorimotor information for perception and cognition (Friston 2002).

Studies of the human brain at rest increased dramatically after the discovery that anatomically separated, but functionally connected regions display a high level of correlated blood oxygen-level dependent (BOLD) signal activity during rest, in the absence of a task. A network of brain regions becomes co-active during rest and the assumption has been that it reflects focus on internal tasks such as daydreaming, imagining the future and reviewing the past (Greicius, Krasnow et al. 2003). As a result, it has been labeled the “default mode network” or DMN. We will use the term DMN here, while acknowledging that it reflects more than processes invoked during passive rest (Binder 2012).

Patients with schizophrenia have been reported to have both hyper- as well as hypo- connectivity within the DMN, and between nodes of the DMN with other cortical and subcortical regions (for reviews see Fornito, Zalesky et al. 2012, Whitfield-Gabrieli and Ford 2012). The deviations seen in schizophrenia during rest are paralleled by EEG and MEG studies showing increased amplitudes in lower delta, theta, and higher beta frequencies, with decreased amplitude in alpha frequency during rest (Boutros, Arfken et al. 2008, Galderisi, Mucci et al. 2009, Siekmeier and Stufflebeam 2010).

The simultaneous acquisition of EEG and fMRI provides a method to link these complementary neuroimaging methodologies. Consistent with alpha band amplitude reflecting a relaxed, alert “DMN-like” state, Jann et al (Jann, Kottlow et al. 2010) reported positive associations between DMN activity and alpha amplitude. Importantly, there is a negative relationship between alpha power and amplitude and sensory networks (Goldman, Stern et al. 2002, Laufs, Krakow et al. 2003, Mantini, Perrucci et al. 2007, Jann, Kottlow et al. 2010). Consistent with the suggestion that DMN reflects more than passive daydreaming and mind wandering (Binder 2012), beta band amplitude and power correlated positively with activity in the DMN and negatively with sensory networks (Mantini, Perrucci et al. 2007, Jann, Kottlow et al. 2010). In accordance with the fact that alpha band power depends on thalamic activity (e.g. de Munck, Goncalves et al. 2007, Tyvaert, Levan et al. 2008) and is dampened during visual tasks (e.g. Toscani, Marzi et al. 2010), there is a positive correlation between amplitude and power in the alpha band and the BOLD response in the thalamus, along with negative correlations between alpha and the BOLD response in executive and visual areas of the brain (e.g. Goldman, Stern et al. 2002, Laufs, Kleinschmidt et al. 2003, Laufs, Krakow et al. 2003, Moosmann, Ritter et al. 2003, Goncalves, de Munck et al. 2006, de Munck, Goncalves et al. 2007, Jann, Kottlow et al. 2010). Thus, while there is a relationship between alpha power and DMN, it is not unique to either alpha or DMN.

It is unknown how spatially distributed brain areas are integrated into transiently stable neural networks, although studies on visual perception suggest integration is instantiated through common-phase synchronization of neurons across areas of the brain (Singer 1999, Singer 2001, Kottlow, Jann et al. 2012). In their review of the literature, Uhlhaas and Singer (2010) noted that schizophrenia was associated with reduced phase locking of beta and gamma band oscillations across electrodes or trials, especially in patients with more severe positive symptoms, such as hallucinations (Uhlhaas and Singer 2010). Global field synchronization (GFS), a multichannel EEG measure, has also been used to assess functional connectivity between brain processes in different frequency bands. In a study of medication naive, first episode patients with schizophrenia, GFS values in the theta band during rest were significantly decreased relative to healthy comparison subjects (Koenig et al., 2001). The authors argued that this finding of reduced functional connectivity in the theta frequency represents

a loss of mutual interdependence of memory functions. Interestingly, another study linking alpha band GFS to fMRI-BOLD signal changes identified regions overlapping with the DMN (Jann et al., 2009). Here, we aimed to extend this important relationship between the EEG-based measure of GFS and fMRI-BOLD to understand schizophrenia in terms of abnormalities of integrative mechanisms that potentially underlie the formation of resting state networks (RSNs).

2. Methods

2.1 Participants

Data were collected at two sites: San Francisco Veterans Affairs Medical Center (SFVAMC) and University Hospital of Psychiatry and Psychotherapy of the University of Bern (PUK Bern), Switzerland.

At the SFVAMC, 20 patients with DSM-IV schizophrenia (N = 13 paranoid type (295.30), N = 4 disorganized type (295.10), N = 2 undifferentiated type (295.90), N = 1 residual type (295.60)) and 5 schizoaffective disorder (295.70; total N = 25; hereinafter referred to as schizophrenia, SZ, patients), and 20 age- and gender-matched healthy comparison (HC) subjects were studied. SZ patients were referred by community outpatient clinicians, and both HC and SZ, were recruited by advertisements and word-of-mouth. At the PUK Bern, 17 psychotic patients and 17 age- and gender-matched HC were studied. Nine patients were diagnosed according to the ICD-10 with schizophrenia (N = 6 paranoid type (F20.0), N = 2 undifferentiated type (F20.3), and N = 1 catatonic type (F20.2), and 8 patients with brief psychotic disorder (F23). At both sites, exclusion criteria for HC included having any past or current history of psychiatric and neurologic disorder, or a first-degree relative with a psychotic disorder. For both groups, exclusion criteria were any past significant medical or neurological illness, head injury resulting in loss of consciousness, or substance abuse in the past three months. Additionally, HC had no history of substance dependence (except caffeine or nicotine), while SZ did not meet criteria for substance dependence within the past year. A trained research assistant, psychiatrist, or clinical psychologist conducted all interviews. Study procedures were approved by the University of California at San Francisco Institutional Review Board and SFVAMC as well as the local ethics committee of the canton of Bern, Switzerland (KEK no. 192/05) and all participants provided written informed consent. Clinical and demographic data are presented in table 1.

		San Francisco V.A. Medical Center				University of Bern, Switzerland				Both sites				
		HC (N = 20)		SZ (N = 25)		HC (N = 17)		SZ (N = 17)		HC (N = 37)		SZ (N = 42)		Group difference
Demographics		*Mean*	*SD*	*Mean*	*SD*	*Mean*	*SD*	*Mean*	*SD*	*Mean*	*SD*	*Mean*	*SD*	*ANOVA*
	Age (years)	37.2	14.2	42.3	13.1	31.5	7.2	34.3	8.4	34.6	11,7	39.1	12.0	F (1.9) p = .168
	Education (years)	15.9	2.3	14.0	2.0	15.4	2.1	12.2	2.6	15.6	2.2	13.2	2.4	F (21.7) p < **0.001**
	Sex (M / F)	16 / 4		23 / 2		13 / 4		14 / 3		29 / 8		37 / 5		
	Handedness (R / L / A)	18 / 1 / 1		23 / 1 / 1		17		17		35 / 1 / 1		40 / 1 / 1		
														Site differences
fMRI	**Mean head displacement (mm)**	*Mean*	*SD*	*Mean*	*SD*	*Mean*	*SD*	*Mean*	*SD*	*Mean*	*SD*	*Mean*	*SD*	*ANOVA*
		0.08	0.05	0.11	0.06	0.04	0.12	0.049	0.035	0.06	0.04	0.08	0.06	F (4.119) p = .**046**
Clinical data	**CPZE (mg)**			362.4	281.9			329.2	174.3			346.8	234.6	F (.166) p = .687
	PANSS positive			17.8	5.8			13.3	4.8			16.0	5.8	F (7.119) p = .**011**
	PANSS negative			18.7	6.3			13.0	7.7			16.4	7.4	F (6.825) p = .**013**
	PANSS general			32.8	8.2			27.5	12.9			30.7	10.5	F (2.647) p = .112
	PANSS total			69.3	15.0			53.8	22.6			63.0	19.6	F (7.133) p = .**011**

Table 1: Demographic, clinical and movement information of subjects from each measuring site separately and merged for healthy controls (HC) and schizophrenia patients (SZ). Sex (M= male, F = female); Handedness (R = right-handed, L = left-handed, A = ambidextrous), CPZE = Chlorpromazine equivalence dosage, PANSS = Positive and negative syndrome scale

2.2 Procedures

At the SFVAMC site, simultaneous EEG-fMRI data were acquired during rest. Participants were instructed to keep their eyes open (EO) and fixated on a white cross (+) in the center of a black screen for six minutes. An Avotec projector behind the scanner was used to project the stimulus on a screen attached inside of the magnet bore, and subjects viewed the screen through a mirror attached to the head coil.

At the PUK Bern, simultaneous EEG-fMRI data were also acquired during rest. Unlike the SFVAMC site, EEG data were also collected outside the scanner for later artifact removal (see section 2.3). Both inside and outside the scanner, participants alternated between two minutes of EO and two minutes eyes closed (EC). During EO inside the scanner, they were instructed to fixate on a white cross on a black screen. During EC, the screen was fully black. Starting with EO, both conditions alternated twice for two minutes each, resulting in eight minutes total time. Three white flashes indicated a switch between conditions. The flashes were not too bright to disturb subjects during EO, but bright enough to be noticed in the EC condition. None of the participants reported any discomfort during the measurement. Stimuli were presented via goggles (VisualStimDigital MR-compatible

video goggles; Resonance Technology Inc., Northridge, CA, USA), with a visual angle of 60°, a resolution of 800x600 pixels and 60Hz refresh rate. To deliver stimulus material, E-Prime (Version 2.0.10.553, Psychology Software Tools, INC.) was used.

At both sites, trained personnel rated the severity of schizophrenia symptoms using the Positive and Negative Syndrome Scale (PANSS; Kay, Fiszbein et al. 1987).

2.3 EEG and fMRI Data Acquisition and Preprocessing

At the SFVAMC, continuous EEG data were collected from 31 standard scalp sites (Fp1, Fp2, F3, F4, C3, C4, P3, P4, O1, O2, F7, F8, T7, T8, P7, P8, Fz, FCz, Cz, Pz, FC1, FC2, CP1, CP2, FC5, FC6, CP5, CP6, POz, TP9, TP10) and another electrode was placed on the lower back to monitor electrocardiograms (ECG). At the Inselspital of Bern, Switzerland, a 92-channel cap was used and two additional channels each served the recording of the electrooculogram (EOG; below the eyes) and the electrocardiogram (ECG; below the clavicles). Both sites mounted the sintered Ag/AgCl ring electrodes in an MR compatible electrode cap from Brain Products (Gilching, Germany; input range: 16.3mV, resolution: 16 bit) according to the 10-10 system and with a sampling rate of 5 kHz. Electrode impedances below 10 kOhm were targeted at the SFVAMC and below 20 kOhm at the Inselspital Bern, while restricting full EEG preparation to one hour avoiding possible tiring of participants, especially patients (SFVAMC: across all subjects, 89.0% of all electrodes had impedances below 25 kOhm, 10% were higher than 30 kOhm and mean impedance was 15.5 kOhm; PUK Bern: across subjects, 88.6% of all electrodes had impedances below 25 kOhm, 7% were higher than 30 kOhm and mean impedance was 17.5 kOhm). The nonmagnetic EEG amplifiers were fixed behind the head coil and powered by a rechargeable power pack placed in the bore of the scanner and stabilized with sandbags. The subject's head was immobilized using cushions. EEG data were transmitted via an MR-compatible fiber optic cable to a BrainAmp USB Adapter that synchronized the EEG acquisition clock to the MRI master clock via a SyncBox (Brain Products) before transferring data via USB to a laptop computer placed outside the scanner room.

To provide a better overview of EEG and fMRI acquisition parameters and preprocessing steps for each site, we assembled the information in table 2 (for a detailed EEG preprocessing description see supplemental materials). Both sites used Brain Vision Analyzer (Version 2.0.4.368, Brain Products, Gilching, Germany) for the preprocessing of the EEG data and SPM8 for the processing of the fMRI data (SPM8; Welcome Department of Imaging Neuroscience, London, http://www.fil.ion.ucl.ac.uk/spm). The SFVAMC additionally had EEG analyses performed in Matlab (Mathworks, Natick, MA). Mean motion for each subject for each condition was computed as the root-mean-square of the translation parameters extracted from the fMRI data (Van Dijk, Sabuncu et al. 2012).

			Measuring site	
			SFVAMC	**PUK Bern**
EEG	**Acquisition parameters**	**♯ channels**	32	92
		Reference / ground electrodes	FCz / AFz	Fz / AFF2
		Online bandpass filter	0.01 – 250Hz	0.1 – 250Hz
	Preprocessing	**MR gradient artifact**	Template subtraction (sliding window: 21)	
		Down-sampling	250Hz	500Hz
		Heart beat detection	Filter ECG channel (1-20Hz)	x
		Cardio ballistic artifact	Template subtraction (sliding window: 21)	
		Filters	x	Bandpass 1-49Hz, Notch filter
		Segmentation	2s-epochs on TR, export to Matlab	x
		Removal of electromyography	Canonical correlation analysis (CCA) in Matlab	x
		Reference	Average reference	
		ICA	EEGLAB: 32 components	Vision Analyzer: 64 components
		Remaining artifacts	single-epoch, single-channel artifacts were flagged with FASTER	Manually marked as bad intervals
		Interpolation	Flagged artifacts: EEGLAB spherical spline interpolation function in Matlab	Bad channels: Spherical spline interpolation
fMRI	**Acquisition parameters**	**Scanner**	3T Siemens Skyra	3T Siemens Magnetom Trio
		EPI Sequenzen	TR = 2000ms, TE = 30ms, flip angle = 77°, 30 slices in ascending order, 3.4x3.4x4.0mm voxel size, 182 frames, 6:08 min	TR = 1960ms, TE = 30ms, flip angle = 90°, 35 slices in interleaved order, 3x3x3mm voxel size, 250 frames, 8:17 min
		T1	TR = 2300ms, TE = 2.98ms, flip angle = 9°, 176 sagittal slices, 1x1x1.2mm voxel size, 1.2mm slice thickness	TR = 2300ms, TE = 2.98ms, flip angle: 9°, 176 sagittal slices, 1x1x1mm voxel size, 1.0mm slice thickness
	Preprocessing	**SPM8**	Motion correction to mean image	Slice time correction
			Slice time correction	Motion correction to mean image
			Co-registration of T1 to the mean image	
			Segmentation into 6 tissue probability maps	
			Normalization and smoothing using a Gaussian FHWH kernel (6x6x6mm)	

Table 2: EEG and fMRI acquisition parameters and preprocessing for each measuring site. EPI = Echo planar imaging; TR = Repetition time; TE = Echo time

2.4 Global field synchronization (GFS) of EEG

Due to site differences in the electrode montages, the EEG data from Bern were reduced from 92 channels to the same 31-channels as used by the SFVAMC site (see section 2.3 above). The GFS values of the Bern data with 92 versus 31 channels were highly correlated (HC mean Pearson *r* = 0.96, SD = 0.019; SZ *r* = 0.95, SD = 0.05). Consequently, we would not expect different results if we would have used all 92 channels of the Bern dataset. The procedures for the computation of GFS are described in previous papers from the PUK Bern (Koenig, Lehmann et al. 2001, Jann, Dierks et al. 2009, Kottlow, Jann et al. 2012) and briefly described as follows: For each subject, EEG data were segmented into 2-second-epochs in relation to the scan markers of each volume (SFVAMC: TR = 2 s, segmentation onset = 0, length = 2 s, total of 181 segments; PUK Bern: TR = 1.96 s, segmentation onset = -0.048, length = 2.048, total of 249 segments). Then, each epoch was frequency transformed using a complex Fast Fourier Transformation (FFT; maximum resolution = 0.48828Hz, zero-padding). The retained sine and cosine values for each electrode and frequency bin could be visualized in a two-dimensional sine-cosine diagram with one point for each electrode at a given frequency. The resulting shape of clouds of all electrodes is an indicator of the amount of zero-lag phase synchronization across electrodes. More specifically, if the cloud is nearly circular, no predominant phase angle is present in the EEG, as opposed to an elongated cloud adverting a common phase across electrodes. The quantification of the shape is done by means of a two-dimensional principal component analysis (PCA): GFS is then defined as the ratio of (E1-E2) to (E1+E2) of the two eigenvalues (E1 and E2; see formula 1), with values ranging from 0 (absence of a common phase angle, minimal synchronization) to 1 (maximal phase synchronization; Koenig, Lehmann et al. 2001). For further analyses, the GFS values were averaged across epochs and frequencies for delta (1 – 3.5Hz), theta (4 – 7.5Hz), alpha1 (8.5 – 10.5Hz), alpha2 (10.5 – 12.5Hz), and beta (13 – 30Hz) band per subject.

$$GFS(f) = \frac{|E(f)_1 - E(f)_2|}{E(f)_1 + E(f)_2}$$

Formula 1: Computation of EEG Global Field Synchronization (GFS) according to Koenig et al. (2001). E (*f*) 1 and E (*f*) 2 are the eigenvalues 1 and 2 obtained from the PCA

2.5 EEG-informed fMRI analysis

To explore the anatomical correlates of GFS at different frequency bands (delta, theta, alpha1, alpha2, and beta) between groups, centered GFS values were used as parametric modulators for first-level fMRI analyses in SPM (SPM8; Welcome Department of Imaging Neuroscience, London, http://www.fil.ion.ucl.ac.uk/spm) using in-house Matlab scripts (Mathworks, Natick, MA) that removed the serial orthogonalization default setting in SPM (Wood, Nuerk et al. 2008). Serial orthogonalization was disabled because within subjects the different GFS frequency bands were not highly correlated with each other (overall mean Pearson *r* = 0.0532, min = 0.0211, max = 0.0828). First level analyses were run separately for SFVAMC and PUK Bern sites due to differences in the resting state acquisitions. In order to exclude bad intervals previously flagged in the EEG data, GFS values were set to zero (SFVAMC: Mean = 5.7, SD = 2.4 of 181 total trials, PUK Bern: Mean = 60.5, SD = 38.8 of 249 total trials; for EO trials: Mean = 25.5, SD = 15.5 of 123 total trials; for different approaches at each site see table 2) and values were centered at each frequency band to get the variance of the GFS predicting BOLD fluctuations. For the second-level analysis, only EO GFS-modulated betas were considered for the comparison of groups across both sites. To evaluate possible differences, the

measuring site (SFVAMC, PUK Bern) was included in the statistical model as a covariate for the within- and between-group analyses.

Our analysis strategy was to explore EEG-fMRI coupled clusters that showed between-group differences first, and then within-group effects. Our initial voxelwise, cluster-finding threshold was set to $p = 0.01$ (two-sided).

3 Results

3.1 EEG-informed fMRI analysis – 2nd level results – Group differences

The EEG-informed fMRI analysis revealed brain clusters that were coupled significantly differently to three of the five GFS frequencies, namely in the delta (1 – 3.5Hz), alpha1 (8.5 – 10.5Hz), and beta (13 – 30Hz) band.

3.1.1 Delta Band

In the delta band, there were seven clusters that differed between groups (cluster 1: 5506 voxels, FWE $p = < 0.001$; cluster 2: 1762 voxels, FWE $p = < 0.001$; cluster 3: 1420 voxels, FWE $p = < 0.001$; cluster 4: 308 voxels, FWE $p = 0.004$; cluster 5: 293 voxels, FWE $p = 0.006$; cluster 6: 232 voxels, FWE $p = 0.022$; cluster 7: 220 voxels, FWE $p = 0.029$; figure 2). Some clusters included regions of the default mode network (DMN), like the precuneus, the posterior cingulate gyrus and the inferior parietal lobule. Other clusters included temporal, parietal, thalamic, cerebellar and limbic regions (for details of regions see supplemental materials, table 1). Looking at the mean beta weights extracted from the between-group clusters for each group, all clusters had negative weights in patients and positive weights in controls (figure 3). Within group analyses revealed two significant positive clusters in healthy controls and eight significant negative clusters in patients (figure 2).

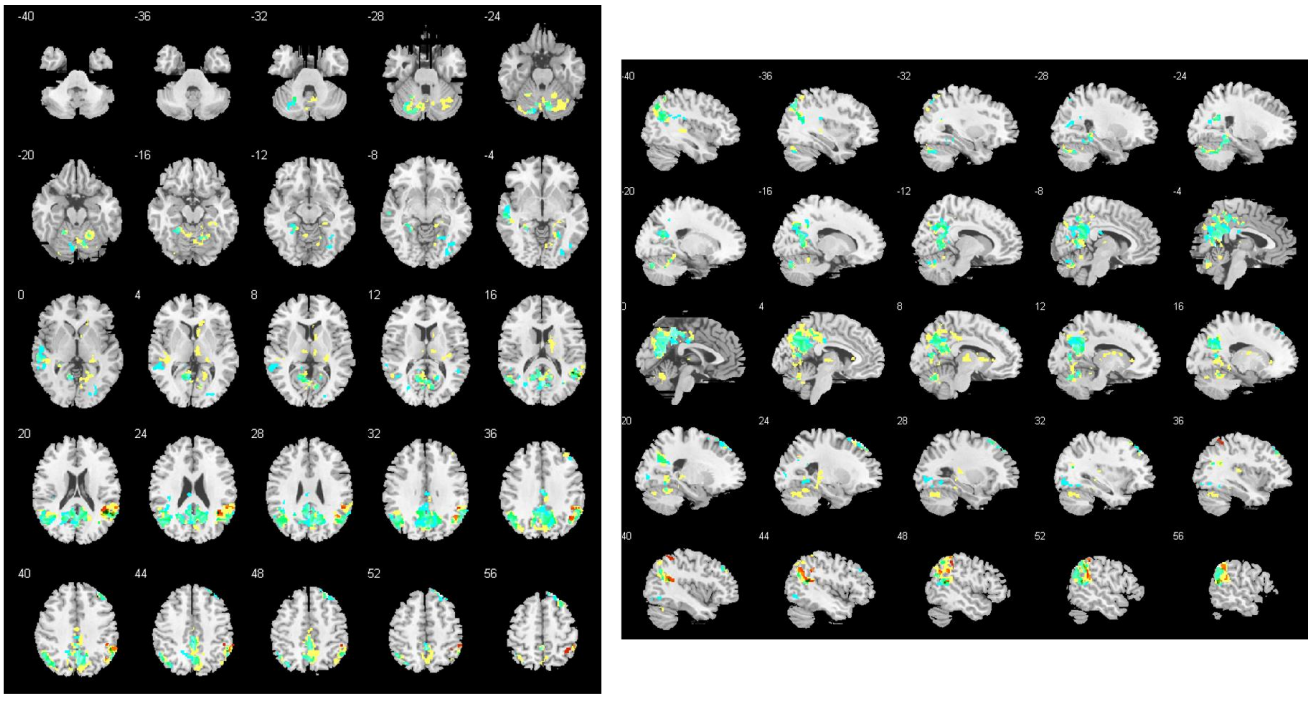

a) b)

Figure 2: GFS Delta band: a) Horizontal b) sagittal view of significant negative clusters between groups (SZ – HC, yellow), positive clusters in HC (red) and negative clusters in SZ (light blue; initial threshold p = 0.01, two-sided)

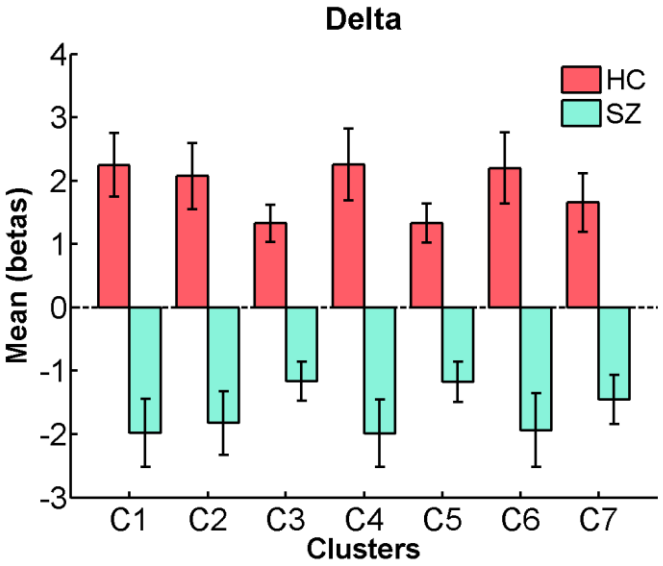

Figure 3: Mean beta weights and standard errors (SE) of significant Delta band clusters for each group

3.1.2 Alpha1 Band

In the alpha1 band, there was one cluster that differed between groups, with controls showing negative coupling between GFS alpha1 and a cluster containing 434 voxels (FWE $p = 0.004$) in left hemispheric occipital, temporal and parietal areas such as the cuneus, precuneus, and Brodmann areas 7, 18, 19, 31 (see figure 4; for details of involved regions see supplemental materials table 1). Within the controls, there were two significant negative clusters overlapping with the cluster of the between-group contrast (figure 4). The mean beta weights reveal that controls showed negative, and patients positive associations explaining the group difference (figure 5).

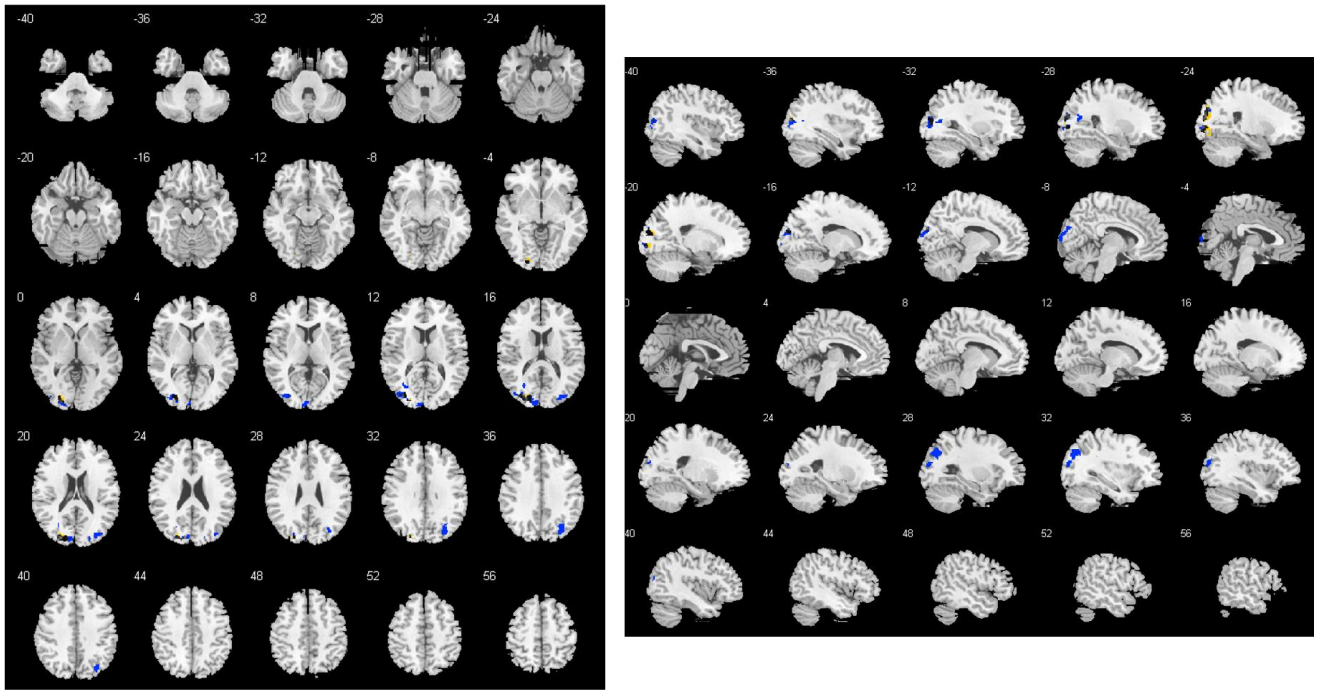

a) b)

Figure 4: GFS Alpha1 band: a) Horizontal b) sagittal view of significant negative cluster between groups (SZ – HC, yellow) and negative clusters in HC (dark blue; initial threshold p = 0.01, two-sided)

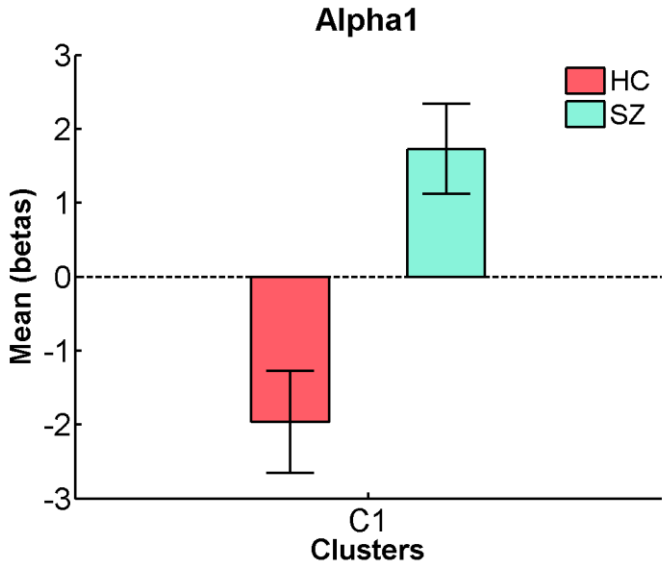

Figure 5: Mean beta weights and standard errors (SE) of significant Alpha1 band cluster for each group

3.1.3 Beta Band

In the beta band, there was one 252-voxel cluster (FWE *p* = 0.0026), located mainly in the right hemispheric precuneus and cuneus that differed between groups (see figure 6; for details of regions see table 1 in supplemental materials). The mean beta weights of that cluster revealed that this difference was explained by patients showing positive GFS beta – BOLD associations, while healthy controls had a negative coupling in that cluster (figure 7).

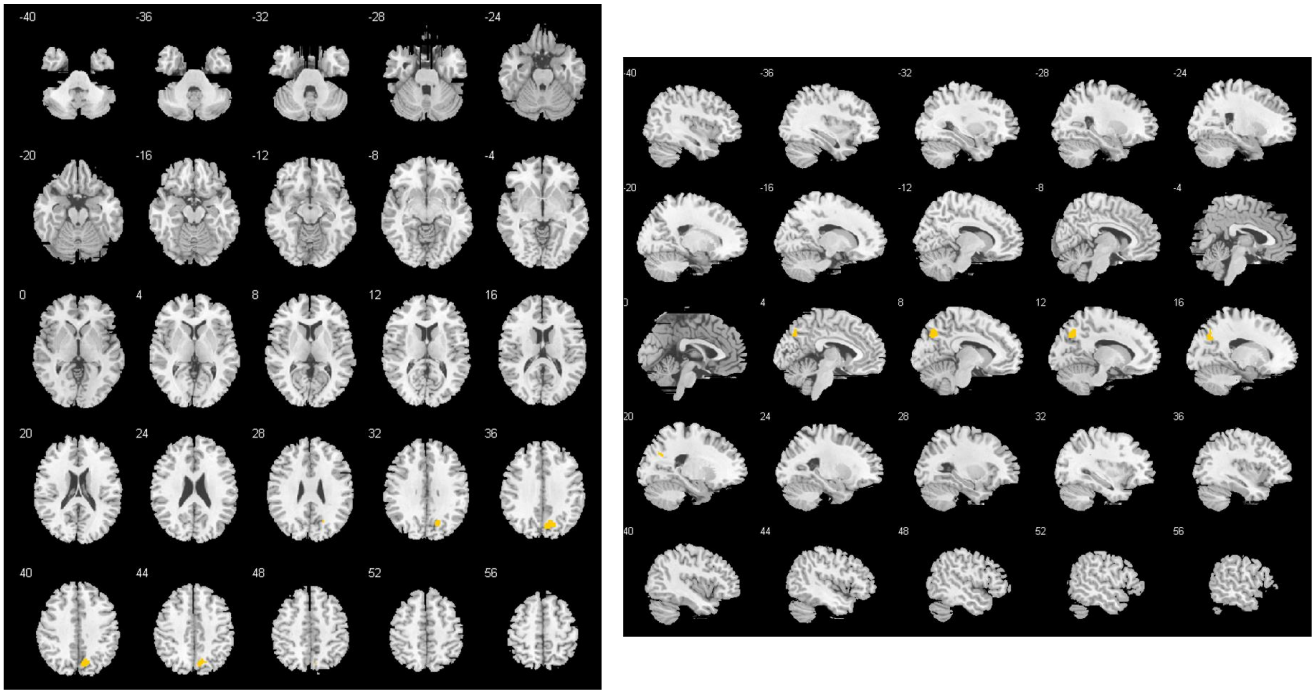

Figure 6: GFS Beta band: a) Horizontal b) sagittal view of significant positive cluster between groups (SZ – HC, initial threshold p = 0.01, two-sided)

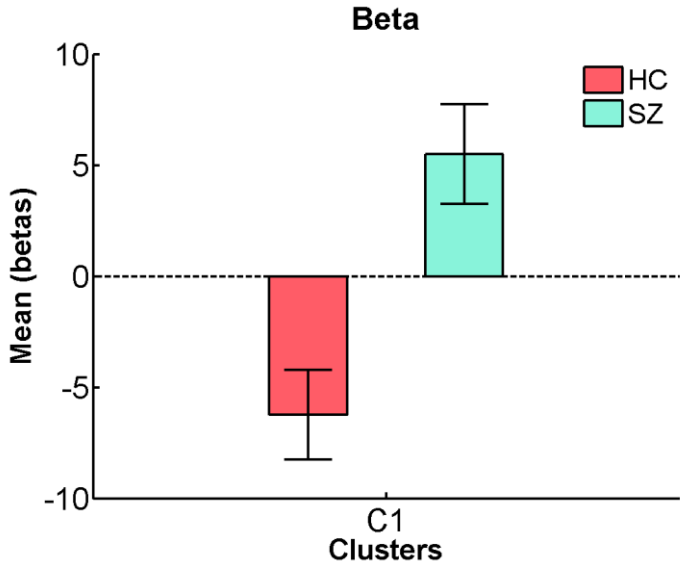

Figure 7: Mean beta weights and standard errors (SE) of significant Beta band cluster for each group

3.2 Follow up analysis – Influence of power across all channels in significant GFS group clusters

To further elucidate how the measure of GFS was related to amplitudes of the corresponding frequency bands, in follow-up analyses, we ran similar first- and second-level analyses, but used mean power across all channels, instead of synchrony (GFS), as parametric modulators. First, the mean power in the three frequency bands, which showed significant group effects in the GFS analysis (delta, alpha1, and beta), was calculated. Mean power and GFS measures within each frequency band were not correlated with each other (overall mean Pearson r = 0.2463, min = 0.0666, max = 0.4814), so we were able to include both as parametric modulators in the same first-level model. In the end, we conducted three separate models, one for each frequency band. There

were no overlapping voxels (initial threshold $p = 0.01$, two-sided; cluster size: 5) for GFS and global power for any of the frequency bands (delta, alpha1, and beta), indicating that these measures indeed capture different aspects of brain function. In addition, there were no significant clusters for global power surviving at the same initial height threshold as used in the main GFS analyses, so these data are not discussed further.

3.3 Relationship between symptoms and brain clusters

We ran ANCOVAs, with site as a covariate, to explore systematic relationships of symptom severity as measured by total scores of positive, negative and general symptoms from the PANSS in SZ on the mean EO GFS-modulator beta weights of the significant between-group brain clusters from the delta, alpha1 and beta bands. None of these tests reached significance (all $p > 0.05$, uncorrected).

3.4 Relationship between movement parameters and brain clusters

Because patients showed significantly stronger mean head displacements than healthy controls (see table 1), we tested the relationship between the mean EO GFS-modulator beta weights of the significant brain clusters including the mean motion parameters as covariate of no interest. The group differences for each brain cluster were still highly significant when controlling for mean head displacements (all p-values < 0.001), thus our between-group results cannot be explained by group differences in head movement.

4 Discussion

The goals of this study were three-fold: To provide further evidence of a relationship between fluctuations in global common-phase neural oscillations and fluctuations in the BOLD response during rest, to determine the relationship between neural activity in specific frequency bands and BOLD activity in specific brain regions, and to ask how this relationship is affected by schizophrenia. Our EEG-informed fMRI analysis using the GFS values pooled into five frequency bands (delta, theta, alpha1, alpha2, and beta) revealed significant brain clusters that differed between groups in the delta, alpha1, and beta band.

4.1 Delta Band

The results in the delta band were the most extensive. They revealed seven clusters, including regions of the well-known default mode network (DMN): the precuneus, the posterior cingulate gyrus and the inferior parietal lobule. The results were driven by a negative relationship between GFS delta and regions of the DMN in the patients. The healthy controls had positive associations, but only with the right inferior parietal sulcus (rIPS) of the DMN. That is, when neuronal oscillations in the delta band were synchronized across the scalp, the DMN was *less* active in patients and *more* active in the healthy controls. Slow EEG oscillations have been linked to inhibitory processes of the brain (Contreras and Steriade 1995) and reduced states of alertness, such as drowsiness, sleep or sedation (Hlinka, Alexakis et al. 2010). Our results suggest that in schizophrenia patients, coordinated neuronal oscillations in the slow delta frequency are coupled with inhibited activity in the DMN. Synchronized delta activity might underlie known alterations of DMN connectivity as well as psychopathology in this patient population. Interestingly, the most preponderant abnormalities in quantitative EEG in schizophrenia are also found in slow rhythms (Boutros, Arfken et al. 2008, Galderisi, Mucci et al. 2009, Siekmeier and Stufflebeam 2010). Our findings may point to a missing link between the extensive literature on fMRI related DMN abnormalities and the equally well-replicated findings of increased slow EEG activity. Nevertheless, because both increased and decreased connectivity of the DMN are reported, the precise nature of the relationship between connectivity within the DMN and common-phase delta synchronization should be further investigated across rest and a variety of tasks.

4.2 Alpha1 Band

There was one cluster including extrastriate visual cortex showing a negative coupling between alpha1 in healthy controls, whereas no such modulation was seen in patients, resulting in the between-group effect. That is, in healthy controls but not patients, greater synchrony in the alpha1 band was related to less activity in visual

cortex. Others have reported a negative relationship between alpha power and occipital brain activity, which has been discussed in terms of “idling” of the brain (Goldman, Stern et al. 2002, Laufs, Kleinschmidt et al. 2003, Laufs, Krakow et al. 2003, Moosmann, Ritter et al. 2003, Goncalves, de Munck et al. 2006, de Munck, Goncalves et al. 2007, Tyvaert, Levan et al. 2008, Jann, Dierks et al. 2009, Jann, Kottlow et al. 2010). Using the same measure of synchronization and definition of lower and upper alpha band that we used, Jann et al (2009) reported a positive relationship between GFS in lower alpha (8.5 – 10.5Hz) and the BOLD signal in brain areas corresponding to the dorsal attention network (dAN), whereas GFS in upper alpha (10.5 – 12.5Hz) was positively correlated to the DMN (Jann, Dierks et al. 2009) in healthy subjects. While the procedures of integrating the alpha band GFS with the fMRI BOLD data were similar, in our healthy controls, we did not see a relationship between GFS alpha1 and the dAN reported by Jann et al (2009). This might be explained by some important differences between the studies: First, in our study, subjects had their eyes open, whereas in Jann et al., eyes were closed. Second, the subjects in the Jann et al study were about 10 years younger than the healthy controls in our study.

4.3 Beta Band

The between-group effect found in the right precuneus originates from patients displaying a positive coupling between GFS in the beta band and activity in the precuneus, with healthy controls showing negative association. The precuneus, a “hub” region of the DMN, is engaged in visuospatial imagery, episodic memory, reflective, self-related processing, awareness and conscious information processing (Cavanna and Trimble 2006, Zhang and Li 2012). As oscillations in the beta frequency range have been associated with polymodal sensory processing, sensory-motor coordination, the maintenance of limb positions, and working memory (Uhlhaas, Haenschel et al. 2008), the positive association between beta GFS and DMN activity in patients may reflect an imbalance between perception/cognition and mind wandering. Findings of decreased induced and evoked beta phase synchronization in circumscribed brain regions were positively correlated with positive symptoms (Uhlhaas and Singer 2010, Uhlhaas 2011), whereas deficits in the perception of Mooney faces in patients coincided with a reduction in global beta phase synchronization, suggesting impairment of large-scale synchronization (Uhlhaas and Singer 2006).

4.4 Conclusion

The associations between BOLD and global common-phase synchronization in low frequency delta, and also the higher frequencies in alpha1 and beta band, were altered in a variety of brain areas in schizophrenia patients, specifically in extrastriate visual areas for the alpha1 and DMN regions for the delta and beta frequency oscillations. The finding that patients and controls showed opposite patterns in their associations between GFS delta and beta band and the DMN, possibly reflects alterations in functional coupling between different nodes of the DMN. The reported results in this study reveal novel aspects of the deficient functional integration in schizophrenia patients suggested by Friston (2002). We argue that by using concurrent EEG and fMRI, links between psychopathology and physiological measures of network integration on different time scales can be established. This may provide a more extensive understanding of schizophrenia and other serious mental illnesses.

4.5 Limitations

The possible influence of antipsychotic medications on the neurobiological data always limits the interpretation of results, and it is not common practice to withdraw patients from medications for scientific studies. Although it is difficult to disentangle the effects of medication from the reasons a particular dose of medication was prescribed, we found no statistically significant relationship between chlorpromazine equivalents and the mean beta weights of the significant group clusters. Despite growing evidence that the EEG gamma band is affected in schizophrenia (e.g. Uhlhaas and Singer 2006, Uhlhaas and Singer 2010, McNally and McCarley 2016), its investigation in EEG-fMRI studies is limited: amplifier gain settings required to remove MRI gradient artifacts

restrict us from measuring small amplitude (i.e., < 0.5 uV) signals like gamma band activity and the noisy environment (e.g., compressor pumps) may contaminate higher frequency bands in particular.

It is difficult for us to compare our findings to others in the literature, as there are few similar studies. This may be for several reasons: First, there are many different methods used to combine neural signals derived from simultaneous EEG and fMRI measurements. Second, most studies that looked for relationships between EEG and fMRI used spectral amplitude of the EEG signal. Third, only two studies (studying healthy subjects only) used a common-phase synchronization measure, and it was sensitive to a different aspect of neuronal oscillatory activation (Jann, Dierks et al. 2009, Kottlow, Jann et al. 2012). Fourth, most studies used eyes-closed (EC) during the resting state, while our subjects had their eyes open (EO), which are two conditions associated with different mental states. The study of Wu and colleagues found that during EC, there were widespread alpha hemodynamic responses and high functional connectivity, whereas during EO these effects were markedly diminished (Wu, Eichele et al. 2010).

Acknowledgements:
We would like to thank all the participants that participated in our studies. Special thanks goes to Laura Diaz Hernandez and Kathryn Heri for helping with the measurements. Andrea Federspiel and Kay Jann for MR-related questions. Nadja Razavi for her help regarding clinical-diagnostic interviews and Ulrich Raub for managing the recruitment process.

Funding:
This work was supported by grants from National Institute of Mental Health (MH58262 to JMF) and the VA (I01 CX000497 to JMF). DHM consults for Boehringer Ingelheim. Furthermore, the Swiss National Science Foundation DocMobility Grant #P1BEP3_158984 and Sinergia Grant CRSII3_136249 supported this work.

5 References

Binder, J. R. (2012). "Task-induced deactivation and the "resting" state." Neuroimage **62**(2): 1086-1091.

Boutros, N. N., C. Arfken, S. Galderisi, J. Warrick, G. Pratt and W. Iacono (2008). "The status of spectral EEG abnormality as a diagnostic test for schizophrenia." Schizophr Res **99**(1-3): 225-237.

Cavanna, A. E. and M. R. Trimble (2006). "The precuneus: a review of its functional anatomy and behavioural correlates." Brain **129**(Pt 3): 564-583.

Contreras, D. and M. Steriade (1995). "Cellular basis of EEG slow rhythms: a study of dynamic corticothalamic relationships." J Neurosci **15**(1 Pt 2): 604-622.

de Munck, J. C., S. I. Goncalves, L. Huijboom, J. P. Kuijer, P. J. Pouwels, R. M. Heethaar and F. H. Lopes da Silva (2007). "The hemodynamic response of the alpha rhythm: an EEG/fMRI study." Neuroimage **35**(3): 1142-1151.

Fornito, A., A. Zalesky, C. Pantelis and E. T. Bullmore (2012). "Schizophrenia, neuroimaging and connectomics." Neuroimage **62**(4): 2296-2314.

Friston, K. J. (1996). "Theoretical neurobiology and schizophrenia." Br Med Bull **52**(3): 644-655.

Friston, K. J. (1998). "The disconnection hypothesis." Schizophr Res **30**(2): 115-125.

Friston, K. J. (2002). "Dysfunctional connectivity in schizophrenia." World Psychiatry **1**(2): 66-71.

Friston, K. J. and C. D. Frith (1995). "Schizophrenia: a disconnection syndrome?" Clin Neurosci **3**(2): 89-97.

Galderisi, S., A. Mucci, U. Volpe and N. Boutros (2009). "Evidence-based medicine and electrophysiology in schizophrenia." Clin EEG Neurosci **40**(2): 62-77.

Goldman, R. I., J. M. Stern, J. Engel, Jr. and M. S. Cohen (2002). "Simultaneous EEG and fMRI of the alpha rhythm." Neuroreport **13**(18): 2487-2492.

Goncalves, S. I., J. C. de Munck, P. J. Pouwels, R. Schoonhoven, J. P. Kuijer, N. M. Maurits, J. M. Hoogduin, E. J. Van Someren, R. M. Heethaar and F. H. Lopes da Silva (2006). "Correlating the alpha rhythm to BOLD using simultaneous EEG/fMRI: inter-subject variability." Neuroimage **30**(1): 203-213.

Greicius, M. D., B. Krasnow, A. L. Reiss and V. Menon (2003). "Functional connectivity in the resting brain: a network analysis of the default mode hypothesis." Proc Natl Acad Sci U S A **100**(1): 253-258.

Hlinka, J., C. Alexakis, A. Diukova, P. F. Liddle and D. P. Auer (2010). "Slow EEG pattern predicts reduced intrinsic functional connectivity in the default mode network: an inter-subject analysis." Neuroimage **53**(1): 239-246.

Jann, K., T. Dierks, C. Boesch, M. Kottlow, W. Strik and T. Koenig (2009). "BOLD correlates of EEG alpha phase-locking and the fMRI default mode network." Neuroimage **45**(3): 903-916.

Jann, K., M. Kottlow, T. Dierks, C. Boesch and T. Koenig (2010). "Topographic electrophysiological signatures of FMRI Resting State Networks." PLoS One **5**(9): e12945.

Kay, S. R., A. Fiszbein and L. A. Opler (1987). "The positive and negative syndrome scale (PANSS) for schizophrenia." Schizophr Bull **13**(2): 261-276.

Koenig, T., D. Lehmann, N. Saito, T. Kuginuki, T. Kinoshita and M. Koukkou (2001). "Decreased functional connectivity of EEG theta-frequency activity in first-episode, neuroleptic-naive patients with schizophrenia: preliminary results." Schizophr Res **50**(1-2): 55-60.

Kottlow, M., K. Jann, T. Dierks and T. Koenig (2012). "Increased phase synchronization during continuous face integration measured simultaneously with EEG and fMRI." Clin Neurophysiol **123**(8): 1536-1548.

Laufs, H., A. Kleinschmidt, A. Beyerle, E. Eger, A. Salek-Haddadi, C. Preibisch and K. Krakow (2003). "EEG-correlated fMRI of human alpha activity." Neuroimage **19**(4): 1463-1476.

Laufs, H., K. Krakow, P. Sterzer, E. Eger, A. Beyerle, A. Salek-Haddadi and A. Kleinschmidt (2003). "Electroencephalographic signatures of attentional and cognitive default modes in spontaneous brain activity fluctuations at rest." Proc Natl Acad Sci U S A **100**(19): 11053-11058.

Mantini, D., M. G. Perrucci, C. Del Gratta, G. L. Romani and M. Corbetta (2007). "Electrophysiological signatures of resting state networks in the human brain." Proc Natl Acad Sci U S A **104**(32): 13170-13175.

McNally, J. M. and R. W. McCarley (2016). "Gamma band oscillations: a key to understanding schizophrenia symptoms and neural circuit abnormalities." Curr Opin Psychiatry **29**(3): 202-210.

Moosmann, M., P. Ritter, I. Krastel, A. Brink, S. Thees, F. Blankenburg, B. Taskin, H. Obrig and A. Villringer (2003). "Correlates of alpha rhythm in functional magnetic resonance imaging and near infrared spectroscopy." Neuroimage **20**(1): 145-158.

Pettersson-Yeo, W., P. Allen, S. Benetti, P. McGuire and A. Mechelli (2011). "Dysconnectivity in schizophrenia: where are we now?" Neurosci Biobehav Rev **35**(5): 1110-1124.

Siekmeier, P. J. and S. M. Stufflebeam (2010). "Patterns of spontaneous magnetoencephalographic activity in patients with schizophrenia." J Clin Neurophysiol **27**(3): 179-190.

Singer, W. (1999). "Neuronal synchrony: a versatile code for the definition of relations?" Neuron **24**(1): 49-65, 111-125.

Singer, W. (2001). "Consciousness and the binding problem." Ann N Y Acad Sci **929**: 123-146.

Stephan, K. E., K. J. Friston and C. D. Frith (2009). "Dysconnection in schizophrenia: from abnormal synaptic plasticity to failures of self-monitoring." Schizophr Bull **35**(3): 509-527.

Toscani, M., T. Marzi, S. Righi, M. P. Viggiano and S. Baldassi (2010). "Alpha waves: a neural signature of visual suppression." Exp Brain Res **207**(3-4): 213-219.

Tyvaert, L., P. Levan, C. Grova, F. Dubeau and J. Gotman (2008). "Effects of fluctuating physiological rhythms during prolonged EEG-fMRI studies." Clin Neurophysiol **119**(12): 2762-2774.

Uhlhaas, P. J. (2011). "High-frequency oscillations in schizophrenia." Clin EEG Neurosci **42**(2): 77-82.

Uhlhaas, P. J., C. Haenschel, D. Nikolic and W. Singer (2008). "The role of oscillations and synchrony in cortical networks and their putative relevance for the pathophysiology of schizophrenia." Schizophr Bull **34**(5): 927-943.

Uhlhaas, P. J. and W. Singer (2006). "Neural synchrony in brain disorders: relevance for cognitive dysfunctions and pathophysiology." Neuron **52**(1): 155-168.

Uhlhaas, P. J. and W. Singer (2010). "Abnormal neural oscillations and synchrony in schizophrenia." Nat Rev Neurosci **11**(2): 100-113.

Van Dijk, K. R., M. R. Sabuncu and R. L. Buckner (2012). "The influence of head motion on intrinsic functional connectivity MRI." Neuroimage **59**(1): 431-438.

Whitfield-Gabrieli, S. and J. M. Ford (2012). "Default mode network activity and connectivity in psychopathology." Annu Rev Clin Psychol **8**: 49-76.

Wood, G., H. C. Nuerk, D. Sturm and K. Willmes (2008). "Using parametric regressors to disentangle properties of multi-feature processes." Behav Brain Funct **4**: 38.

Wu, L., T. Eichele and V. D. Calhoun (2010). "Reactivity of hemodynamic responses and functional connectivity to different states of alpha synchrony: a concurrent EEG-fMRI study." Neuroimage **52**(4): 1252-1260.

Zhang, S. and C. S. Li (2012). "Functional connectivity mapping of the human precuneus by resting state fMRI." Neuroimage **59**(4): 3548-3562.

2.3.1 Supplemental material of Paper 3

Supplemental materials:

DELTA (1 – 3.5Hz)														ALPHA 1 (8.5 – 10.5Hz)		BETA (13 – 30Hz)	
Cluster 1 5506 voxels Peak intensity: 1		Cluster 2 1762 voxels Peak intensity: 1		Cluster 3 1420 voxels Peak intensity: 1		Cluster 4 308 voxels Peak intensity: 1		Cluster 5 293 voxels Peak intensity: 1		Cluster 6 232 voxels Peak intensity: 1		Cluster 7 220 voxels Peak intensity: 1		Cluster 1 434 voxels Peak intensity: 4.218		Cluster 1 252 voxels Peak intensity: 3.9384	
# voxels (≥ 10)	structure	# voxels (≥ 10)	structure	# voxels (≥ 10)	structure	# voxels (≥ 10)	structure	# voxels (≥ 10)	structure	# voxels (≥ 10)	structure	# voxels (≥ 10)	structure	# voxels (≥ 10)	structure	# voxels (≥ 10)	structure
2196	Right Cerebrum	1761	Right Cerebrum	1401	Left Cerebrum	286	Right Cerebrum	293	Left Cerebrum	226	Frontal Lobe	208	Right Cerebrum	434	Left Cerebrum	252	Right Cerebrum
1917	Left Cerebrum	1194	White Matter	865	White Matter	218	Gray Matter	279	Temporal Lobe	226	Right Cerebrum	114	White Matter	421	Occipital Lobe	250	Precuneus
1882	Precuneus	1103	Parietal Lobe	825	Parietal Lobe	132	Thalamus	176	Temporal Mid L	175	Superior Frontal G	83	Gray Matter	355	White Matter	244	Parietal Lobe
1839	White Matter	632	Inferior Parietal L	672	Angular L	114	Thalamus R	169	White Matter	134	Frontal Sup R	66	Limbic Lobe	293	Occipital Mid L	163	Precuneus R
1774	Parietal Lobe	614	Temporal Lobe	563	Temporal Lobe	97	Caudate R	157	Sup. Temporal G	115	Gray Matter	62	Parahippocampal G	189	Middle Occipital G	144	White Matter
1600	Gray Matter	576	Angular R	491	Gray Matter	86	Caudate	112	Gray Matter	87	White Matter	41	Thalamus	159	Cuneus	93	Brodmann area 7
1391	Limbic Lobe	498	Gray Matter	330	Inferior Parietal L	80	White Matter	85	Mid. Temporal G	85	Frontal Mid R	38	Parahhippocampal R	87	Occipital Sup L	93	Gray Matter
1169	Precuneus R	392	Supramarginal G	283	Temporal Mid L	72	Medial Dorsal N	67	Temporal Sup L	81	Brodmann area 8	32	Pulvinar	75	Gray Matter	84	Cuneus R
853	Cerebellum Post Lobe	385	Superior Temporal G	262	Sup. Temporal G	49	Caudate Body	54	Brodmann area 21	51	Middle Frontal G	29	Hippocampus R	37	Brodmann area 19		
850	Precuneus L	307	SupraMarginal R	246	Middle Temporal G	37	Caudate Head	33	Brodmann area 22	27	Brodmann area 9	26	Insula	32	Lingual Gyrus		
832	Declive	306	Brodmann area 40	233	Brodmann area 39	30	Corpus Callosum	10	Insula			22	Fusiform R	28	Brodmann area 18		
800	Posterior Cingulate	292	Parietal Inf R	202	Supramarginal G	22	Thalamus L					15	Thalamus R	25	Occipital Inf L		
712	Right Cerebellum	206	Temporal Mid R (aal)	198	Parietal Inf L	20	Left Cerebrum					14	Brodmann area 13				
628	Brodmann area 7	183	Temporal Sup R (aal)	194	Angular G	19	Ventral Lateral N					14	Insula R				
604	Occipital Lobe	124	Angular Gyrus	127	Brodmann area 40							11	Heschl R				
534	Left Cerebellum	106	Middle Temporal G	120	Occipital Mid L							10	Culmen				
499	Cingulate Gyrus	105	Brodmann area 39	91	Precuneus							10	Cerebellum Anter. L				
494	Brodmann area 31	53	Brodmann area 13	63	Sup. Parietal L							10	Temporal Lobe				
415	Cerebelum 6 R	42	Insula	59	Brodmann area 7							10	Right Cerebellum				
393	Cerebellum Anterior L	40	Occipital Mid R	51	SupraMarginal L												
365	Culmen	21	Brodmann area 7	51	Brodmann area 19												
308	Calcarine L	14	Parietal Sup R	35	Parietal Sup L												
254	Cingulum Mid L	13	Sup Parietal Lobule	21	Brodmann area 22												
248	Cerebelum Crus1 L	13	Brodmann area 22	17	Temporal Sup L												
228	Cingulum Mid R			13	Occipital Lobe												
222	Cuneus L																
206	Lingual R																
203	Cuneus R																
176	Calcarine R																
172	Cingulum Post L																
169	Cuneus																
167	Lingual Gyrus																
163	Frontal Lobe																
160	Paracentral L																
131	Brodmann area 30																
120	Brodmann area 23																
112	Cerebelum 6 L																
107	Cerebelum 4/5 R																
106	Temporal Lobe																
94	Parahippocampa G																
91	Cerebelum 4/5 L																
91	Vermis 6																
88	Lingual L																
74	Cingulum Post R																
63	Brodmann area 18																
62	Fusiform L																
45	Brodmann area 5																
40	Cerebelum Crus1 R																
32	Occipital Sup L																
32	Vermis 7																
31	Parahippocampal L																
27	Brodmann area 29																
26	Brodmann area 19																
25	Hippocampus L																
24	Vermis 4/5																
24	Brodmann area 24																
19	Occipital Sup R																
19	Fusiform Gyrus																
18	Vermis 8																
15	Hippocampus																
14	Nodule																
13	Corpus Callosum																
12	Declive of Vermis																
12	Brodmann area 36																
12	Brodmann area 37																
11	Cerebelum Crus 2 L																

Table 1: Significant between-group clusters in GFS delta, alpha1 and beta band

Detailed procedure for EEG preprocessing at both sites:

SFVAMC:

1. Correction for MR gradient artifacts using artifact subtraction proposed by Allen et al. (Allen, Josephs et al. 2000) as implemented in Brain Vision Analyzer. The correction involved subtracting an artifact template from the raw data, using a baseline-corrected sliding average of 21 consecutive volumes to generate the template.
2. Down-sampling of EEG data to 250Hz.
3. Removal of ballistocardiac artifact by subtracting a heartbeat template from the EEG, using a sliding average of 21 (±10 centered on a given pulse) heartbeat events as originally proposed (Allen, Polizzi et al. 1998) and done by others (Schulz, Regenbogen et al. 2015, Shams, Alain et al. 2015). Parameters of the semi-automatic heartbeat detection in Brain Vision Analyzer were: high temporal correlation (r >.5) and above threshold amplitude (0.6-1.7) with trained research assistants adjusting templates, search windows, and manually identifying pulses as needed.
6. Canonical correlation analysis (CCA) was used as a blind source separation technique to remove broadband or electromyography (EMG) noise from single trial data using a method similar to that used by others (De Clercq, Vergult et al. 2006, Ries, Janssen et al. 2013) with some important differences. The CCA de-noising procedure involves correlating time series data from all channels with the one-sample time-lagged series from all channels, which is the multivariate equivalent of auto-regressive time series correlation. Each set of canonical correlation coefficients (one for each electrode resulting in 31 for this study) has an associated time series (i.e., linear function of the coefficients and raw data called canonical variates). The Fast Fourier Transformed (FFT) power spectra of these canonical variate time series have been used to identify EMG components by taking the ratio of high (e.g., 15 to 30Hz) to low (e.g., <15Hz) power and removing components with ratios greater than a pre-determined limit (e.g., if high/low > 1/5 in (Ries, Janssen et al. 2013). This is a very rough heuristic for determining if a canonical variate's power spectrum has Power-law scaling (e.g., $1/f^{\beta}$ or f^{α}, where $-\beta=\alpha$) where log-transformed power decreases linearly with increasing log-transformed frequency. Previous studies (Pereda, Gamundi et al. 1998, Freeman, Holmes et al. 2003) have suggested that the exponent, α, is less than -1 in human EEG, while white noise or EMG would have an exponent of approximately zero. Using simple linear regression, we estimated α by predicting log-power with log-frequency. For each trial and canonical variate, a bootstrap confidence interval was constructed for the estimated α by randomly sampling, without replacement, half of the frequency bins between 1-125Hz from the FFT one thousand times to avoid potential contamination by a few frequencies (i.e., 60Hz or alpha-band). If the interval contained values less than -1, the component was retained while all others were algebraically removed during back-projection to the original EEG epoch space.
7. Single trial data were re-referenced to an average reference, and data were obtained for the prior reference channel, FCz.
8. Outlier trials were rejected based on previously established criteria from FASTER (Nolan, Whelan et al. 2010, Ford, Palzes et al. 2014)
9. Independent components analysis (ICA) was then performed on each subject in EEGLAB (Delorme and Makeig 2004), generating 32 independent components.
10. Noise components were identified by FASTER criteria (Nolan, Whelan et al. 2010), and also spatial correlations of $|r|>0.8$ with eye blink and ballistocardiac artifact templates. The eyeblink template was created by averaging components resembling frontal-only activity, while the ballistocardiac template was created by setting midline electrodes to 0 and the two hemispheres with opposing signs, resembling a dipole effect (see

figure 1). These noise components were then removed from the data during back-projection (in controls: mean = 7.1, SD =2.1; in patients: mean = 8.0, SD = 3.2 out of 32 components).

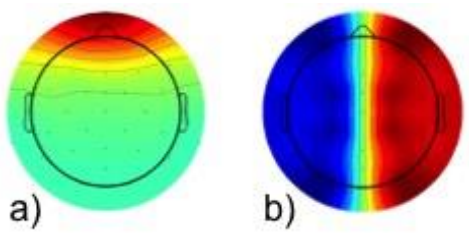

Figure 1: Templates for removal of a) eyeblink and b) ballistocardiac artifacts using FASTER

PUK Bern:

The procedures used for artifact removal are based on previous literature (Jann, Dierks et al. 2009, Jann, Kottlow et al. 2010, Kottlow, Jann et al. 2012, Razavi, Jann et al. 2013, Kottlow, Schlaepfer et al. 2015) and briefly summarized here:

1. By means of average artifact subtraction with a sliding window of 21 (Allen, Josephs et al. 2000), the EEG was corrected for MR related artifacts including scan-pulse and cardio-ballistic artifact.
2. EEG files from outside and inside of the scanner were down-sampled to 500Hz and concatenated.
3. Application of a bandpass filter (1 – 49Hz and a notch filter) to the concatenated file and disabling of bad channels.
4. Further cleaning of the EEG from remaining scan-pulse, cardio-ballistic and eye movement artifacts using an ICA-based approach (number of ICA components removed in controls: mean = 20.5, SD = 2.7; in patients: mean = 18.4, SD = 3.4 out of 64 components). By visual inspection of the components' temporal dynamics, topographic maps, and the comparison of their power spectra from inside versus outside of the scanner, components loading for artifacts were identified. Then, the EEG of each subject was reconstructed from the remaining factors.
5. Manual marking of epochs containing residual scanner or movement artifacts and interpolating of disabled channels using a spherical spline interpolation.
6. After removal of the ECG and EOG channels, the EEG was recalculated to average reference.

References

Allen, P. J., O. Josephs and R. Turner (2000). "A method for removing imaging artifact from continuous EEG recorded during functional MRI." Neuroimage **12**(2): 230-239.

Allen, P. J., G. Polizzi, K. Krakow, D. R. Fish and L. Lemieux (1998). "Identification of EEG events in the MR scanner: the problem of pulse artifact and a method for its subtraction." Neuroimage **8**(3): 229-239.

De Clercq, W., A. Vergult, B. Vanrumste, W. Van Paesschen and S. Van Huffel (2006). "Canonical correlation analysis applied to remove muscle artifacts from the electroencephalogram." IEEE Trans Biomed Eng **53**(12 Pt 1): 2583-2587.

Delorme, A. and S. Makeig (2004). "EEGLAB: an open source toolbox for analysis of single-trial EEG dynamics including independent component analysis." J Neurosci Methods **134**(1): 9-21.

Ford, J. M., V. A. Palzes, B. J. Roach and D. H. Mathalon (2014). "Did I do that? Abnormal predictive processes in schizophrenia when button pressing to deliver a tone." Schizophr Bull **40**(4): 804-812.

Freeman, W. J., M. D. Holmes, B. C. Burke and S. Vanhatalo (2003). "Spatial spectra of scalp EEG and EMG from awake humans." Clin Neurophysiol **114**(6): 1053-1068.

Jann, K., T. Dierks, C. Boesch, M. Kottlow, W. Strik and T. Koenig (2009). "BOLD correlates of EEG alpha phase-locking and the fMRI default mode network." Neuroimage **45**(3): 903-916.

Jann, K., M. Kottlow, T. Dierks, C. Boesch and T. Koenig (2010). "Topographic electrophysiological signatures of FMRI Resting State Networks." PLoS One **5**(9): e12945.

Kottlow, M., K. Jann, T. Dierks and T. Koenig (2012). "Increased phase synchronization during continuous face integration measured simultaneously with EEG and fMRI." Clin Neurophysiol **123**(8): 1536-1548.

Kottlow, M., A. Schlaepfer, A. Baenninger, L. Michels, D. Brandeis and T. Koenig (2015). "Pre-stimulus BOLD-network activation modulates EEG spectral activity during working memory retention." Front Behav Neurosci **9**: 111.

Nolan, H., R. Whelan and R. B. Reilly (2010). "FASTER: Fully Automated Statistical Thresholding for EEG artifact Rejection." J Neurosci Methods **192**(1): 152-162.

Pereda, E., A. Gamundi, R. Rial and J. Gonzalez (1998). "Non-linear behaviour of human EEG: fractal exponent versus correlation dimension in awake and sleep stages." Neurosci Lett **250**(2): 91-94.

Razavi, N., K. Jann, T. Koenig, M. Kottlow, M. Hauf, W. Strik and T. Dierks (2013). "Shifted coupling of EEG driving frequencies and fMRI resting state networks in schizophrenia spectrum disorders." PLoS One **8**(10): e76604.

Ries, S., N. Janssen, B. Burle and F. X. Alario (2013). "Response-locked brain dynamics of word production." PLoS One **8**(3): e58197.

Schulz, M. A., C. Regenbogen, C. Moessnang, I. Neuner, A. Finkelmeyer, U. Habel and T. Kellermann (2015). "On utilizing uncertainty information in template-based EEG-fMRI ballistocardiogram artifact removal." Psychophysiology **52**(6): 857-863.

Shams, N., C. Alain and S. Strother (2015). "Comparison of BCG artifact removal methods for evoked responses in simultaneous EEG-fMRI." J Neurosci Methods **245**: 137-146.

3. GENERAL DISCUSSION

This project intended to provide novel insights into functional network properties in schizophrenia patients as determined by simultaneous EEG-fMRI measurements during rest and from prestimulus to task-related states in the framework of state dependency.

In our second study, we could replicate findings in healthy controls from the first study: Mainly, it could be shown that there are consistent relationships between TCNs and EEG frequency bands, even in a timely lagged manner (especially the inverse relationship between prestimulus DMN and FM theta power). Furthermore, EEG load effects and the averaged fluctuations of TCNs seemed comparable in healthy controls between both studies. Thus, it can be concluded that reliable findings in healthy controls were detected to which data from patients with schizophrenia were put into context. Both studies performed on patient's data (studies 2&3) gave evidence of alterations in the activation level, functional state, and integrative mechanisms of TCNs or brain regions comprised in typical TCNs. In the second study (based on study 1 including healthy subjects only), participants performed a verbal WM task and we examined the coupling between prestimulus TCNs and power of EEG frequencies during the retention period. The third study explored brain regions involved in common-phase synchronization of oscillatory brain activity (assumed to be a binding mechanism of TCNs) during eyes open (EO) resting state. In both studies, unexpectedly, the results indicated that mainly the DMN appeared to be affected in patients with schizophrenia, which will be discussed in the following.

3.1 The default mode network (DMN) from rest to task-related states

The DMN is the most investigated TCN and disruptions have already been linked to different psychiatric and neurological disorders, as indicated in the introductory chapter. In schizophrenia, despite numerous studies, the results remain ambiguous. Both hyper- and hypoconnectivity within the DMN and between nodes of the DMN to other TCNs during rest as well as different cognitive tasks have been reported (for reviews see Greicius 2008, Broyd, Demanuele et al. 2009, Fornito, Zalesky et al. 2012, Whitfield-Gabrieli and Ford 2012), and no useful predictor has been established so far. We will use the term *dysconnectivity* instead of *disconnectivity* of networks from now on as the former allows both hypo- as well as hyperconnectivity, whereas the latter

historically referred to disruptions in the sense of hypoconnectivity of networks. What can be deduced from the conducted studies within this project in relation to the current status of research?

a) Alteration of the functional state during rest

During EO resting state, regions of the DMN were differently integrated through common-phase synchronization as measured with GFS (study 3). Most extensive differences were found in the delta band with hub regions of the DMN including the PrC, the PCC, and the IPL being negatively related in patients but positively in controls. The opposite was found in the PrC in association with GFS beta band.

Further support for changed electrophysiological signatures of the DMN is provided by the EEG-fMRI study of Razavi et al (2013). They showed that patient's DMN was coupled to lower frequencies (theta and alpha band) than controls (beta band) during EC resting state (Razavi, Jann et al. 2013). Also, a Magnetoencephalography (MEG) study during EO rest revealed increased involvement of theta, alpha and beta band power in the PCC in schizophrenia patients compared to controls using source analyses (Kim, Shin et al. 2014).

b) No activation deficit in the DMN at prestimulus

Using an ICA approach on the fMRI-BOLD data in our second study, no preparatory deficit in DMN activity was seen, as activation levels were comparable between groups at prestimulus. However, it is theoretically possible that hemodynamic fluctuations of some regions are hyper- and others hypoconnected within the DMN, but that the network in its entirety is comparable to healthy controls due to an equalization of effects.

c) Lack of task-related suppression of the DMN

In line with previous reports of reduced task-related DMN modulations in subjects at high risk and with first episode psychosis (e.g. Pomarol-Clotet, Salvador et al. 2008, Whitfield-Gabrieli, Thermenos et al. 2009, Fryer, Woods et al. 2013), patients had significantly less suppression of the DMN during the retention period of the WM task compared to healthy controls (study 2). It was shown that a reduced suppression is related to impaired task performance as seen in prolonged reaction times or lower accuracy rates in healthy controls (e.g. Drummond, Bischoff-Grethe et al. 2005, Weissman, Roberts et al. 2006, Eichele, Debener et al. 2008, Anticevic, Repovs et al.

2010) as well as schizophrenia patients (e.g. Whitfield-Gabrieli, Thermenos et al. 2009, Zhou, Pu et al. 2016).

d) Alterations of the coupling from pre-to-post stimulus

We additionally observed changes in the relationship between prestimulus DMN with theta (especially FM theta) band power during the retention period of higher WM load trials in patients, indicating that they could not rally task-related memory functions similarly as healthy controls (study 2).

To some degree, the findings of a different functional state of the DMN during rest (a) and from pre-to-post stimulus (d) in the WM task might be explained by long-lasting evidence of heightened power in lower EEG frequencies as delta and especially theta band during resting state (e.g. Boutros, Arfken et al. 2008, Galderisi, Mucci et al. 2009). Previous studies showed that in general, especially alpha and beta were positively and FM theta band negatively related to the DMN in healthy controls (see Chapter 1.2.3.1). Derived from other studies (Mantini, Perrucci et al. 2007, Jann, Kottlow et al. 2010), a specific TCN is not only related to a single frequency band, thus subregions of a TCN can be modulated by different oscillatory frequencies at the time. A further aspect increasing the complexity to relate DMN activity to mental disorders in general is that particular DMN hub regions maintain different mental functions and thus altered functional states of certain hubs can cause diverse functional impairments. The mPFC for example is activated in tasks containing social cognition as well as self-referential processing (e.g. Gusnard, Akbudak et al. 2001, Bzdok, Langner et al. 2013). The PCC was related to the retrieval of autobiographic episodic memory and self-referential tasks (e.g. Fink, Markowitsch et al. 1996, Piefke, Weiss et al. 2003, D'Argembeau, Collette et al. 2005) and the PrC to reflective, self-related processing, visuospatial imagery, episodic memory, awareness and conscious information processing (Cavanna and Trimble 2006, Zhang and Li 2012).

e) Linking rest and pre-to-post stimulus findings

Despite the lack of fMRI-BOLD differences in the DMN during the prestimulus period (b), its functional state at rest (a) and from pre-to-post stimulus (d) was altered in addition to a deficient task-related suppression (c). Consequently, it seems that the DMN cannot be modulated appropriately to task-related requirements due to its functional deviations, which could be paralleled by hyper- and/or hypo-activations

between hub regions within the DMN or between the DMN and task-positive networks as the dAN.

To sum up, the DMN seems to be a key TCN in the detection of possible biological markers in various mental and neurologic disorders, but the specificity and validity of DMN alterations in schizophrenia need to be further investigated. However, Seeley et al showed that other TCNs as the saliency network (Seeley, Menon et al. 2007) were more sensitive to neurodegenerative diseases such as fronto-temporal dementia (Seeley, Allman et al. 2007). It is perspicuous that TCNs facilitating functions that are deficient in the patient population of interest would be predominantly affected, leading to characteristic symptoms or cognitive deficits observed. Finally, as presented in the introduction (see Chapters 1.2.2.1, 1.4), TCNs are interdependent and thus, not only the DMN, but also other TCNs are of interest in gaining further insights into schizophrenia.

3.2 Interplay of networks and modulation of EEG frequencies

For effective information processing, many different factors play together. First of all, brain activation elicited by a task relies on the prestimulus or resting state as explained by the theory of state dependency (Chapter 1.4). Furthermore, TCNs are interdependent and if one specific TCN is affected, it certainly has a further (causal) effect on other TCNs. And finally, different EEG frequency bands modulate the functional state of TCNs, may it be in either an inhibitory or excitatory way. Consequently, how all those possible factors influence cognitive functions in the healthy and diseased brain is complex, but we will shortly discuss what can be abstracted from our performed studies.

a) Reduced anti-correlation between the DMN and dAN

The second study demonstrated that the anti-correlation between the functionally opposed DMN and dAN was overall reduced at higher WM load in patients. Thus, patients seem to have deficient orientation of attention to internal versus external events. As this anti-correlation has been linked to more efficient cognitive processing as seen in shorter reaction times (RTs; e.g. Drummond, Bischoff-Grethe et al. 2005, Weissman, Roberts et al. 2006) and fewer error rates (e.g. Daselaar, Prince et al. 2004, Eichele, Debener et al. 2008, Anticevic, Repovs et al. 2010), this reduction could partly account for the increased RTs seen in patients when performing the task and impairments in cognitive tasks more in general. As stated earlier, we found altered

coupling of prestimulus DMN with EEG theta power (see 3.1 d)) during high load WM retention, but also a cross-load similarity in the dAN with theta power for lower load in patients compared to higher load in healthy controls. This implies a disturbance of the functional states of both TCNs, which could explain their reduced anti-correlation to some degree.

b) Missing lateralization effect of WMNs

Furthermore, in healthy controls there was a lateralization towards the left WMN over whole trial durations for the WM task, whereas this lateralization was missing in patients, besides an even higher involvement of the right WMN. As the WM task was of a verbal nature and it has been shown that left hemispheric WMN is recruited for verbal as compared to the right WMN in spatial WM tasks (Walter, Wunderlich et al. 2003), there is a twofold interpretation of these results: Either, patients were unable to inhibit the task-irrelevant right hemisphere or it is a compensation effect as they needed more resources to be able to perform the WM task. Overall, our results support the hypothesis that patients were still within, but close to the limit of their cognitive capacities.

3.3 Remaining questions and limitations

Some explanations for observed discrepancies of DMN functional connectivity between studies could be the following: First, different methodologies were used to explore functional connectivity. The two main categories are either seed-based or ROI analyses versus ICA. Using either approach, there are differences in their statistical implementations, as for example the a priori selection of the ROI within DMN hub regions or the amount of components chosen to run the ICA. Second, the variety of paradigms including simple perceptual to higher cognitive tasks as well as EO versus EC resting state might account for different findings. And third, different subgroups of schizophrenia patients were studied including first-degree relatives, first episode psychosis, and chronic schizophrenia patients, which further complicates the comparability of studies.

An important limitation of the studies presented in this thesis is the following: The comparableness of the findings between the studies including patient's data is restricted, as we used different methodologies (EEG-informed fMRI versus fMRI-informed EEG analysis) during different conditions (rest, task-related states), which hinder clear statements about the relationship between them. Future studies trying to

incorporate different network properties during rest as well as in interaction with task states could further help to strengthen the importance of the presented findings.

Another question that remains to be solved is if deviations of TCN captured by means of EEG and fMRI are disorder–specific and if they could be used to classify patients based on the pattern of present alterations. Encouraging findings in Alzheimer's disease, which received the most attention from investigations, exist where healthy controls and Alzheimer patients could be classified with high level of sensitivity (85%) and specificity (77%) in reference to a DMN template (Greicius, Srivastava et al. 2004). Also, whether deficits represent state or trait markers of the disorder have to be resolved. However, parametrical reductions of task-induced DMN suppression was reported as a continuum from unaffected siblings, youth at high-risk for psychosis to first episode psychosis (Pomarol-Clotet, Salvador et al. 2008, de Leeuw, Kahn et al. 2013, Fryer, Woods et al. 2013), arguing for DMN activity reflecting an endophenotype. There is a lack of data in acute patients, but the performance of tasks and especially MRI acquisitions are hardly feasible in this patient group: First, the understanding of the study and task has to be affirmed. Second, subjects need to be able to lie still and quietly in the scanner for a longer period of time in addition to further time requirements for preparation. Hence, a minimum of attentional and cognitive resources is already required. Also, despite the known advantages of simultaneous EEG and fMRI measurements and their common neuronal basis (Chapter 1.2.3), there is still a lack of understanding the exact nature of the neurovascular coupling and further studies are needed. As a final remark, the results from our presented functional connectivity studies within this thesis project are of descriptive character and do not give any causal explanations (further discussed *Perspectives*).

3.4 Concluding remarks

Our results point towards a multitude of changed indices of functional networks, especially the DMN, at rest and from pre-to-post stimulus states in WM processes (an overview of the discussed findings is presented in Table 2). Taken together, the resting and prestimulus states provide important information to understand the baseline state of the brain and how they relate to subsequent information processing in a demand-dependent manner. The observed changes in patients might partly explain their experienced symptomatology as well as detrimental performance in cognitive tasks such as WM. For example, the altered functional coupling of the DMN and dAN as well

as the reduced anti-correlation between them might explain a problematic balance between internal versus externally oriented attention. It seems promising to further explore TCNs as possible biomarkers and targets for treatments as will be further elaborated in the consecutive chapter *Perspectives*.

	DIFFERENT MENTAL STATES			
	RESTING STATE	**TASK-RELATED STATES**		
		PRESTIMULUS	**ON-TASK**	**PRE-TO-POST STIMULUS**
DMN	(a) Different association of GFS Delta and Beta band with regions of the DMN	(b) No difference in DMN activation	(c) Reduced DMN suppression	(d) Different coupling of DMN with theta band
Interplay between TCNs	Not investigated	(a) Reduced anti-correlation between DMN & dAN		
		(b) Missing lateralization effect in WMNs		

Table 2: Overview of main findings from studies including patient's data (studies 2&3)

4. PERSPECTIVES

4.1 The search for valid biomarkers

As long as the diagnosis of schizophrenia is based on the collection of a bundle of descriptive symptoms, finding viable biomarker remains difficult. As mentioned in the introduction, it is still ambiguous how results of altered functional TCNs can be related to the etiology, pathophysiological mechanisms and the finally observed clinical symptoms in schizophrenia. Additionally, the complexity of the brain makes it hard to understand all processes that are relevant for schizophrenia and therefore, methods of systems science could be helpful tools to overcome this limitation (Tretter and Scherer 2006). Functional connectivity alone cannot reveal causes of TCN dysconnectivity, as the direction of information flow remains hidden. Hence, effective connectivity analyses are beneficial to overcome this gap, given the interactions are causal.

In an exemplary study, looking at the fronto-parietal (FP) network, Schmidt et al (2014) pointed out what connectivity changes were found for different endophenotypes of psychosis (looking at psychosis as a continuum). The authors further suggested modeling approaches, which could help to increase the specificity and validity of an early diagnosis and prevention of onset of illness. They mentioned two approaches that should be used complementary: First, graph theory could help to detect network connectivity endophenotypes by using whole-brain connectivity

patterns. As a second step, those results could inform constrained models of effective connectivity such as in dynamic causal modeling (DCM; Schmidt, Diwadkar et al. 2014). Another analysis technique that could help to classify disease mechanisms in individual patients is the so-called *generative embedding* based again on DCM introduced by Brodersen et al (Brodersen, Haiss et al. 2011). Applying this method to data from schizophrenia patients, they could determine three clinically distinct subgroups based on neurophysiological patterns that differed significantly in their negative symptom severity (Brodersen, Deserno et al. 2014).

Besides exploring functionally connected brain networks, we further need to elucidate the relationship between structural and functional connectivity as they are interrelated (see Chapter 1.2).

4.2 Linking structure and function of the brain

It was proven that typical TCNs such as the DMN show underlying structural connectivity as measured by means of diffusion tensor imaging (DTI; Greicius, Supekar et al. 2009, van den Heuvel, Mandl et al. 2009). Anatomical connections are necessary to give raise to functionally co-activated regions, but regions being functionally co-activated do not necessarily need to be directly connected to each other. As Stephan et al (2009) commented, the link between dysconnectivity of networks could result either from aberrant synaptic plasticity, aberrant wiring of connections or both (Stephan, Friston et al. 2009).

Therefore, analyses incorporating structural and functional data to check whether abnormalities are overlapping between both modalities or not are promising. Within the DMN, several studies found overlapping abnormalities between structural and functional indices in schizophrenia patients. Pomarol-Clotet et al (2010) showed in chronic patients that a predominant reduction of grey matter volume in the medial frontal cortex coincided with failures to deactivate the DMN during an n-back task (Pomarol-Clotet, Canales-Rodriguez et al. 2010). Another study reported on reduced task-induced deactivations of anterior and posterior midline nodes of the DMN besides structural data overlapping with decreased grey matter volume in these areas (Salgado-Pineda, Fakra et al. 2011). It has to be mentioned that those studies included grey matter volume, which is not a direct measure of axonal connections and hence structural connectivity. To this end, DTI measures are needed, as they inform about white matter tracks of the brain. One such study combining DTI and fMRI found that a

reduced functionally connected DMN in anterior nodes (mPFC, ACC) was paralleled by less white matter subjacent to this area (Camchong, MacDonald et al. 2011). Consequently, there is prove of common abnormalities in structural and functional imaging data, but there are also studies revealing the opposite, again using measures of grey matter volume in combination with fMRI (Calhoun, Adali et al. 2006, Lui, Deng et al. 2009). An interesting data-driven method calculating whole-brain inter-correlations between structural and functional MRI data concluded that the linkage between grey matter and functional activations was reduced in schizophrenia patients compared to healthy controls (Michael, Baum et al. 2010). The continuation of joint functional and structural data analyses (especially using DTI and fMRI connectivity measures) could help to detect hidden traits in complex disorders such as schizophrenia. Furthermore, they could provide information to further confine the interpretation of dysconnectivity reported in fMRI studies.

4.3 Possible therapeutic interventions

The main objective of investigations in psychiatric disorders in addition to increasing understanding of their neurophysiological basis, is to develop new or improve existing treatment options. In schizophrenia, roughly 30% of patients are not responding well to typical conventional and atypical antipsychotic medication (Lieberman, Stroup et al. 2005, Harvey and Rosenthal 2016) and show severe side effects, reducing quality of life and potentially increase the mortality risk (Chapter 1.1.1).

There are suggestions that pharmacological agents targeting specific network hubs could be used to normalize activation patterns within TCNs. Those agents would be assumed to have a more specific effect on symptoms related to activation changes in the respective TCN (e.g. Gebicke-Haerter 2016). Still, effective non-invasive approaches would be preferable over medication.

Among non-invasive techniques, neurofeedback represents a possible treatment option where subject learn usually via visual or auditory feedback to self-regulate brain states. A recent study from our group suggested the feasibility of EEG microstate D neurofeedback in healthy participants (Diaz Hernandez, Rieger et al. 2016). As this microstate is shortened in schizophrenia patients, especially during auditory verbal hallucinations (Kindler, Hubl et al. 2011), it seems to be appropriate trying to translate it to patients. Other non-invasive brain stimulation techniques such as transcranial direct current stimulation (tDCS), or transcranial magnetic stimulation (TMS) could be

used to target specific hub regions within TCNs (e.g. the DMN or dAN). Regions shown to be either hyper- or hypoactive would be stimulated in an inhibitory or excitatory way, respectively, to reestablish the balance within and between specific TCNs. Palm et al (2016) recently presented findings of a tDCS protocol applied on the prefrontal cortex causing a reduction of symptomatology (especially negative symptoms) as well changes in functional connectivity within frontal-thalamic-temporo-parietal networks (Palm, Keeser et al. 2016).

As described by Mantini et al (2007), we might think of TCNs representing a "*finite set of spatiotemporal basis functions from which task-networks are then dynamically assembled and modulated during different behavioral states*" (Mantini, Perrucci et al. 2007). Consequently, by modulating the activation level and/or functional state of a particular TCN, it most certainly will influence the efficiency of other TCNs (especially regarding TCNs that are anti-correlated to each other as the DMN and any task-positive network including the dAN). Based on the presented results of altered TCNs, mainly the DMN and dAN, during rest and from pre-to-post states, I would recommend continuing the exploration of TCNs, especially the DMN, to gain reliable and possibly valid biomarkers for this severe mental illness. If this point will be achieved, it seems promising to try to normalize the activation patterns and functional states of the DMN, as this network represents a basic, intrinsic function of the brain that further influences the activation patterns when confronted with task situations.

REFERENCES

Addington, J. and R. Heinssen (2012). "Prediction and prevention of psychosis in youth at clinical high risk." Annu Rev Clin Psychol **8**: 269-289.

Allen, A. J., M. E. Griss, B. S. Folley, K. A. Hawkins and G. D. Pearlson (2009). "Endophenotypes in schizophrenia: a selective review." Schizophr Res **109**(1-3): 24-37.

Andreasen, N. C. (2000). "Schizophrenia: the fundamental questions." Brain Res Brain Res Rev **31**(2-3): 106-112.

Anticevic, A., G. Repovs, G. L. Shulman and D. M. Barch (2010). "When less is more: TPJ and default network deactivation during encoding predicts working memory performance." Neuroimage **49**(3): 2638-2648.

Auquier, P., C. Lancon, F. Rouillon, M. Lader and C. Holmes (2006). "Mortality in schizophrenia." Pharmacoepidemiol Drug Saf **15**(12): 873-879.

Bak, N., E. Rostrup, H. B. Larsson, B. Y. Glenthoj and B. Oranje (2014). "Concurrent functional magnetic resonance imaging and electroencephalography assessment of sensory gating in schizophrenia." Hum Brain Mapp **35**(8): 3578-3587.

Beckmann, C. F. and S. M. Smith (2004). "Probabilistic independent component analysis for functional magnetic resonance imaging." IEEE Trans Med Imaging **23**(2): 137-152.

Biessmann, F., S. Plis, F. C. Meinecke, T. Eichele and K. R. Muller (2011). "Analysis of multimodal neuroimaging data." IEEE Rev Biomed Eng **4**: 26-58.

Biswal, B., F. Z. Yetkin, V. M. Haughton and J. S. Hyde (1995). "Functional connectivity in the motor cortex of resting human brain using echo-planar MRI." Magn Reson Med **34**(4): 537-541.

Bluhm, R. L., J. Miller, R. A. Lanius, E. A. Osuch, K. Boksman, R. W. Neufeld, J. Theberge, B. Schaefer and P. Williamson (2007). "Spontaneous low-frequency fluctuations in the BOLD signal in schizophrenic patients: anomalies in the default network." Schizophr Bull **33**(4): 1004-1012.

Boutros, N. N., C. Arfken, S. Galderisi, J. Warrick, G. Pratt and W. Iacono (2008). "The status of spectral EEG abnormality as a diagnostic test for schizophrenia." Schizophr Res **99**(1-3): 225-237.

Brandt, C. L., T. Eichele, I. Melle, K. Sundet, A. Server, I. Agartz, K. Hugdahl, J. Jensen and O. A. Andreassen (2014). "Working memory networks and activation patterns in schizophrenia and bipolar disorder: comparison with healthy controls." Br J Psychiatry **204**: 290-298.

Britz, J. and C. M. Michel (2011). "State-dependent visual processing." Front Psychol **2**: 370.

Brodersen, K. H., L. Deserno, F. Schlagenhauf, Z. Lin, W. D. Penny, J. M. Buhmann and K. E. Stephan (2014). "Dissecting psychiatric spectrum disorders by generative embedding." Neuroimage Clin **4**: 98-111.

Brodersen, K. H., F. Haiss, C. S. Ong, F. Jung, M. Tittgemeyer, J. M. Buhmann, B. Weber and K. E. Stephan (2011). "Model-based feature construction for multivariate decoding." Neuroimage **56**(2): 601-615.

Broyd, S. J., C. Demanuele, S. Debener, S. K. Helps, C. J. James and E. J. Sonuga-Barke (2009). "Default-mode brain dysfunction in mental disorders: a systematic review." Neurosci Biobehav Rev **33**(3): 279-296.

Buckner, R. L., J. R. Andrews-Hanna and D. L. Schacter (2008). "The brain's default network: anatomy, function, and relevance to disease." Ann N Y Acad Sci **1124**: 1-38.

Burwick, T. (2014). "The binding problem." Wiley Interdiscip Rev Cogn Sci **5**(3): 305-315.

Buxton, R. B., K. Uludag, D. J. Dubowitz and T. T. Liu (2004). "Modeling the hemodynamic response to brain activation." Neuroimage **23 Suppl 1**: S220-233.

Bzdok, D., R. Langner, L. Schilbach, D. A. Engemann, A. R. Laird, P. T. Fox and S. B. Eickhoff (2013). "Segregation of the human medial prefrontal cortex in social cognition." Front Hum Neurosci **7**: 232.

Calhoun, V., L. Wu, K. Kiehl, T. Eichele and G. Pearlson (2010). "Aberrant Processing of Deviant Stimuli in Schizophrenia Revealed by Fusion of FMRI and EEG Data." Acta Neuropsychiatr **22**(3): 127-138.

Calhoun, V. D., T. Adali, N. R. Giuliani, J. J. Pekar, K. A. Kiehl and G. D. Pearlson (2006). "Method for multimodal analysis of independent source differences in schizophrenia: combining gray matter structural and auditory oddball functional data." Hum Brain Mapp **27**(1): 47-62.

Calhoun, V. D., K. A. Kiehl and G. D. Pearlson (2008). "Modulation of temporally coherent brain networks estimated using ICA at rest and during cognitive tasks." Hum Brain Mapp **29**(7): 828-838.

Camchong, J., A. W. MacDonald, 3rd, C. Bell, B. A. Mueller and K. O. Lim (2011). "Altered functional and anatomical connectivity in schizophrenia." Schizophr Bull **37**(3): 640-650.

Cavanna, A. E. and M. R. Trimble (2006). "The precuneus: a review of its functional anatomy and behavioural correlates." Brain **129**(Pt 3): 564-583.

Chong, H. Y., S. L. Teoh, D. B. Wu, S. Kotirum, C. F. Chiou and N. Chaiyakunapruk (2016). "Global economic burden of schizophrenia: a systematic review." Neuropsychiatr Dis Treat **12**: 357-373.

Corbetta, M. and G. L. Shulman (2002). "Control of goal-directed and stimulus-driven attention in the brain." Nat Rev Neurosci **3**(3): 201-215.

Cordes, D., V. M. Haughton, K. Arfanakis, G. J. Wendt, P. A. Turski, C. H. Moritz, M. A. Quigley and M. E. Meyerand (2000). "Mapping functionally related regions of brain with functional connectivity MR imaging." AJNR Am J Neuroradiol **21**(9): 1636-1644.

D'Argembeau, A., F. Collette, M. Van der Linden, S. Laureys, G. Del Fiore, C. Degueldre, A. Luxen and E. Salmon (2005). "Self-referential reflective activity and its relationship with rest: a PET study." Neuroimage **25**(2): 616-624.

da Silva, F. H., T. H. van Lierop, C. F. Schrijer and W. S. van Leeuwen (1973). "Organization of thalamic and cortical alpha rhythms: spectra and coherences." Electroencephalogr Clin Neurophysiol **35**(6): 627-639.

Damoiseaux, J. S., S. A. Rombouts, F. Barkhof, P. Scheltens, C. J. Stam, S. M. Smith and C. F. Beckmann (2006). "Consistent resting-state networks across healthy subjects." Proc Natl Acad Sci U S A **103**(37): 13848-13853.

Daselaar, S. M., S. E. Prince and R. Cabeza (2004). "When less means more: deactivations during encoding that predict subsequent memory." Neuroimage **23**(3): 921-927.

de Leeuw, M., R. S. Kahn, B. B. Zandbelt, C. G. Widschwendter and M. Vink (2013). "Working memory and default mode network abnormalities in unaffected siblings of schizophrenia patients." Schizophr Res **150**(2-3): 555-562.

De Luca, M., C. F. Beckmann, N. De Stefano, P. M. Matthews and S. M. Smith (2006). "fMRI resting state networks define distinct modes of long-distance interactions in the human brain." Neuroimage **29**(4): 1359-1367.

de Munck, J. C., S. I. Goncalves, L. Huijboom, J. P. Kuijer, P. J. Pouwels, R. M. Heethaar and F. H. Lopes da Silva (2007). "The hemodynamic response of the alpha rhythm: an EEG/fMRI study." Neuroimage **35**(3): 1142-1151.

De Pisapia, N., M. Turatto, P. Lin, J. Jovicich and A. Caramazza (2012). "Unconscious priming instructions modulate activity in default and executive networks of the human brain." Cereb Cortex **22**(3): 639-649.

Diaz Hernandez, L., K. Rieger, A. Baenninger, D. Brandeis and T. Koenig (2016). "Towards Using Microstate-Neurofeedback for the Treatment of Psychotic Symptoms in Schizophrenia. A Feasibility Study in Healthy Participants." Brain Topogr **29**(2): 308-321.

Drummond, S. P., A. Bischoff-Grethe, D. F. Dinges, L. Ayalon, S. C. Mednick and M. J. Meloy (2005). "The neural basis of the psychomotor vigilance task." Sleep **28**(9): 1059-1068.

Efron, R. (1970). "The minimum duration of a perception." Neuropsychologia **8**(1): 57-63.

Eichele, T., S. Debener, V. D. Calhoun, K. Specht, A. K. Engel, K. Hugdahl, D. Y. von Cramon and M. Ullsperger (2008). "Prediction of human errors by maladaptive changes in event-related brain networks." Proc Natl Acad Sci U S A **105**(16): 6173-6178.

Feige, B., K. Scheffler, F. Esposito, F. Di Salle, J. Hennig and E. Seifritz (2005). "Cortical and subcortical correlates of electroencephalographic alpha rhythm modulation." J Neurophysiol **93**(5): 2864-2872.

Fink, G. R., H. J. Markowitsch, M. Reinkemeier, T. Bruckbauer, J. Kessler and W. D. Heiss (1996). "Cerebral representation of one's own past: neural networks involved in autobiographical memory." J Neurosci **16**(13): 4275-4282.

Ford, J. M. (1999). "Schizophrenia: the broken P300 and beyond." Psychophysiology **36**(6): 667-682.

Fornito, A., A. Zalesky, C. Pantelis and E. T. Bullmore (2012). "Schizophrenia, neuroimaging and connectomics." Neuroimage **62**(4): 2296-2314.

Foucher, J. R., D. Luck, C. Marrer, B. T. Pham, D. Gounot, P. Vidailhet and H. Otzenberger (2011). "fMRI working memory hypo-activations in schizophrenia come with a coupling deficit between arousal and cognition." Psychiatry Res **194**(1): 21-29.

Fox, M. D., M. Corbetta, A. Z. Snyder, J. L. Vincent and M. E. Raichle (2006). "Spontaneous neuronal activity distinguishes human dorsal and ventral attention systems." Proc Natl Acad Sci U S A **103**(26): 10046-10051.

Fox, M. D. and M. E. Raichle (2007). "Spontaneous fluctuations in brain activity observed with functional magnetic resonance imaging." Nat Rev Neurosci **8**(9): 700-711.

Fox, M. D., A. Z. Snyder, J. L. Vincent, M. Corbetta, D. C. Van Essen and M. E. Raichle (2005). "The human brain is intrinsically organized into dynamic, anticorrelated functional networks." Proc Natl Acad Sci U S A **102**(27): 9673-9678.

Fox, M. D., A. Z. Snyder, J. M. Zacks and M. E. Raichle (2006). "Coherent spontaneous activity accounts for trial-to-trial variability in human evoked brain responses." Nat Neurosci **9**(1): 23-25.

Fransson, P. (2005). "Spontaneous low-frequency BOLD signal fluctuations: an fMRI investigation of the resting-state default mode of brain function hypothesis." Hum Brain Mapp **26**(1): 15-29.

Friston, K. J. (1996). "Theoretical neurobiology and schizophrenia." Br Med Bull **52**(3): 644-655.

Friston, K. J. (1998). "The disconnection hypothesis." Schizophr Res **30**(2): 115-125.

Friston, K. J. (1999). "Schizophrenia and the disconnection hypothesis." Acta Psychiatr Scand Suppl **395**: 68-79.

Friston, K. J. (2002). "Dysfunctional connectivity in schizophrenia." World Psychiatry **1**(2): 66-71.

Friston, K. J. (2011). "Functional and effective connectivity: a review." Brain Connect **1**(1): 13-36.

Friston, K. J. and C. D. Frith (1995). "Schizophrenia: a disconnection syndrome?" Clin Neurosci **3**(2): 89-97.

Friston, K. J., C. D. Frith, P. F. Liddle and R. S. Frackowiak (1993). "Functional connectivity: the principal-component analysis of large (PET) data sets." J Cereb Blood Flow Metab **13**(1): 5-14.

Fryer, S. L., S. W. Woods, K. A. Kiehl, V. D. Calhoun, G. D. Pearlson, B. J. Roach, J. M. Ford, V. H. Srihari, T. H. McGlashan and D. H. Mathalon (2013). "Deficient Suppression of Default Mode Regions during Working Memory in Individuals with Early Psychosis and at Clinical High-Risk for Psychosis." Front Psychiatry **4**: 92.

Galderisi, S., A. Mucci, U. Volpe and N. Boutros (2009). "Evidence-based medicine and electrophysiology in schizophrenia." Clin EEG Neurosci **40**(2): 62-77.

Garrity, A. G., G. D. Pearlson, K. McKiernan, D. Lloyd, K. A. Kiehl and V. D. Calhoun (2007). "Aberrant "default mode" functional connectivity in schizophrenia." Am J Psychiatry **164**(3): 450-457.

Gebicke-Haerter, P. J. (2016). "Systems psychopharmacology: A network approach to developing novel therapies." World J Psychiatry **6**(1): 66-83.

Global Burden of Disease Study, C. (2015). "Global, regional, and national incidence, prevalence, and years lived with disability for 301 acute and chronic diseases and injuries in 188 countries, 1990-2013: a systematic analysis for the Global Burden of Disease Study 2013." Lancet **386**(9995): 743-800.

Goldman, R. I., J. M. Stern, J. Engel, Jr. and M. S. Cohen (2002). "Simultaneous EEG and fMRI of the alpha rhythm." Neuroreport **13**(18): 2487-2492.

Gray, C. M., P. Konig, A. K. Engel and W. Singer (1989). "Oscillatory responses in cat visual cortex exhibit inter-columnar synchronization which reflects global stimulus properties." Nature **338**(6213): 334-337.

Gray, C. M. and W. Singer (1989). "Stimulus-specific neuronal oscillations in orientation columns of cat visual cortex." Proc Natl Acad Sci U S A **86**(5): 1698-1702.

Greicius, M. (2008). "Resting-state functional connectivity in neuropsychiatric disorders." Curr Opin Neurol **21**(4): 424-430.

Greicius, M. D., B. Krasnow, A. L. Reiss and V. Menon (2003). "Functional connectivity in the resting brain: a network analysis of the default mode hypothesis." Proc Natl Acad Sci U S A **100**(1): 253-258.

Greicius, M. D. and V. Menon (2004). "Default-mode activity during a passive sensory task: uncoupled from deactivation but impacting activation." J Cogn Neurosci **16**(9): 1484-1492.

Greicius, M. D., G. Srivastava, A. L. Reiss and V. Menon (2004). "Default-mode network activity distinguishes Alzheimer's disease from healthy aging: evidence from functional MRI." Proc Natl Acad Sci U S A **101**(13): 4637-4642.

Greicius, M. D., K. Supekar, V. Menon and R. F. Dougherty (2009). "Resting-state functional connectivity reflects structural connectivity in the default mode network." Cereb Cortex **19**(1): 72-78.

Gusnard, D. A., E. Akbudak, G. L. Shulman and M. E. Raichle (2001). "Medial prefrontal cortex and self-referential mental activity: relation to a default mode of brain function." Proc Natl Acad Sci U S A **98**(7): 4259-4264.

Hampson, M., I. R. Olson, H. C. Leung, P. Skudlarski and J. C. Gore (2004). "Changes in functional connectivity of human MT/V5 with visual motion input." Neuroreport **15**(8): 1315-1319.

Haque, R. U., J. H. Wittig, Jr., S. R. Damera, S. K. Inati and K. A. Zaghloul (2015). "Cortical Low-Frequency Power and Progressive Phase Synchrony Precede Successful Memory Encoding." J Neurosci **35**(40): 13577-13586.

Harvey, P. D. and J. B. Rosenthal (2016). "Treatment resistant schizophrenia: Course of brain structure and function." Prog Neuropsychopharmacol Biol Psychiatry.

Hirano, S., Y. Hirano, T. Maekawa, C. Obayashi, N. Oribe, T. Kuroki, S. Kanba and T. Onitsuka (2008). "Abnormal neural oscillatory activity to speech sounds in schizophrenia: a magnetoencephalography study." J Neurosci **28**(19): 4897-4903.

Hunter, M. D., S. B. Eickhoff, T. W. Miller, T. F. Farrow, I. D. Wilkinson and P. W. Woodruff (2006). "Neural activity in speech-sensitive auditory cortex during silence." Proc Natl Acad Sci U S A **103**(1): 189-194.

Ives, J. R., S. Warach, F. Schmitt, R. R. Edelman and D. L. Schomer (1993). "Monitoring the patient's EEG during echo planar MRI." Electroencephalogr Clin Neurophysiol **87**(6): 417-420.

Jafri, M. J., G. D. Pearlson, M. Stevens and V. D. Calhoun (2008). "A method for functional network connectivity among spatially independent resting-state components in schizophrenia." Neuroimage **39**(4): 1666-1681.

Jann, K., T. Dierks, C. Boesch, M. Kottlow, W. Strik and T. Koenig (2009). "BOLD correlates of EEG alpha phase-locking and the fMRI default mode network." Neuroimage **45**(3): 903-916.

Jann, K., M. Kottlow, T. Dierks, C. Boesch and T. Koenig (2010). "Topographic electrophysiological signatures of FMRI Resting State Networks." PLoS One **5**(9): e12945.

Jann, K., R. Wiest, M. Hauf, K. Meyer, C. Boesch, J. Mathis, G. Schroth, T. Dierks and T. Koenig (2008). "BOLD correlates of continuously fluctuating epileptic activity isolated by independent component analysis." Neuroimage **42**(2): 635-648.

Kapur, S. (2011). "Looking for a "biological test" to diagnose"schizophrenia": are we chasing red herrings?" World Psychiatry **10**(1): 32.

Kapur, S., A. G. Phillips and T. R. Insel (2012). "Why has it taken so long for biological psychiatry to develop clinical tests and what to do about it?" Mol Psychiatry **17**(12): 1174-1179.

Kelly, A. M., L. Q. Uddin, B. B. Biswal, F. X. Castellanos and M. P. Milham (2008). "Competition between functional brain networks mediates behavioral variability." Neuroimage **39**(1): 527-537.

Kennedy, D. P., E. Redcay and E. Courchesne (2006). "Failing to deactivate: resting functional abnormalities in autism." Proc Natl Acad Sci U S A **103**(21): 8275-8280.

Kikuchi, M., T. Koenig, Y. Wada, M. Higashima, Y. Koshino, W. Strik and T. Dierks (2007). "Native EEG and treatment effects in neuroleptic-naive schizophrenic patients: time and frequency domain approaches." Schizophr Res **97**(1-3): 163-172.

Kim, D. I., D. S. Manoach, D. H. Mathalon, J. A. Turner, M. Mannell, G. G. Brown, J. M. Ford, R. L. Gollub, T. White, C. Wible, A. Belger, H. J. Bockholt, V. P. Clark, J. Lauriello, D. O'Leary, B. A. Mueller, K. O. Lim, N. Andreasen, S. G. Potkin and V. D. Calhoun (2009). "Dysregulation of working memory and default-mode networks in schizophrenia using independent component analysis, an fBIRN and MCIC study." Hum Brain Mapp **30**(11): 3795-3811.

Kim, H. (2015). "Encoding and retrieval along the long axis of the hippocampus and their relationships with dorsal attention and default mode networks: The HERNET model." Hippocampus **25**(4): 500-510.

Kim, J. S., K. S. Shin, W. H. Jung, S. N. Kim, J. S. Kwon and C. K. Chung (2014). "Power spectral aspects of the default mode network in schizophrenia: an MEG study." BMC Neurosci **15**: 104.

Kindler, J., D. Hubl, W. K. Strik, T. Dierks and T. Koenig (2011). "Resting-state EEG in schizophrenia: auditory verbal hallucinations are related to shortening of specific microstates." Clin Neurophysiol **122**(6): 1179-1182.

Kleinloog, D., A. Uit den Boogaard, A. Dahan, R. Mooren, E. Klaassen, J. Stevens, J. Freijer and J. van Gerven (2015). "Optimizing the glutamatergic challenge model for psychosis, using S+ - ketamine to induce psychomimetic symptoms in healthy volunteers." J Psychopharmacol **29**(4): 401-413.

Koenig, T., D. Lehmann, N. Saito, T. Kuginuki, T. Kinoshita and M. Koukkou (2001). "Decreased functional connectivity of EEG theta-frequency activity in first-episode, neuroleptic-naive patients with schizophrenia: preliminary results." Schizophr Res **50**(1-2): 55-60.

Koenig, T., L. Prichep, D. Lehmann, P. V. Sosa, E. Braeker, H. Kleinlogel, R. Isenhart and E. R. John (2002). "Millisecond by millisecond, year by year: normative EEG microstates and developmental stages." Neuroimage **16**(1): 41-48.

Koenig, T., and J. Wakermann (2009). "Overview of analytical approaches". In Michel, C.M., T. Koenig, D. Brandeis, L.R.R. Gianotti and J. Wackermann, eds. Electrical Neuroimaging. (pp. 93-110). Cambridge, M.A: Cambridge University Press

Kottlow, M., K. Jann, T. Dierks and T. Koenig (2012). "Increased phase synchronization during continuous face integration measured simultaneously with EEG and fMRI." Clin Neurophysiol **123**(8): 1536-1548.

Kottlow, M., A. Schlaepfer, A. Baenninger, L. Michels, D. Brandeis and T. Koenig (2015). "Pre-stimulus BOLD-network activation modulates EEG spectral activity during working memory retention." Front Behav Neurosci **9**: 111.

Lachaux, J. P., N. George, C. Tallon-Baudry, J. Martinerie, L. Hugueville, L. Minotti, P. Kahane and B. Renault (2005). "The many faces of the gamma band response to complex visual stimuli." Neuroimage **25**(2): 491-501.

Laufs, H., A. Kleinschmidt, A. Beyerle, E. Eger, A. Salek-Haddadi, C. Preibisch and K. Krakow (2003). "EEG-correlated fMRI of human alpha activity." Neuroimage **19**(4): 1463-1476.

Laufs, H., K. Krakow, P. Sterzer, E. Eger, A. Beyerle, A. Salek-Haddadi and A. Kleinschmidt (2003). "Electroencephalographic signatures of attentional and cognitive default modes in spontaneous brain activity fluctuations at rest." Proc Natl Acad Sci U S A **100**(19): 11053-11058.

Lauritzen, M. (2001). "Relationship of spikes, synaptic activity, and local changes of cerebral blood flow." J Cereb Blood Flow Metab **21**(12): 1367-1383.

Lauritzen, M. and L. Gold (2003). "Brain function and neurophysiological correlates of signals used in functional neuroimaging." J Neurosci **23**(10): 3972-3980.

Lehmann, D. (1971). "Multichannel topography of human alpha EEG fields." Electroencephalogr Clin Neurophysiol **31**(5): 439-449.

Lehmann, D., H. Ozaki and I. Pal (1987). "EEG alpha map series: brain micro-states by space-oriented adaptive segmentation." Electroencephalogr Clin Neurophysiol **67**(3): 271-288.

Lehmann, D., W. K. Strik, B. Henggeler, T. Koenig and M. Koukkou (1998). "Brain electric microstates and momentary conscious mind states as building blocks of spontaneous thinking: I. Visual imagery and abstract thoughts." Int J Psychophysiol **29**(1): 1-11.

Leicht, G., S. Vauth, N. Polomac, C. Andreou, J. Rauh, M. Mussmann, A. Karow and C. Mulert (2016). "EEG-Informed fMRI Reveals a Disturbed Gamma-Band-Specific Network in Subjects at High Risk for Psychosis." Schizophr Bull **42**(1): 239-249.

Li, C. S., P. Yan, K. L. Bergquist and R. Sinha (2007). "Greater activation of the "default" brain regions predicts stop signal errors." Neuroimage **38**(3): 640-648.

Liang, M., Y. Zhou, T. Jiang, Z. Liu, L. Tian, H. Liu and Y. Hao (2006). "Widespread functional disconnectivity in schizophrenia with resting-state functional magnetic resonance imaging." Neuroreport **17**(2): 209-213.

Lieberman, J. A., D. Perkins, A. Belger, M. Chakos, F. Jarskog, K. Boteva and J. Gilmore (2001). "The early stages of schizophrenia: speculations on pathogenesis, pathophysiology, and therapeutic approaches." Biol Psychiatry **50**(11): 884-897.

Lieberman, J. A., T. S. Stroup, J. P. McEvoy, M. S. Swartz, R. A. Rosenheck, D. O. Perkins, R. S. Keefe, S. M. Davis, C. E. Davis, B. D. Lebowitz, J. Severe, J. K. Hsiao and I. Clinical Antipsychotic Trials of Intervention Effectiveness (2005). "Effectiveness of antipsychotic drugs in patients with chronic schizophrenia." N Engl J Med **353**(12): 1209-1223.

Linden, D. (2013). "Biological psychiatry: time for new paradigms." Br J Psychiatry **202**(3): 166-167.

Linkenkaer-Hansen, K., V. V. Nikulin, S. Palva, R. J. Ilmoniemi and J. M. Palva (2004). "Prestimulus oscillations enhance psychophysical performance in humans." J Neurosci **24**(45): 10186-10190.

Littow, H., V. Huossa, S. Karjalainen, E. Jaaskelainen, M. Haapea, J. Miettunen, O. Tervonen, M. Isohanni, J. Nikkinen, J. Veijola, G. Murray and V. J. Kiviniemi (2015). "Aberrant Functional Connectivity in the Default Mode and Central Executive Networks in Subjects with Schizophrenia - A Whole-Brain Resting-State ICA Study." Front Psychiatry **6**: 26.

Llinas, R. R. (1988). "The intrinsic electrophysiological properties of mammalian neurons: insights into central nervous system function." Science **242**(4886): 1654-1664.

Logothetis, N. K. (2002). "The neural basis of the blood-oxygen-level-dependent functional magnetic resonance imaging signal." Philos Trans R Soc Lond B Biol Sci **357**(1424): 1003-1037.

Logothetis, N. K. (2008). "What we can do and what we cannot do with fMRI." Nature **453**(7197): 869-878.

Logothetis, N. K., J. Pauls, M. Augath, T. Trinath and A. Oeltermann (2001). "Neurophysiological investigation of the basis of the fMRI signal." Nature **412**(6843): 150-157.

Lowe, M. J., B. J. Mock and J. A. Sorenson (1998). "Functional connectivity in single and multislice echoplanar imaging using resting-state fluctuations." Neuroimage **7**(2): 119-132.

Lui, S., W. Deng, X. Huang, L. Jiang, X. Ma, H. Chen, T. Zhang, X. Li, D. Li, L. Zou, H. Tang, X. J. Zhou, A. Mechelli, D. A. Collier, J. A. Sweeney, T. Li and Q. Gong (2009). "Association of cerebral deficits with clinical symptoms in antipsychotic-naive first-episode schizophrenia: an optimized voxel-based morphometry and resting state functional connectivity study." Am J Psychiatry **166**(2): 196-205.

Mantini, D., M. G. Perrucci, C. Del Gratta, G. L. Romani and M. Corbetta (2007). "Electrophysiological signatures of resting state networks in the human brain." Proc Natl Acad Sci U S A **104**(32): 13170-13175.

McGrath, J., S. Saha, D. Chant and J. Welham (2008). "Schizophrenia: a concise overview of incidence, prevalence, and mortality." Epidemiol Rev **30**: 67-76.

McIntosh, A. R. (1999). "Mapping cognition to the brain through neural interactions." Memory **7**(5-6): 523-548.

McIntosh, A. R. (2000). "Towards a network theory of cognition." Neural Netw **13**(8-9): 861-870.

McKiernan, K. A., B. R. D'Angelo, J. N. Kaufman and J. R. Binder (2006). "Interrupting the "stream of consciousness": an fMRI investigation." Neuroimage **29**(4): 1185-1191.

McKiernan, K. A., J. N. Kaufman, J. Kucera-Thompson and J. R. Binder (2003). "A parametric manipulation of factors affecting task-induced deactivation in functional neuroimaging." J Cogn Neurosci **15**(3): 394-408.

Meltzer, J. A., M. Negishi, L. C. Mayes and R. T. Constable (2007). "Individual differences in EEG theta and alpha dynamics during working memory correlate with fMRI responses across subjects." Clin Neurophysiol **118**(11): 2419-2436.

Metzak, P. D., J. D. Riley, L. Wang, J. C. Whitman, E. T. Ngan and T. S. Woodward (2012). "Decreased efficiency of task-positive and task-negative networks during working memory in schizophrenia." Schizophr Bull **38**(4): 803-813.

Michael, A. M., S. A. Baum, T. White, O. Demirci, N. C. Andreasen, J. M. Segall, R. E. Jung, G. Pearlson, V. P. Clark, R. L. Gollub, S. C. Schulz, J. L. Roffman, K. O. Lim, B. C. Ho, H. J. Bockholt and V. D. Calhoun (2010). "Does function follow form?: methods to fuse structural and functional brain images show decreased linkage in schizophrenia." Neuroimage **49**(3): 2626-2637.

Michels, L., K. Bucher, R. Luchinger, P. Klaver, E. Martin, D. Jeanmonod and D. Brandeis (2010). "Simultaneous EEG-fMRI during a working memory task: modulations in low and high frequency bands." PLoS One **5**(4): e10298.

Milz, P., P. L. Faber, D. Lehmann, T. Koenig, K. Kochi and R. D. Pascual-Marqui (2016). "The functional significance of EEG microstates--Associations with modalities of thinking." Neuroimage **125**: 643-656.

Mobascher, A., T. Warbrick, J. Brinkmeyer, F. Musso, T. Stoecker, N. Jon Shah and G. Winterer (2012). "Nicotine effects on anterior cingulate cortex in schizophrenia and healthy smokers as revealed by EEG-informed fMRI." Psychiatry Res **204**(2-3): 168-177.

Moosmann, M., P. Ritter, I. Krastel, A. Brink, S. Thees, F. Blankenburg, B. Taskin, H. Obrig and A. Villringer (2003). "Correlates of alpha rhythm in functional magnetic resonance imaging and near infrared spectroscopy." Neuroimage **20**(1): 145-158.

Moussavi, S., S. Chatterji, E. Verdes, A. Tandon, V. Patel and B. Ustun (2007). "Depression, chronic diseases, and decrements in health: results from the World Health Surveys." Lancet **370**(9590): 851-858.

Mulert, C., V. Kirsch, R. Pascual-Marqui, R. W. McCarley and K. M. Spencer (2011). "Long-range synchrony of gamma oscillations and auditory hallucination symptoms in schizophrenia." Int J Psychophysiol **79**(1): 55-63.

Newman, M. E. (2006). "Modularity and community structure in networks." Proc Natl Acad Sci U S A **103**(23): 8577-8582.

Nicholson, C. (1973). "Theoretical analysis of field potentials in anisotropic ensembles of neuronal elements." IEEE Trans Biomed Eng **20**(4): 278-288.

Nir, Y., U. Hasson, I. Levy, Y. Yeshurun and R. Malach (2006). "Widespread functional connectivity and fMRI fluctuations in human visual cortex in the absence of visual stimulation." Neuroimage **30**(4): 1313-1324.

Obata, T., T. T. Liu, K. L. Miller, W. M. Luh, E. C. Wong, L. R. Frank and R. B. Buxton (2004). "Discrepancies between BOLD and flow dynamics in primary and supplementary motor areas: application of the balloon model to the interpretation of BOLD transients." Neuroimage **21**(1): 144-153.

Ogawa, S., T. M. Lee, A. R. Kay and D. W. Tank (1990). "Brain magnetic resonance imaging with contrast dependent on blood oxygenation." Proc Natl Acad Sci U S A **87**(24): 9868-9872.

Otten, L. J., A. H. Quayle, S. Akram, T. A. Ditewig and M. D. Rugg (2006). "Brain activity before an event predicts later recollection." Nat Neurosci **9**(4): 489-491.

Palm, U., D. Keeser, A. Hasan, M. J. Kupka, J. Blautzik, N. Sarubin, F. Kaymakanova, I. Unger, P. Falkai, T. Meindl, B. Ertl-Wagner and F. Padberg (2016). "Prefrontal Transcranial Direct Current Stimulation for Treatment of Schizophrenia With Predominant Negative Symptoms: A Double-Blind, Sham-Controlled Proof-of-Concept Study." Schizophr Bull.

Pascual-Marqui, R.D., K. Sekihara, D. Braneis, C.M. Michel. In Michel, C.M., T. Koenig, D. Brandeis, L.R.R. Gianotti and J. Wackermann, eds. Electrical Neuroimaging. (pp. 49-77). Cambridge, M.A: Cambridge University Press

Pessoa, L. and S. Padmala (2005). "Quantitative prediction of perceptual decisions during near-threshold fear detection." Proc Natl Acad Sci U S A **102**(15): 5612-5617.

Pettersson-Yeo, W., P. Allen, S. Benetti, P. McGuire and A. Mechelli (2011). "Dysconnectivity in schizophrenia: where are we now?" Neurosci Biobehav Rev **35**(5): 1110-1124.

Pfurtscheller, G. and F. H. Lopes da Silva (1999). "Event-related EEG/MEG synchronization and desynchronization: basic principles." Clin Neurophysiol **110**(11): 1842-1857.

Piefke, M., P. H. Weiss, K. Zilles, H. J. Markowitsch and G. R. Fink (2003). "Differential remoteness and emotional tone modulate the neural correlates of autobiographical memory." Brain **126**(Pt 3): 650-668.

Plum, F. (1972). "Prospects for research on schizophrenia. 3. Neurophysiology. Neuropathological findings." Neurosci Res Program Bull **10**(4): 384-388.

Pomarol-Clotet, E., E. J. Canales-Rodriguez, R. Salvador, S. Sarro, J. J. Gomar, F. Vila, J. Ortiz-Gil, Y. Iturria-Medina, A. Capdevila and P. J. McKenna (2010). "Medial prefrontal cortex pathology in schizophrenia as revealed by convergent findings from multimodal imaging." Mol Psychiatry **15**(8): 823-830.

Pomarol-Clotet, E., R. Salvador, S. Sarro, J. Gomar, F. Vila, A. Martinez, A. Guerrero, J. Ortiz-Gil, B. Sans-Sansa, A. Capdevila, J. M. Cebamanos and P. J. McKenna (2008). "Failure to deactivate in the prefrontal cortex in schizophrenia: dysfunction of the default mode network?" Psychol Med **38**(8): 1185-1193.

Raichle, M. E., A. M. MacLeod, A. Z. Snyder, W. J. Powers, D. A. Gusnard and G. L. Shulman (2001). "A default mode of brain function." Proc Natl Acad Sci U S A **98**(2): 676-682.

Razavi, N., K. Jann, T. Koenig, M. Kottlow, M. Hauf, W. Strik and T. Dierks (2013). "Shifted coupling of EEG driving frequencies and fMRI resting state networks in schizophrenia spectrum disorders." PLoS One **8**(10): e76604.

Rieger, K., L. Diaz Hernandez, A. Baenninger and T. Koenig (2016). "15 Years of Microstate Research in Schizophrenia - Where Are We? A Meta-Analysis." Front Psychiatry **7**: 22.

Rodriguez, E., N. George, J. P. Lachaux, J. Martinerie, B. Renault and F. J. Varela (1999). "Perception's shadow: long-distance synchronization of human brain activity." Nature **397**(6718): 430-433.

Rosburg, T., N. N. Boutros and J. M. Ford (2008). "Reduced auditory evoked potential component N100 in schizophrenia--a critical review." Psychiatry Res **161**(3): 259-274.

Rosenkranz, K. and L. Lemieux (2010). "Present and future of simultaneous EEG-fMRI." MAGMA **23**(5-6): 309-316.

Rossiter, H. E., S. F. Worthen, C. Witton, S. D. Hall and P. L. Furlong (2013). "Gamma oscillatory amplitude encodes stimulus intensity in primary somatosensory cortex." Front Hum Neurosci **7**: 362.

Saha, S., D. Chant, J. Welham and J. McGrath (2005). "A systematic review of the prevalence of schizophrenia." PLoS Med **2**(5): e141.

Sala-Llonch, R., C. Pena-Gomez, E. M. Arenaza-Urquijo, D. Vidal-Pineiro, N. Bargallo, C. Junque and D. Bartres-Faz (2012). "Brain connectivity during resting state and subsequent working memory task predicts behavioural performance." Cortex **48**(9): 1187-1196.

Salgado-Pineda, P., E. Fakra, P. Delaveau, P. J. McKenna, E. Pomarol-Clotet and O. Blin (2011). "Correlated structural and functional brain abnormalities in the default mode network in schizophrenia patients." Schizophr Res **125**(2-3): 101-109.

Scheeringa, R., M. C. Bastiaansen, K. M. Petersson, R. Oostenveld, D. G. Norris and P. Hagoort (2008). "Frontal theta EEG activity correlates negatively with the default mode network in resting state." Int J Psychophysiol **67**(3): 242-251.

Scheidegger, O., R. Wiest, K. Jann, T. Konig, K. Meyer and M. Hauf (2013). "Epileptogenic developmental venous anomaly: insights from simultaneous EEG/fMRI." Clin EEG Neurosci **44**(2): 157-160.

Schmidt, A., V. A. Diwadkar, R. Smieskova, F. Harrisberger, U. E. Lang, P. McGuire, P. Fusar-Poli and S. Borgwardt (2014). "Approaching a network connectivity-driven classification of the psychosis continuum: a selective review and suggestions for future research." Front Hum Neurosci **8**: 1047.

Seeley, W. W., J. M. Allman, D. A. Carlin, R. K. Crawford, M. N. Macedo, M. D. Greicius, S. J. Dearmond and B. L. Miller (2007). "Divergent social functioning in behavioral variant frontotemporal dementia and Alzheimer disease: reciprocal networks and neuronal evolution." Alzheimer Dis Assoc Disord **21**(4): S50-57.

Seeley, W. W., V. Menon, A. F. Schatzberg, J. Keller, G. H. Glover, H. Kenna, A. L. Reiss and M. D. Greicius (2007). "Dissociable intrinsic connectivity networks for salience processing and executive control." J Neurosci **27**(9): 2349-2356.

Shenton, M. E., C. C. Dickey, M. Frumin and R. W. McCarley (2001). "A review of MRI findings in schizophrenia." Schizophr Res **49**(1-2): 1-52.

Shulman, G. L., J. A. Fiez, M. Corbetta, R. L. Buckner, F. M. Miezin, M. E. Raichle and S. E. Petersen (1997). "Common Blood Flow Changes across Visual Tasks: II. Decreases in Cerebral Cortex." J Cogn Neurosci **9**(5): 648-663.

Siekmeier, P. J. and S. M. Stufflebeam (2010). "Patterns of spontaneous magnetoencephalographic activity in patients with schizophrenia." J Clin Neurophysiol **27**(3): 179-190.

Singer, W. (1999). "Neuronal synchrony: a versatile code for the definition of relations?" Neuron **24**(1): 49-65, 111-125.

Singer, W. (2001). "Consciousness and the binding problem." Ann N Y Acad Sci **929**: 123-146.

Singh, K. D. and I. P. Fawcett (2008). "Transient and linearly graded deactivation of the human default-mode network by a visual detection task." Neuroimage **41**(1): 100-112.

Soravia, L. M., J. S. Witmer, S. Schwab, M. Nakataki, T. Dierks, R. Wiest, K. Henke, A. Federspiel and K. Jann (2016). "Prestimulus default mode activity influences depth of processing and recognition in an emotional memory task." Hum Brain Mapp **37**(3): 924-932.

Spencer, K. M., P. G. Nestor, R. Perlmutter, M. A. Niznikiewicz, M. C. Klump, M. Frumin, M. E. Shenton and R. W. McCarley (2004). "Neural synchrony indexes disordered perception and cognition in schizophrenia." Proc Natl Acad Sci U S A **101**(49): 17288-17293.

Sponheim, S. R., B. A. Clementz, W. G. Iacono and M. Beiser (2000). "Clinical and biological concomitants of resting state EEG power abnormalities in schizophrenia." Biol Psychiatry **48**(11): 1088-1097.

Sporns, O., D. R. Chialvo, M. Kaiser and C. C. Hilgetag (2004). "Organization, development and function of complex brain networks." Trends Cogn Sci **8**(9): 418-425.

Stephan, K. E., K. J. Friston and C. D. Frith (2009). "Dysconnection in schizophrenia: from abnormal synaptic plasticity to failures of self-monitoring." Schizophr Bull **35**(3): 509-527.

Strogatz, S. H. (2001). "Exploring complex networks." Nature **410**(6825): 268-276.

Sullivan, P. F., K. S. Kendler and M. C. Neale (2003). "Schizophrenia as a complex trait: evidence from a meta-analysis of twin studies." Arch Gen Psychiatry **60**(12): 1187-1192.

Tallon-Baudry, C., O. Bertrand, C. Delpuech and J. Permier (1997). "Oscillatory gamma-band (30-70 Hz) activity induced by a visual search task in humans." J Neurosci **17**(2): 722-734.

Tretter, F. and J. Scherer (2006). "Schizophrenia, neurobiology and the methodology of systemic modeling." Pharmacopsychiatry **39 Suppl 1**: S26-35.

Tyvaert, L., P. Levan, C. Grova, F. Dubeau and J. Gotman (2008). "Effects of fluctuating physiological rhythms during prolonged EEG-fMRI studies." Clin Neurophysiol **119**(12): 2762-2774.

Uhlhaas, P. J., F. Roux, W. Singer, C. Haenschel, R. Sireteanu and E. Rodriguez (2009). "The development of neural synchrony reflects late maturation and restructuring of functional networks in humans." Proc Natl Acad Sci U S A **106**(24): 9866-9871.

Uhlhaas, P. J. and W. Singer (2006). "Neural synchrony in brain disorders: relevance for cognitive dysfunctions and pathophysiology." Neuron **52**(1): 155-168.

Uhlhaas, P. J. and W. Singer (2010). "Abnormal neural oscillations and synchrony in schizophrenia." Nat Rev Neurosci **11**(2): 100-113.

van den Heuvel, M. P., R. C. Mandl, R. S. Kahn and H. E. Hulshoff Pol (2009). "Functionally linked resting-state networks reflect the underlying structural connectivity architecture of the human brain." Hum Brain Mapp **30**(10): 3127-3141.

Varela, F., J. P. Lachaux, E. Rodriguez and J. Martinerie (2001). "The brainweb: phase synchronization and large-scale integration." Nat Rev Neurosci **2**(4): 229-239.

Vatansever, D., D. K. Menon, A. E. Manktelow, B. J. Sahakian and E. A. Stamatakis (2015). "Default Mode Dynamics for Global Functional Integration." J Neurosci **35**(46): 15254-15262.

Wagner, A. D., D. L. Schacter, M. Rotte, W. Koutstaal, A. Maril, A. M. Dale, B. R. Rosen and R. L. Buckner (1998). "Building memories: remembering and forgetting of verbal experiences as predicted by brain activity." Science **281**(5380): 1188-1191.

Walter, H., A. P. Wunderlich, M. Blankenhorn, S. Schafer, R. Tomczak, M. Spitzer and G. Gron (2003). "No hypofrontality, but absence of prefrontal lateralization comparing verbal and spatial working memory in schizophrenia." Schizophr Res **61**(2-3): 175-184.

Weissman, D. H., K. C. Roberts, K. M. Visscher and M. G. Woldorff (2006). "The neural bases of momentary lapses in attention." Nat Neurosci **9**(7): 971-978.

Whitfield-Gabrieli, S. and J. M. Ford (2012). "Default mode network activity and connectivity in psychopathology." Annu Rev Clin Psychol **8**: 49-76.

Whitfield-Gabrieli, S., H. W. Thermenos, S. Milanovic, M. T. Tsuang, S. V. Faraone, R. W. McCarley, M. E. Shenton, A. I. Green, A. Nieto-Castanon, P. LaViolette, J. Wojcik, J. D. Gabrieli and L. J. Seidman (2009). "Hyperactivity and hyperconnectivity of the default network in schizophrenia and in first-degree relatives of persons with schizophrenia." Proc Natl Acad Sci U S A **106**(4): 1279-1284.

Wiest, R., L. Estermann, O. Scheidegger, C. Rummel, K. Jann, M. Seeck, K. Schindler and M. Hauf (2013). "Widespread grey matter changes and hemodynamic correlates to interictal epileptiform discharges in pharmacoresistant mesial temporal epilepsy." J Neurol **260**(6): 1601-1610.

Zhang, S. and C. S. Li (2012). "Functional connectivity mapping of the human precuneus by resting state fMRI." Neuroimage **59**(4): 3548-3562.

Zhou, L., W. Pu, J. Wang, H. Liu, G. Wu, C. Liu, T. E. Mwansisya, H. Tao, X. Chen, X. Huang, D. Lv, Z. Xue, B. Shan and Z. Liu (2016). "Inefficient DMN Suppression in Schizophrenia Patients with Impaired Cognitive Function but not Patients with Preserved Cognitive Function." Sci Rep **6**: 21657.

Zhou, Y., M. Liang, L. Tian, K. Wang, Y. Hao, H. Liu, Z. Liu and T. Jiang (2007). "Functional disintegration in paranoid schizophrenia using resting-state fMRI." Schizophr Res **97**(1-3): 194-205.

ACKNOWLEDGMENTS

I would like to express my sincere gratefulness to the many people who contributed over the whole PhD period in manifold ways to make this thesis possible and an enriching personal experience.

All the **participants**, who took part in the studies and expressed their interest in research.

Thomas Koenig, my thesis advisor, for his guidance and encouragement throughout this period. His creative ideas and methodological skills were inspiring and indispensable for my work. Especially, the positive attitude and the "open door" policy he follows with his students creates a very nice working atmosphere. **Roland Wiest** for being the co-advisor of the thesis. With his knowledge from clinical neuroradiology, he contributed meaningfully discussing our results, especially in the 2nd year examination. **Thomas Dierks** for providing the framework to realize all the work included, being it the physical workspace or the performance of all the MR measurements at the Inselspital. The **TRC team** for creating a stimulating and amicable working field. Also to previous members of the TRC: **Axel**, **Ingrida, Jennifer, Kay**, **Lester, Philipp, Simon**, **Stéphanie**, **Nadia**, **Nadja**, **Keiichiro**, **Mara**, **Masahito**, **Miranka**, **Melanie** and **Othmar.**

My deepest appreciation goes to my office colleagues and friends **Laura Diaz Hernandez** and **Kathryn Heri** for assisting many times early in the morning with the measurements, but especially for sharing all the fun as well as stressful moments of that period - thanks roomies!

A special thank goes to **Sonia Nauer** and **Lilo Badertscher** for the many administrative and organizational efforts they made throughout those years.

Nadja Razavi for being such a good instructor into the clinical field and for generously sharing her knowledge and experience for the performance of the clinical interviews. **Ulrich Raub** for maintaining the recruiting system. Regarding MRI measurements, I would like express my gratitude to **Andrea Federspiel**, **Kay Jann** and **Simon Schwab** for their versatile support in explaining physical basics, good practice with the data, as well as preprocessing and analysis procedures. And also the **MTRA team** of the Inselpital for helping to conduct all the measurements.

The Singergia team: **Dani, Lutz, Peter, Thomas, Mara, Anthony, Carina, Laura D.H**. and **Laura T.** I always enjoyed being part of this "bigger" project including the enriching exchange and also the informal and humorous parts of the meetings we had. A special

thanks goes to **Mara Kottlow** for organizing all the educational programs and for her scientific assistance, but also her friendship and being such a good host to me several times in Zurich.

The BIEEGL in San Francisco: **Brian**, **Dan**, **Christopher**, **Holly**, **Jamie**, **Judy**, **Julianne**, **Kate**, **Kayla, Kia, Naomi**, **Nick**, **Nina**, **Susanna**, **Taihao**, **Tara**, and **Vanessa**. Thank you all, especially **Judy**, for welcoming me so nicely and introducing me into the scientific life of this beautifully located lab.

I deeply thank **Laura Diaz Hernandez, Jamie Ferrie**, **Holly Hamilton**, and **Kathryn Heri** for proofreading my thesis.

Axel Kohler, an important person for paving my way into neuroscience. As supervisor of my master thesis, I could benefit from his profound knowledge in the field of EEG as well as in statistical methods. Especially, I am grateful for his encouragement to pursue scientific research.

My very deep gratitude goes to my family and friends for their priceless support over all those years, and beyond: My love goes to my parents, **Vera** and **Fred Bänninger**. **Simone**, for sharing all the way from the studies through the graduate school together – merci buuz! Other close friends for being so awesome: **Anouk**, **Carla**, **Jessy**, **Muriel**, **Nicole**, **Nice**, **Noémi**, and **Lytschi –** you made me thrive in different ways. **Manu**, thank you for your encouragement and for providing a "home" for me ☺

Finally, I would like to mention the **Graduate School for Health Sciences** for providing educational program and financial support and further organizations who funded my project: **The Swiss National Science Foundation** (Sinergia Grant #136249, DocMobility Grant #P1BEP3_158984), and the **Center for Cognition, Learning and Memory** of the University of Bern.

CURRICULUM VITAE

PERSONAL INFORMATION

Name	**Anja Katharina Bänninger**
Office address	Psychiatric Electrophysiology Unit Translational Research Center University Hospital of Psychiatry and Psychotherapy University of Bern Bolligenstrasse 111 3000 Bern 60
Office phone	+41 (0)31 932 88 27
E-Mail	anja.baenninger@puk.unibe.ch
Birth date	22nd of December 1984
Place of origin	Embrach (ZH), Switzerland

PROFESSIONAL EXPERIENCE

03. 2015 – 12.2014	**Visitor graduate with a DocMobility from the SNSF** Brain Imaging and EEG Laboratory (BIEEGL) San Francisco Veteran Affairs Medical Center University of San Francisco, California Supervisor: Prof. Dr. Judith M. Ford
08. 2010 – 07. 2011	**Research internship in line with the master thesis** Translational Research Center University Hospital of Psychiatry and Psychotherapy University of Bern Supervisor: Dr. Axel Kohler
01. 2010 – 06. 2010	**Internship in Neuropsychology** Department of Cognitive and Restorative Neurology Anna Seiler – Haus, Inselspital Bern

EDUCATION

02. 2012 – current	**PhD student** Psychiatric Electrophysiology Unit Translational Research Center University Hospital of Psychiatry and Psychotherapy University of Bern

Thesis advisor: Prof. Dr. Thomas Koenig
Title of thesis: "From rest to task: Functional brain networks in schizophrenia"

09. 2008 – 07. 2011 **Master of Science in Psychology**
Specialization in Neuropsychology and Clinical Psychology
University of Bern
Title of Master thesis: "Investigating the dynamics of brain networks in visuospatial processing using EEG"

10. 2004 – 07. 2007 **Bachelor of Science in Psychology with minor in Sport Sciences**
University of Bern

TEACHING EXPERIENCE

16. – 18. 07. 2014 **Assisting EEG Course for students**
University of Bern
Course leader: Prof. Dr. Thomas Koenig

09. – 13. 09. 2013 **Assisting EEG Course for students**
University of Bern
Course leader: Prof. Dr. Thomas Koenig

ORGANIZATIONAL ACTIVITIES

28. 9. – 1. 10. 2014 Assistant in organization of the Monte Verita conference '**Resting-States and State Dependent Information Processing in Health and Disease**'
Centro Stefano Franscini, Monte Veritá, Ascona, Switzerland
Organizing committee: Thomas Koenig, Daniel Brandeis, Peter Achermann, Lutz Jäncke, and Mara Kottlow

27. – 29. 06. 2012 Organization of the **6th Swiss Mapping Meeting (SMM)** in Brione (TI; together with Laura Diaz Hernandez)
Scientific leader: Prof. Dr. Thomas Koenig

CONFERENCES & MEETINGS

31. 03. 2016 Clinical Neuroscience Meeting Bern (CNB), Switzerland
14. – 18. 06. 2015 Organization for Human Brain Mapping (OHBM), Honolulu, Hawaii
08. – 12. 06. 2014 Organization for Human Brain Mapping (OHBM), Hamburg, Germany

19. – 20. 03. 2014	First Zurich Computational Psychiatry Meeting, Switzerland
24. – 25. 01. 2014	Swiss Society for Neuroscience (SSN) and Clinical Neuroscience Meeting Bern (CNB), Switzerland
05. – 08. 09. 2013	First international conference on Basic and Clinical multimodal Imaging (BaCI), Geneva, Switzerland
04. 12. 2012	Clinical Neuroscience Meeting Bern (CNB), Switzerland
27. – 30. 08. 2012	Swiss Mapping Meeting (SSM), Brione (TI), Switzerland
09. – 13. 01. 2012	Alpine Brain Imaging Meeting (ABIM), Champéry, Switzerland

GRANTS

DocMobility "P1BEP3_158984" from the Swiss National Science Foundation (SNSF)

LIST OF PUBLICATIONS

Relevant for the PhD thesis:

Baenninger A, Diaz Hernandez L, Rieger K, Ford JM, Kottlow M, Koenig T. Inefficient preparatory fMRI-BOLD network activations predict working memory dysfunctions in patients with schizophrenia. Front. Psychiatry 7:29.

Kottlow M, Schlaepfer A, **Baenninger A**, Michels L, Brandeis D, Koenig T. Pre-stimulus BOLD-network activation modulates EEG spectral activity during working memory retention. Front. Behav.Neurosci.9:111.

Baenninger A, Palzes VA, Roach BJ, Mathalon DH, Judith M Ford JM, Koenig T. Delta EEG synchronization linked to DMN activity in schizophrenia (submitted to NeuroImage Clinical)

Other publications:

Diaz Hernandez L, Rieger K, **Baenninger A**, Brandeis D, Koenig T. 2016. Towards Using Microstate- Neurofeedback for the Treatment of Psychotic Symptoms in Schizophrenia: A Feasibility Study in Healthy Participants. Brain Topogr 29:308–321

Rieger K*, Diaz Hernandez L*, **Baenninger A**, Koenig T. 2016 15 years of microstate research in schizophrenia – where are we? A meta-analysis. Frontiers in Psychiatry

Antonova I*, **Bänninger A***, Dierks T, Griskova-Bolanova I, Koenig T, Kohler A. Differential recruitment of brain networks during visuospatial and color processing: evidence from ERP microstates. Neuroscience 305 (2015) 128–138 137

(* shared first authorship)

DECLARATION OF ORIGINALITY

Last name, first name: Bänninger, Anja

Matriculation number: 04-104-980

I hereby declare that this thesis represents my original work and that I have used no other sources except as noted by citations.

All data, tables, figures and text citations which have been reproduced from any other source, including the internet, have been explicitly acknowledged as such.

I am aware that in case of non-compliance, the Senate is entitled to withdraw the doctorate degree awarded to me on the basis of the present thesis, in accordance with the "Statut der Universität Bern (Universitätsstatut; UniSt)", Art. 69, of 7 June 2011.

Place, date

Bern, 20.5.2016

Signature